DESIGN RECOMMENDATION FOR STORAGE TANKS AND THEIR SUPPORTS WITH EMPHASIS ON SEISMIC DESIGN

(2010 EDITION)

ARCHITECTURAL INSTITUTE OF JAPAN

Foreword

The Architectural Institute of Japan set up a "Sub-Committee for Design of Storage Tanks" to provide a recommendation of the seismic design for the various types of storage tanks in common use throughout Japan. The Sub-Committee first published "Design Recommendation for Storage Tanks and Their Supports" in 1984, and amended it in the 1990, 1996 and 2010 publications. This current revised recommendation provides bulk material pressures for silos and further guidance on seismic design methods for storage tanks based on the horizontal load-carrying capacity in the structure.

It is envisaged by publishing the English version of "Design Recommendation for Storage Tanks and Their Supports" that the above unique design recommendation will be promoted to the overseas countries who are concerned on the design of storage tanks and the activities of the Architectural Institute of Japan will be introduced them too. It is addressed how this recommendation is in an advanced standard in terms of the theory of the restoring force characteristics of the structure considering the Elephant Foot Bulge (EFB), the effect of the uplifting tank and the plastic deformation of the bottom plate at the shell-to-bottom juncture in the event of earthquake, the design spectrum for sloshing in tanks, the design pressure for silos, and the design methods for the under-ground storage tanks as well. The body of the recommendation was completely translated into English but the translation of the commentary was limited to the minimum necessary parts for understanding and utilising the theories and equations in the body. The sections 2.7 Timbers and 4.9 Wooden Storage Tanks are omitted as they are not common in overseas countries. Listing of some Japanese references are omitted and some new references are added in this English version.

It is worthy of note that the contents of this recommendation have been verified and their efficacy confirmed by reference to data obtained from the tanks and silos damaged during recent earthquakes in Japan, including the Hanshin-Awaji Great Earthquake in 1995 and the Niigataken Chuetu-oki Earthquake in 2007.

Introduction

There are several types of storage tanks, e.g., above-ground, flat-bottomed, cylindrical tanks for the storage of refrigerated liquefied gases, petroleum, etc., steel or concrete silos for the storage of coke, coal, grains, etc., steel, aluminium, concrete or FRP tanks including elevated tanks for the storage of water, spherical tanks (pressure vessels) for the storage of high pressure liquefied gases, and under-ground tanks for the storage of water and oil. The trend in recent years is for larger tanks, and as such the seismic design for these larger storage tanks has become more important in terms of safety and the environmental impact on society as a whole.

The failure mode of the storage tank subjected to a seismic force varies in each structural type, with the structural characteristic coefficient (D_s) being derived from the relationship between the failure mode and the seismic energy transferred to, and accumulated in the structure. A cylindrical steel tank is the most common form of storage tank and its normal failure mode is a buckling of the cylindrical shell, either in the so called Elephant Foot Bulge (EFB), or as Diamond Pattern Buckling (DPB). The D_s value was originally calculated with reference to experimental data obtained from cylindrical shell buckling, but was later re-assessed and modified based on the restoring force characteristics of the structure after buckling. Those phenomena at the Hanshin-Awaji Great Earthquake and the Niigataken Chuetu-oki Earthquake were the live data to let us review the D_s value. For the EFB, which is the typical buckling mode of a cylindrical shell storage tank for petroleum, liquefied hydrocarbon gases, etc., it became possible to ascertain the buckling strength by experiments on a cylindrical shell by applying an internal hydrodynamic pressure, an axial compressive force, and a shear force simultaneously. Details of these experiments are given in Chapter 3.

The seismic design calculations for other types of storage tanks have been similarly reviewed and amended to take into account data obtained from recent experience and experiments.

Design recommendation for sloshing phenomena in tanks has been added in this publication. Design spectra for sloshing, spectra for long period range in other words, damping ratios for the sloshing phenomena and pressures by the sloshing on the tank roof have been presented.

For above-ground vertical cylindrical storage tanks without any restraining element, such as anchor bolts or straps, to prevent any overturning moment, only the bending resistance due to the uplift of the rim of bottom plate exists. This recommendation shows how to evaluate the energy absorption value given by plasticity of the uplifted bottom plate for unanchored tanks, as well as the D_s value of an anchored cylindrical steel-wall tank.

As the number of smaller under-ground tanks used for the storage of water and fuel is increasing in Japan, the Sub-committee has added them in the scope of the recommendation and provided a framework for the seismic design of under-ground tanks. The recommendation has accordingly included a new response displacement method and a new earth pressure calculation method, taking into account the design methods adopted by the civil engineering fraternity.

For silo design, additional local pressure which depends on eccentricity of discharge outlet, and equations which give approximate stress produced by this pressure are given in this 2010 publication.

August 2011
Sub-committee for Design of Storage Tanks
The Architectural Institute of Japan

Table of Contents

1. General

1.1 Scope

This Design Recommendation is applied to the structural design of water storage tanks, silos, spherical storage tanks (pressure vessels), flat-bottomed, cylindrical above-ground storage tanks and under-ground storage tanks.

Commentary:

This Design Recommendation is applied to the structural design, mainly the seismic design, of water storage tanks, silos, spherical storage tanks (pressure vessels), flat-bottomed, cylindrical, above-ground storage tanks and under-ground storage tanks. As common requirements chapter 2 calls for material specifications which are applicable to the above -mentioned tanks, and chapter 3 calls for loads and buckling designs. Chapter 3 especially highlights the modified seismic coefficient method and the modal analysis as approved evaluation methods of seismic design based on the reference design acceleration response spectrum and the structural characteristic coefficient D_s. The seismic design method adopted in the Recommendation is the allowable stress method modified with B, the ratio of the horizontal load-carrying capacity in the structure to the short-term allowable yield strength. The design for each tank is described in chapter 4 and onwards. Chapters 4 and 5 call for general requirements of structural design of tanks and their supporting structures for water storage tanks and silos, respectively. Chapters 6 calls for requirements of seismic design only for supporting structures of spherical storage tanks. Chapters 7 and 8 calls for requirements of flat-bottomed, cylindrical above-ground storage tanks and under-ground storage tanks, respectively.

Examples of design procedure for each type of tanks in chapters 4 through 8 are included in appendices.

1.2 Notations

The following notations are applicable as common notations through the chapters in this Recommendation, and each chapter includes some additional notations to be specifically used in the chapter.

B ratio of the horizontal load-carrying capacity in the structure to the short-term allowable yield strength

C design yield shear force coefficient

C_j design yield shear force coefficient at the *j*-th natural mode

D_s structural characteristic coefficient $D_h \times D_\eta$

D_h coefficient determined by the damping of the structure

D_η coefficient determined by the ductility of the structure

E Young's modulus (N/mm^2)

F yield strength (N/ mm^2)

$_bf_{cr}$ allowable bending stress in the cylindrical wall (N/mm^2)

$_cf_{cr}$ allowable compressive stress in the cylindrical wall (N/mm^2)

$_sf_{cr}$ allowable shear stress in the cylindrical wall (N/mm^2)

g acceleration of gravity (= 9.8m/s^2)

h damping ratio

I importance factor

j order of natural frequency

K lateral design seismic coefficient

K_H lateral design seismic coefficient in the ground

K_V vertical design seismic coefficient in the ground

K_{HS} lateral design seismic coefficient at the ground surface

K_{HB} lateral design seismic coefficient at the bedrock surface

k the maximum number of vibration modes which largely influence to seismic responses

n total number of mass points

Q_d design yield shear force at the base of the structure (N)

Q_{di} design shear force imposed just below the i-th mass in case that the structure is assumed the n-th lumped mass vibration system (N)

R_G ground amplification factor

r radius of cylindrical tank (mm)

S_v design velocity response spectrum (m/s)

S_a design acceleration response spectrum (m/s^2)

S_{a1} acceleration response at the first natural period (m/s^2)

S_{aj} acceleration response at the j-th natural period (m/s^2)

S_{v1} design velocity response at the first natural period in the sloshing mode (m/s)

T the first natural period of the structure (s)

T_j j-th natural period of the structure (s)

T_G critical period determined by the ground classification (s)

$U_{H(z)}$ horizontal displacement at the depth z from the ground surface (m)

$U_{V(z)}$ vertical displacement at the depth z from the ground surface (m)

u_{ij} j-th natural mode at the i-th mass

W design weight imposed on the base of the structure (N)

W_i weight of the i-th mass (N)

Z_s seismic zoning factor

σ_b bending stress in the cylindrical wall (N/mm^2)

σ_c average compressive stress in the cylindrical wall (N/mm^2)

σ_h average hoop tensile stress in the cylindrical wall (N/mm^2)

τ shear stress in the cylindrical wall (N/mm^2)

2.   Materials

2.1   Scope

This chapter calls for the recommended materials used in the tanks and their supports. Allowable stresses of the materials are determined in accordance with the recommended method set up in each chapter for each type of storage tank.

2.2   Steels

Steel materials listed in Table 2.1 should apply for.

Table 2.1 Specifications for Steels

Specification	Type of steel Grades
JIS G 3136	Rolled Steels for Building Structure; SN400A/B/C, SN490B/C
JIS G 3101	Rolled Steels for General Structure; SS400, SS490, SS540
JIS G 3106	Rolled Steels for Welded Structure; SM400A/B/C, SM490A/B/C, SM490YA/YB, SM520B/C, SM570
JIS G 3444	Carbon Steel Tubes for General Structural Purposes; STK400, STK490
JIS G 3466	Carbon Steel Square Pipes for General Structural Purposes; STKR400, STKR490
JIS G 5101	Carbon Steel Castings
JIS G 3201	Carbon Steel Forgings for General Use
JIS G 3115	Steel Plates for Pressure Vessels for Intermediate Temperature Service; SPV235, SPV315, SPV355, SPV450, SPV490
JIS G 3120	Manganese-Molybdenum and Manganese-Molybdenum-Nickel Alloy Steel Plates Quenched and Tempered for Pressure Vessels; SQV1A/1B, SQV 2A/2B, SQV 3A/3B
JIS G 3126	Carbon Steel Plates for Pressure Vessels for Low Temperature Service; SLA235A/B, SLA325A/B, SLA365
JIS B 1186	Sets of High Strength Hexagon Bolt, Hexagon Nut and Plain Washers for Friction Grip Joints
JIS Z 3211	Covered Electrodes for Mild Steel
JIS Z 3212	Covered Electrodes for High Tensile Strength Steel
JIS Z 3351	Submerged Arc Welding Solid Wires for Carbon Steel and Low Alloy Steel
JIS Z 3352	Submerged Arc Welding Fluxes for Carbon Steel and Low Alloy Steel
JIS G 3112	Steel Bars for Concrete Reinforcement
JIS G 3117	Rerolled Steel Bars for Concrete Reinforcement
JIS G 3551	Welded Steel Wires and Bar Fabrics
JIS G 3536	Uncoated Stress-Relieved Steel Wires and Strands for Prestressed Concrete
JIS G 3538	Hard Drawn Steel Wires for Prestressed Concrete
JIS G 3109	Steel Bars for Prestressed Concrete

JIS : Japanese Industrial Standards

2.3 Stainless Steels

Stainless steel materials listed in Table 2.2 should apply for.

Table 2.2 Specifications for Stainless Steels

Specification	Type of steel Grades
JIS G 4304	Hot Rolled Stainless Steel Plates, Sheets and Strips; SUS304, SUS304L, SUS316, SUS316L, SUS444, SUS329 J 4 L
JIS G 4305	Cold Rolled Stainless Steel Plates, Sheets and Strips; SUS304, SUS304L, SUS316, SUS316L, SUS444, SUS329 J 4 L
JIS G 3601	Stainless Clad Steels; SUS304, SUS304L, SUS316, SUS316L, SUS444
JIS G 3459	Stainless Steel Pipes; SUS304TP, SUS304LTP, SUS316TP, SUS316LTP, SUS444TP, SUS329 J 4 LTP
JIS Z 3221	Stainless Steel Covered Electrodes
JIS Z 3321	Stainless Steel, Wire Rods and Solid Wires

2.4 Concrete

2.4.1 Concrete materials should comply with JASS 5 (Japanese Architectural Standard Specifications and Commentary for Reinforced Concrete Works (2003)) 5.4 "Concrete Materials" except that par. 5N.13.3 "Pre-stressed Concrete" of JASS 5N "Reinforced Concrete Work at Nuclear Power Plants (2001)" should apply for pre-stressed concrete.

2.4.2 Quality of concrete materials should comply with Table 2.3 and below.

- JASS 5.5 "Mixing Proportion"
- JASS 5.6 "Production of Concrete"
- JASS 5.7 "Transportation and Placement"
- JASS 5.8 "Curing" etc.

JASS 5N.13.3 "Pre-stressed Concrete" should apply for pre-stressed concrete.

Table 2.3 Specifications for Concrete Materials

Specification	Minimum Value of F_c (N/mm^2)	Aggregate	
		Coarse	Fine
Normal Weight Concrete	18	Gravel or Crushed Stone	Sand or Crushed Sand

2.5 Aluminium Alloys

Aluminium alloys used for structural members should be selected from those

designated in Table 2.5 which are in accordance with the specifications of Japanese Industrial Standards in Table 2.4.

Table 2.4 Aluminium and Aluminium Alloy Materials

Specification	Title
JIS H 4000	Aluminium and Aluminium Alloy Sheets and Plates, Strips and Coiled Sheets
JIS H 4040	Aluminium and Aluminium Alloy Rods, Bars and Wires
JIS H 4080	Aluminium and Aluminium Alloy Extruded Tubes and Cold-drawn Tubes
JIS H 4090	Aluminium and Aluminium Alloy Welded Pipes and Tubes
JIS H 4100	Aluminium and Aluminium Alloy Extruded Shape
JIS H 4140	Aluminium and Aluminium Alloy Forgings
JIS H 5202	Aluminium Alloy Castings
JIS Z 3232	Aluminium and Aluminium Alloy Welding Rods and Wires

Table 2.5 Grades of Aluminium Alloy Materials

A 1060	A 5052	A 5652	A 7003-T5
A 1070	A 5056	A 6061-T4	
A 1080	A 5083	A 6061-T6	
A 1100	A 5086	A 6063-T5	
A 1200	A 5154	A 6063-T6	
A 3003	A 5254	A 7 N 01-T4	
A 3203	A 5454	A 7 N 01-T6	

2.6   FRP

2.6.1   Resins used for FRP (Fibre Reinforced Plastics) materials should be equal to or better than the quality of the UP-G (Unsaturated Polyester Resin-Gneral) specified in the Japanese Industrial Standard JIS K 6919 (Liquid unsaturated polyester resins for fibre reinforced plastics), and should have excellent weather and water resistant properties.

2.6.2   Glass fibre used for FRP materials should be of the no alkali glass type in accordance with the Japanese Industrial Standards indicated in Table 2.6. Any additional processed glass fibres should also be manufactured using these fibres as raw materials.

Table 2.6 Types of glass fibre for FRP

Specification	Type
JIS R 3411	Textile glass chopped strand mats
JIS R 3412	Textile glass rovings
JIS R 3413	Textile glass yarns
JIS R 3415	Textile glass tapes
JIS R 3416	Finished textile glass fabrics
JIS R 3417	Woven roving glass fabrics

2.6.3   FRP materials should be processed using the resins and glass fibres specified above, and by adding any necessary fillers, coloring agents, artificial fibres, etc., as required to ensure that the performance requirements stipulated in Table 2.7 are satisfied.

Table 2.7 Physical Properties of FRP Materials

Property	Performance	Testing Method
Tensile strength	$> 59 \text{N/mm}^2$	JIS K 7054
Flexural strength	$> 78 \text{N/mm}^2$	JIS K 7055
Flexural modulus	$> 5.9 \times 10^3 \text{ N/mm}^2$	JIS K 7055
Glass content	$> 25 \text{wt}\%$	JIS K 7052
Barcol hardness	> 30	JIS K 7060
Water absorption	$< 1.0\%$	JIS K 6919

2.7   Timber

This section is omitted in this English version.

Commentary

1.   Component Materials of FRP

FRP basically consists of a fibre reinforcement in a resin matrix. FRP used for water tanks, use a compound resin consisting of hardening agents, colouring agents, mineral fillers, etc., in an unsaturated polyester resin. The fibre reinforcement is generally glass fibre of the no alkali glass type bundled from 50 ~ 2000 filaments of 8 ~ 13 μ m in diameter in a processed mat, cloth or roving state depending upon the intended use. The resin, glass fibre, additional fillers, and other materials should be equal to or better than the requirements specified in the relevant Japanese Industrial Standards indicated in sections 2.6.1, 2.6.2 and 2.6.3 above. Additional consideration should be given to the hygiene requirements for materials used in drinking water tanks.

2.   Performance and Allowable Stress of FRP

The performance of FRP may be changed by varying the combinations of the resin, glass fibre, and other agents to meet the requirements indicated. For water tanks, the combinations should be such that the mechanical and physical performance criteria specified in 2.6.3 are satisfied.

An approximation of the relationship of tensile stress and strain of FRP is shown in Fig. 2.6.1. FRP material with a tensile strength greater than 59N/mm^2 is used provided the material characteristics satisfy the minimum requirements noted in 2.6.3. The strain at break point is between 2% ~ 3%. Allowable stress of FRP is determined for the static properties at normal temperature, taking into account degradation within the durable period, material deviations, etc. Tables 2.6.1, 2.6.2, and 2.6.3 show the current method used to determine the allowable stresses in the design of FRP water tanks. In this illustration, the static properties of FRP at normal temperature are determined as the standard value, the limited value - considering the degradation within durable period (15years) - is then calculated, and finally the allowable stress is calculated by dividing the limited value by a safety factor (See Table 2.6.3.).
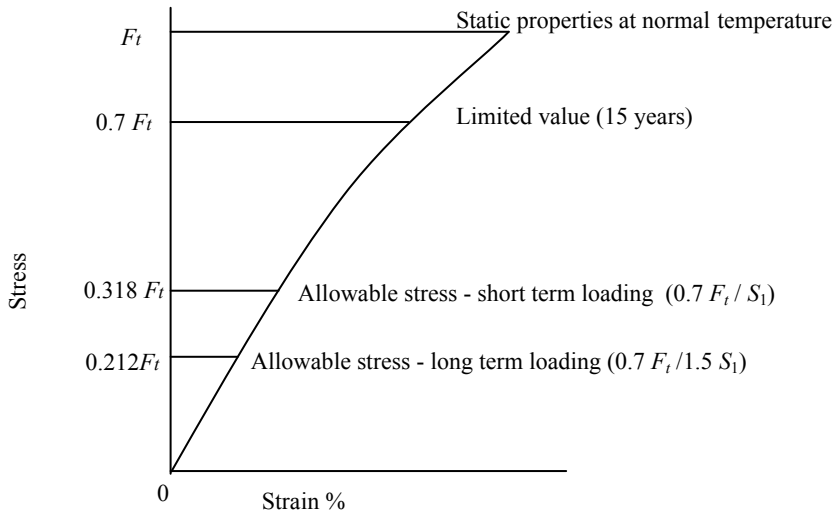
Fig. 2.6.1 Characteristics of tensile stress and strain of FRP and an example of allowable stress determination. In this case, $S_1=2.2$ (Mat hand-lay-up material).

Table 2.6.1 Allowable stress based on fracture strength

Fracture Strength	*Standard Value* [1]	*Limited Value*	*Allowable Stress*	
			Short Term [2]	*Long Term* [3]
Tensile strength	F_t	$0.7\,F_t$	$0.7\,F_t\,/\,S_1$ [4]	$0.7\,F_t\,/\,1.5S_1$
Flexural strength	F_b	$0.6\,F_b$	$0.6\,F_b\,/\,S_1$	$0.6\,F_b\,/\,1.5S_1$
In-plane shear strength	F_s	$0.7\,F_s$	$0.7\,F_s\,/\,S_1$	$0.7\,F_s\,/\,1.5S_1$
Interlaminar shear strength	F_{IS}	$0.7\,F_{IS}$	$0.7\,F_{IS}\,/\,S_1$	$0.7\,F_{IS}\,/\,1.5S_1$
Transverse shear strength	F_T	$0.6\,F_T$	$0.6\,F_T\,/\,S_1$	$0.6\,F_T\,/\,1.5S_1$
Compressive strength	F_B	$0.7\,F_B$	$0.7\,F_B\,/\,S_1$	$0.7\,F_B\,/\,1.5S_1$

[1]   *Standard value -static properties at normal temperature*
[2]   *Short-term - considering short-term loading*
[3]   *Long-term - considering long-term loading*
[4]   *The definition of S_1 is given in Table 2.6.3.*

For long-term loading, hydrostatic pressure, dead loads, etc., should be divided by 1.5 to take into account creep phenomena.

Table 2.6.2   Allowable Properties of Modulus

Modulus	Standard Value	Limited Value	Allowable Properties
Tensile Modulus	E_t	$0.8\ E_t$	$0.8\ E_t / S_2$*
Flexural Modulus	E_b	$0.8\ E_b$	$0.8\ E_b / S_2$
In-Plane Shear Modulus	G	$0.8\ G$	$0.8\ G / S_2$

* The definition of S_2 is given in Table 2.6.3.

Table 2.6.3   Safety factor of FRP (S_1, S_2)

Strength Criteria of Material (S_1)	Stiffness Criteria of Structure (S_2)
$1.72\ L_S$	$1.58\ L_S$

L_S is the coefficient of dispersion for material properties of FRP.
(In the case of fracture strength, tensile strength and flexural strength; in the case of stiffness, tensile modulus and flexural modulus.)

L_S is determined by the following equation, based on material properties obtained from more than 10 test pieces.

$$L_S = 1/\{1-3.09(\sigma / \overline{x})\}$$

where:
$\overline{x}$ = average of material properties
σ = standard deviation.

The allowable properties to be determined depends on the criteria of fracture strength or stiffness; i.e., if the criteria is based on strength of material, the allowable stress should be determined on the base of strength, and if the criteria is based on stiffness of structure, the allowable properties should be determined on the base of stiffness. The safety factor should be the value considering the effect of circumstance temperature of water tanks used, and deviation of material properties.

The material properties of FRP should be determined by the following test methods.

JIS K 7051:	General rules for testing methods of glass fibre reinforced plastics.
JIS K 7054:	Testing method for tensile properties of glass fibre reinforced plastics.
JIS K 7055:	Testing method for flexural properties of glass fibre reinforced plastics.
JIS K 7056:	Testing method for compressive properties of glass fibre reinforced plastic.
JIS K 7057:	Fibre-reinforced plastic composites - Determination of apparent interlaminar shear strength by short-beam method.
JIS K 7059:	Testing method for in-plane shear properties of glass fibre reinforced plastics.

3 Design Loads

3.1 General

3.1.1 Loads should be applied to the structural design of a tank according to its intended use, size, structure type, materials, design lifetime, location and environment, in order to assure life safety and to maintain its essential functions.

3.1.2 The applied loads should be as follows, and their combinations should be defined considering the actual probability of occurrence.

(i) Dead loads
(ii) Live loads
(iii) Snow loads
(iv) Wind loads
(v) Seismic loads
(vi) Impulse and suction due to content sloshing, and pressure due to content
(vii) Thermal stresses
(viii) Shock, e. g., by crane
(ix) Fatigue loads
(x) Soil and water pressures
(xi) Others. e.g., load from mechanical device.

3.2 Dead Loads

Dead loads are the sum of the weights of the tank, its associated piping and equipment and other fixed appurtenances.

3.3 Live Loads

3.3.1 Live loads should be considered to be the contents of the tank, the temporary weight of personnel, and the weight of other temporary equipment not normally fixed to the tank. If such loads involve a impulsive force, they should be increased by a suitable impulse factor.

3.3.2 Temporary live loads may be discounted if they have been taken into consideration with other load combinations.

3.3.3 For seismic designs, the weight of the tank contents should be considered as being divided into fixed weight (impulsive mass) and free weight (convective mass).

3.4 Snow Loads

Snow loads should be defined by considering the location, topography, environment, density of the snow, snow accumulating period, and the shape and temperature of the tank, as defined in "Recommendations for Loads on Buildings" (AIJ- 2004).

3.5   Wind loads

Wind loads should be defined by considering the shape of the tank, its structural characteristics, the location, and environment, as defined in "Recommendations for Loads on Buildings" (AIJ - 2004).

3.6   Seismic Loads

3.6.1   Seismic Loads for Above-ground Storage Tanks

3.6.1.1   Design for Impulsive Mass

Design seismic loads for above-ground storage tanks should be calculated by either one of the following methods:

(i)   Modified Seismic Coefficient Method, or
(ii)   Modal Analysis

The Modified Seismic Coefficient Method should be used for the design seismic loads of tank foundations.

3.6.1.2   Modified Seismic Coefficient Analysis

Design yield shear force, Q_d, should be calculated using equations (3.1) and (3.2).

(3.1) $Q_d = CW$

(3.2) $C = Z_s ID_s \dfrac{S_{a1}}{g}$

where:
$C \geq 0.3Z_sI$

Notations:
Q_d design yield shear force (N)
C design yield shear force coefficient
W design weight imposed on the base of the structure, which is equal to the sum of dead weight of structure and weight of impulsive mass of liquid content (N)
S_{a1} design acceleration response spectrum corresponding to the first natural period, given in par. 3.6.1.6 (m/s^2)
g acceleration of gravity $= 9.8$ (m/s^2)
Z_s seismic zone factor, which is the value stipulated in the Building Standards Law and the local government
I importance factor, given in par. 3.6.1.7
D_s structural characteristic coefficient, which is the value calculated in equation (3.3) and as further detailed in Chapters 4, 5, 6, and 7.

(3.3) $D_s = D_h D_\eta$

where:
D_h is the coefficient determined by the damping of the structure
D_η is the coefficient determined by the ductility of the structure

When the structure is assumed to have the *n* mass vibration system, the design shear force imposed just below the *i*-th mass, Q_{di}, should be calculated using equation (3.4).

(3.4) $$Q_{di} = Q_d \frac{\sum\limits_{m=i}^{n} W_m h_m}{\sum\limits_{m=1}^{n} W_m h_m}$$

where:
Q_{di} is the vertical distribution of the design shear force imposed just below the *i*-th mass (N)

Notations:
n   total number of masses
h_i height at the *i*-th mass from the ground level (m)
W_i weight of the *i*-th mass (N)

3.6.1.3   Modal Analysis

When the structure is considered as the vibration of an *n* mass-system, the design yield shear force imposed just below the *i*-th mass, Q_{di}, should be calculated using equation (3.5).

(3.5) $$Q_{di} = \left[\sum_{j=1}^{k} \left\{ C_j \sum_{m=i}^{n} W_m \beta_j u_{mj} \right\}^2 \right]^{1/2}$$

(3.6) $$C_j = Z_s ID_s \frac{S_{aj}}{g}$$

where:
$Q_{d1} \geq 0.3 Z_s IW$

Notations:
j   order of natural frequency
k   the maximum number of vibration modes which largely influences seismic responses
n   total number of masses
W_i weight of the *i*-th mass (N)
β_j participation factor of the *j*-th natural mode
u_{ij} *j*-th natural mode at the *i*-th mass
C_j design yield shear force coefficient at the *j*-th natural mode
S_{aj} design acceleration response spectrum at the *j*-th natural period, given in par. 3.6.1.6 (m/s^2)

3.6.1.4   Design Seismic Loads of Weight of Convective Mass

When the stored content is liquid, the design seismic loads of the weight of convective mass should be obtained from the design velocity response spectrum, S_{v1}, corresponding to the first natural period of the convective mass. See also chapter 7.

3.6.1.5   Design Seismic Loads of Tank Foundation

The sum of the lateral force, which is obtained from the dead weight multiplied by the horizontal design seismic coefficient, K, as shown in (3.7), and the shear force transmitted from the upper structure should be the design seismic load acting on the tank foundation.

(3.7) $K \geq 0.15$

3.6.1.6   Design Response Spectra

Design velocity response spectrum, S_{vj}, and design acceleration response spectrum, S_{aj}, should be obtained from the equation (3.8) or (3.9).

(3.8)   when $T_j < T_G$ $S_{vj} = 1.56 \, T_j$
                                        $S_{aj} = 9.8$

(3.9)   when $T_j \geq T_G$ $S_{vj} = 1.56 \, T_G$
                                        $S_{aj} = 9.8 \, T_G / T_j$

Notations:
T_j j-th natural period of the structure (s)
T_G critical period determined by the ground classification shown in Table 3.1 below (s).

Table 3.1   Critical Period, T_G (s)

Classification of Ground	Ground Conditions	T_G (s)
Type 1	(1) the ground before the Tertiary (hereinafter called bedrock) (2) diluviums (3) alluviums which are less than 10m in thickness to bedrock	0.64
Type 2	alluviums which are less than 25 m in thickness to bedrock and of which the soft layer is less than 5 m in thickness	0.96
Type 3	(1) the ground other than the above (2) the ground which is unknown in properties	1.28

3.6.1.7   Importance Factor

An importance factor is determined corresponding to the classification of the seismic design I, II, III, or IV given in Table 3.2 in consideration of significance of earthquake damages and consequence to environment.

Table 3.2   Importance Factor, I

Classification of Seismic Design	Description	I
I	Storage tanks which have small capacities and do not contain hazardous materials	0.6 and greater
II	Storage tanks which have medium to large capacities, do not contain hazardous materials, and will not have any significant consequential effect in the event of earthquake damage.	0.8 and greater
III	Storage tanks to which the significance of earthquake damages is equivalent to common use buildings	1.0 and greater
IV	Storage tanks which contain hazardous materials and the failure of which will constitute a secondary disaster	1.2 and greater

3.6.1.8   Design Seismic Loads for Allowable Stress Design

The allowable design stress for storage tanks should be obtained from the design story shear force, Q_{ei}, given in equation (3.10).

(3.10) $$Q_{ei} = \frac{Q_{di}}{B}$$

Notations:
Q_{ei} design story shear force for allowable stress design (N)
B ratio of horizontal load-carrying capacity in the structure to short-term allowable yield strength, the value of which should be between 1.0 ~ 1.5 and should be determined for each type of structure specified in the commentary to chapter 3 and the body of chapter 4 onwards.

3.6.1.9   Horizontal Load-carrying Capacity

Horizontal load-carrying capacity of storage tanks should be obtained from the allowable stresses given in par. 3.7.4.

Commentary:

Essentially seismic design as applied to storage tanks follows the requirements prescribed by the Building Standard Law where the importance of structures is not explicitly considered. However, as storage tanks are more versatile than normal building structures in that they include a range of structures covering silo containing forages and tanks for toxic materials, an importance factor, I, is introduced to accommodate these differences. Whilst this chapter summarises the common features of seismic design for above-ground storage tanks, specific design considerations - including the importance factor, is given in the chapters dedicated to each principal tank design type.

1.   Seismic Input

The seismic energy input, E_D, the principal cause for a structure's elasto-plastic deformation, is approximately expressed as shown in equation (3.6.1) as follows[3.13]:

(3.6.1) $$E_D = \frac{M S_v^{\,2}}{2}$$

Notations:
M   total mass of a structure
S_v velocity response spectrum

The acceleration response spectrum, S_a, prescribed by the Building Standard Law, is obtained from equation (3.6.2):

(3.6.2) $$S_a = C_0 R_t g$$

Notations:
C_0 standard design shear force coefficient
R_t vibration characteristic coefficient
g   acceleration of gravity

S_a and S_v are related to each other as shown in the following equation (3.6.3).

(3.6.3) $$S_a = \frac{2\pi}{T} S_v$$

Notations:
T   natural period for the 1st mode of a structure

S_a and S_v are indicated by broken lines in the curves shown in Figure 3.6.1, whilst the solid lines represent the simplified curves expressed in equations (3.8) and (3.9).
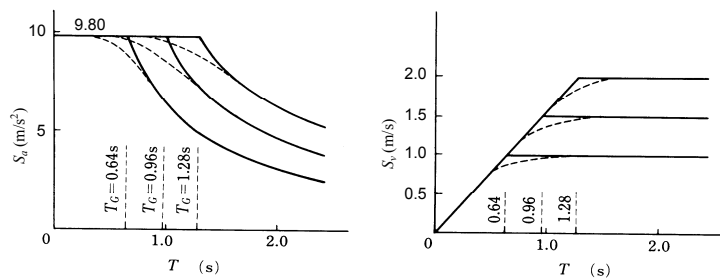

Fig.3.6.1 Design Response Spectra

2. *Seismic Design Loads*

For the sake of determining seismic design loads, storage tanks can be simplified to a single mass system, the restoring force characteristics of which are assumed to be of the elasto-plastic type with yield shear force Q_y.

It is also assumed that the structure develops cumulative plastic deformation, δ_0 , in both positive and negative directions under severe earthquake conditions as shown in Figure 3.6.2.
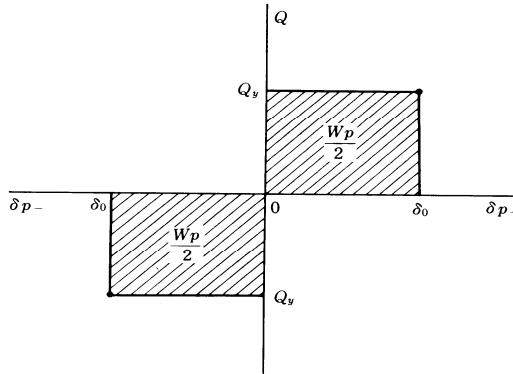
Fig.3.6.2 Damage and Cumulative Plastic Deformation

The relationship between the total energy input exerted by an earthquake and the damage of a structure is expressed by equation (3.6.4) as follows:

(3.6.4)
$$W_p + W_e = E - W_h = \frac{E}{\left(1 + 3h + 1.2\sqrt{h}\right)^2}$$

Notations:
E   *total energy input*
W_p *damage to a structure (cumulative plastic strain energy)*
W_e *elastic vibrational energy*
W_h *energy absorbed by damping*
h   *damping ratio*

$E - W_h$ can be approximately expressed by the following equation (3.6.5):

(3.6.5)
$$E - W_h = \frac{MS_v^2}{2}$$

Notations:
M   *mass of a single-mass system*

The spectra shown in Figure 3.6.1 are given for h = 0.05. E may then be expressed by equation (3.6.6):

(3.6.6)
$$E = \frac{1.42^2 MS_v^2}{2}$$

W_p and W_e are expressed by equations (3.6.7) and (3.6.8) respectively:

(3.6.7)
$$W_p = 2Q_y\delta_0$$

$$(3.6.8) \qquad W_e = \frac{Q_y \delta_y}{2}$$

Where the yield deformation, δ_y, and the yield shear force, Q_y, are determined by equations (3.6.9) and (3.6.10) respectively.

$$(3.6.9) \qquad \delta_y = \frac{Q_y}{k}$$

$$(3.6.10) \qquad Q_y = MgC$$

Notations:
Q_y	yield shear force
δ_y	yield deformation
k	spring constant of a singl-mass system
C	yield shear coefficient

The natural period of a single-mass system, T, is expressed by equation (3.6.11).

$$(3.6.11) \qquad T = 2\pi \left(\frac{M}{k}\right)^{1/2}$$

C is obtained by substituting (3.6.7) and (3.6.8) into (3.6.4) and using (3.6.9) - (3.6.11) as shown in equation (3.6.12) as follows:

$$(3.6.12) \qquad C = \frac{1}{\sqrt{1+4\eta}} \frac{1.42}{1+3h+1.2\sqrt{h}} \frac{2\pi}{T} \frac{S_v}{g}$$

$$(3.6.13) \qquad \eta = \frac{\delta_0}{\delta_y}$$

Notations:
η	averaged cumulative plastic deformation ratio as shown in equation (3.6.13).

Knowing that $S_a = 2\pi S_v/T$, and applying $Z_s = I = 1.0$, D_s in (3.3) is determined by comparing (3.2) and (3.6.12) using equations (3.6.14) and (3.6.15) as follows:

$$(3.6.14) \qquad D_h = \frac{1.42}{1+3h+1.2\sqrt{h}}$$

$$(3.6.15) \qquad D_\eta = \frac{1}{\sqrt{1+4\eta}}$$

(1)   Value of D_h

Large diameter storage tanks, such as oil storage tanks, are subject to an interaction between the soil and the structure. Assuming that a structure in direct contact with the ground is a continuous shear stratum, the one dimensional wave propagation theory yields an estimate of damping ratio, h, due to energy dissipation through the soil - structure interaction as illustrated in equation (3.6.16).

$$(3.6.16) \qquad h = \frac{2}{\pi} \frac{\rho_0 V_0}{\rho_1 V_1}$$

Notations:

ρ_0, ρ_1 densities of structure and the ground, respectively (kg/m³)

V_0, V_1 shear wave velocities of structure and the ground, respectively (m/s)

ρ_0 and V_0 are expressed by equations. (3.6.17) and (3.6.18).

(3.6.17) $$\rho_0 = \frac{M}{HA_0}$$

(3.6.18) $$V_0 = \frac{4H}{T}$$

Notations:
M   mass of structure (kg)
H   height of structure (m)
A_0 bottom area of structure (m²)
T   fundamental period of structure (s)

$\rho_0 V_0$ is approximately expressed by equation (3.6.19).

(3.6.19) $$\rho_0 V_0 = \frac{4M}{A_0 T}$$

Assuming $\rho_1 = 2.4 \times 10^3$ kg/m³ and $V_1 = 150$ m/s for Type 3 Classification of Ground with some margin, $\rho_1 V_1$ is expressed by equation (3.6.20).

(3.6.20) $$\rho_1 V_1 = \frac{360}{a_h} \cdot 10^3$$

Where a_h is shown in Table 3.6.1.

Damping ratio, h, is then expressed by equation (3.6.21) by substituting equations (3.6.19) and (3.6.20) into equation (3.6.16).

(3.6.21) $$h = \frac{7a_h M}{A_0 T} \cdot 10^{-6}$$

If a large –scale cylindrical LPG storage tank on soft soil (Type 3) is given for an example, and assuming the diameter of the tank D=60m, liquid height H=25m, T=0.32s, $A_0=3,120m^2$ and M=2.12 × 10⁷kg, $\rho_0 V_0$ is estimated as $\rho_0 V_0 = 8.5 \times 10^4 kg/(s \cdot m^2)$. The damping ratio is then determined as, h=0.15, from equation (3.6.21).

These values are consistent with the damage noted after the Miyagiken-oki and other earthquakes, and are confirmed by the analytical results of a three-dimensional thin-layer element model.

Equation (3.6.21) is applicable to flat tanks such as large-scale cylindrical oil storage tanks build on soft ground. For non-flat tanks, the damping ratio is smaller.

The ρ_1 and V_1 for equation (3.6.16) can also be directly measured by velocity logging etc., if necessary.

Table.3.6.1 Value of α_h

Classification of Ground	α_h
Type 1	0.6
Type 2	0.75
Type 3	1.0

* The classification, Type 1~3, is defined in Table 3.1.

(2) Value of D_η

As there are many variations in the design of storage tanks, estimating approximate values of η is accordingly dependent on the information provided. It is therefore essential that sufficient details are provided about the structural design to enable a reasonable estimation to be made. As a tentative measure, the minimum value of η, and D_η as obtained from equation (3.6.15) should be used (see Table 3.6.2).

Table.3.6.2 Value of D_η

Structural Type		η	D_η
Frame Structure		1.3	0.40
Wall Structure	RC	1.0	0.45
	S	0.75~0.25	0.5~0.7

RC : reinforced concrete
S : steel

3. *Relationship between modified seismic coefficient method and modal analysis*

   A seismic load can be obtained by the modified seismic coefficient method or by modal analysis. The advantage of the modified seismic coefficient method lies in its simplicity of application, whereas modal analysis is a little bit more complicated, as indicated by equations (3.5) and (3.6), and can result in a smaller seismic load than the modified seismic coefficient method.

   When comparison of the design yield shear force at the base of structure is made using the modal analysis and the modified seismic coefficient method for structures in which shear deformation is dominant, the ratio of the design yield shear force given by the modal analysis, Q_{d1}, to the design yield shear force given by the modified seismic coefficient method, Q_d, lies between 1.0 and 0.8.

   When flexural deformation is added, the ratio may be further decreased. Provided that structural parameters can be adequately estimated, the lower seismic loads given by modal analysis may be applied. However, in view of the uncertainty in estimating structural parameters, it is preferable that Q_{d1} is limited to ensure that,

   (3.6.22) $\qquad Q_{d1} \geq 0.7\, Q_d$

4. *Design seismic load applied to liquid sloshing*

   The sloshing oscillation of a contained liquid is obtained from the velocity response spectrum. Although the velocity response spectra in the range of longer periods are not yet fully clarified, equation(7.7) is considered to be a valid conservative estimate.

5. *Evaluation of seismic resistance*

   The seismic resistance of structures can be evaluated by the following alternative methods:

   (1) Horizontal load-carrying capacity design

   Horizontal load-carrying capacity in each part of a structure is checked to ensure that the criteria contained in equation (3.6.23) are satisfied.

   (3.6.23) $\qquad Q_{yi} \geq Q_{di}$

   Notations:
   Q_{yi} horizontal load-carrying capacity in the i-th mass
   Q_{di} design yield shear force in the i-th mass

(2) Allowable stress design

Similarly, the design shear force in each storey, Q_{ei}, is checked to confirm that the stresses caused by this force and the vertical loads are less than the allowable stresses. Q_{ei} is obtained using equation (3.6.24).

(3.6.24)
$$Q_{ei} = \frac{Q_{di}}{B}$$

Notations:
Q_{ei} design story shear force in the i-th mass point
B the ratio of the horizontal load-carrying capacity to the short-term allowable horizontal strength (≥ 1.0)

The first method corresponds to the ultimate strength design, whilst the second method corresponds to the conventional allowable stress design. The second method is needed, because the first one is not established yet for some types of storage tanks. Generally B is greater than unity, and when applied to ordinary building structures, the following values can be taken:

For frame structures   B   =   1.2 ~1.5
For wall structures   B   =   1.0

3.6.2   Seismic Load for Under-ground Storage Tanks

3.6.2.1   General

The following paragraphs give details of under-ground seismic intensity and under-ground soil displacement as applicable to the seismic intensity and the response displacement methods. Further details of their application can be found in Chapter 8 Seismic Design of under-ground Tanks, and Appendix B.

3.6.2.2   Under-ground seismic intensity

Horizontal seismic intensity, K_H, is based on the linear relation to the depth, and should be determined according to equation (3.11) below.

(3.11)
$$K_H = K_{HS} - (K_{HS} - K_{HB})\frac{z}{H}$$

where:
K_{HS} horizontal seismic intensity at the ground surface as calculated by equation (3.12) below,
K_{HB} horizontal seismic intensity at the bedrock surface as calculated by equation (3.13) below,
z depth from the ground surface (m),
H depth from the ground surface to the bedrock surface.

(3.12)
$$K_{HS} = Z_S R_G K_0$$

(3.13)
$$K_{HB} = \frac{3}{4} Z_S K_0$$

where:
Z_S seismic zone factor,
R_G soil amplification factor given in Table 3.3 below,

K_0 standard seismic intensity obtained from equation (3.14).

(3.14) $K_0 = 0.2$

Vertical seismic intensity K_V should be determined by equation (3.15).

(3.15) $K_V = \dfrac{1}{2} K_H$

Table 3.3   Soil Amplification Factor R_G

Ground Type	Soil Amplification Factor - R_G
Type 1 Ground (diluvial deposit)	1.0
Type 2 Ground (alluvium)	1.1
Type 3 Ground (soft ground)	1.2

Note: 1) R_G may be 0.9 for bedrock.

          2) The classification, Type 1~3, is defined in Table 3.1.

3.6.2.3   Under-ground soil displacement

Horizontal and vertical displacements U_H and U_V of under-ground soil should be determined in accordance with equations (3.16) and (3.17).

(3.16) $U_H = \dfrac{2}{\pi^2} S_V K_{HB} T_S \dfrac{H - z}{H}$

(3.17) $U_V = \dfrac{1}{2} U_H$

where:

U_H horizontal displacement of under-ground soil at the depth z from the ground surface (m),

U_V vertical displacement of under-ground soil at the depth z from the ground surface (m),

S_V design velocity response spectrum for a unit seismic intensity determined according to the surface soil natural period T_S (m/s),

T_S natural period of the ground surface layer which is determined by equation (3.18), taking into account the shear strain level of the surface soil (s)

(3.18) $T_S = 1.25 T_0$

(3.19) $T_0 = \displaystyle\sum_{i=1}^{n} \dfrac{4H_i}{V_{si}}$

where:

H_i thickness of the stratum at the i-th layer (m),

V_{si} mean shear wave velocity at the i-th layer (m/s),

However, when the bedrock surface level is close to the tank bottom level, U_H may be determined by equation (3.20)

(3.20) $$U_H = \frac{2}{\pi^2} S_V K_{HB} T_S \cos(\frac{\pi z}{2H})$$

Commentary:

1.   *Under-ground seismic intensity*

Under-ground seismic intensity may be calculated as a linear function of the depth using the seismic intensities at the ground and the bedrock surfaces provided the surface layers around the tank are nearly uniform. The term "bedrock" here is defined as 25 or more N-value for clay, 50 or more N-value for sand, or 300m/sec. or more shear wave velocity .

2.   *Under-ground soil displacement*

Because under-ground tanks are bound by the surrounding soil, the seismic response is influenced more by the deformation of the soil than that of their structural characteristics. Therefore, regarding the soil deformation as forced displacement, as well as inertia force of the structure, is consistent with actual condition.

The recommendation published in 1990 adopted a sine curve distribution for under-ground soil displacement, where a dynamic shear deformation equation for homogeneous one-layer soil was used with a sine curve assumption for shear wave form in the soil. Later FEM simulations confirmed that assumed sine curve distribution gives a smaller relative displacement (deformation) than the FEM results to tanks in deep bedrock cases, because a relatively soft soil rigidity gives larger relative displacement in the surface region. Accordingly, it is recommended that linear distribution of soil displacement for deep bedrock cases and sine curve distribution for shallow bedrock cases are used in the seismic design for under-ground tanks.

Appendix B examines the seismic design of Under-ground storage tanks and gives the basis for deep bedrock cases, whereas the basis for shallow bedrock cases is given in the following paragraphs.

Although soil displacements during earthquakes are very complicated with the actual conditions depending on the propagating earthquake, for design purposes it is assumed that all movements are in shear wave. Sine wave motion and cosine ($\pi z / 2H$) distribution in depth are assumed as in Figure 3.6.3.
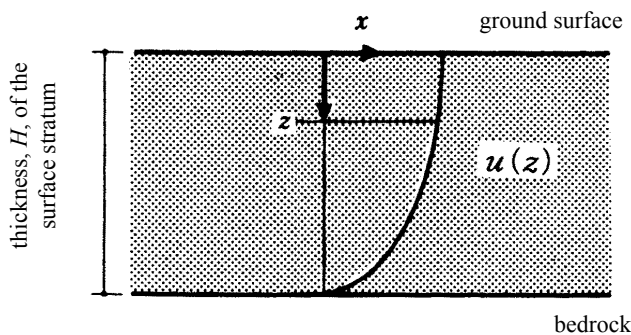

Figure 3.6.3   Under-ground soil displacement

If a homogeneous one-layer soil is assumed, the vibration equation for shear waves is as given in equation (3.6.25).

$(3.6.25)$
$$\gamma_t \frac{\partial^2 u}{\partial t^2} + C\frac{\partial u}{\partial t} - \frac{\partial}{\partial z}(G\frac{\partial u}{\partial z}) = -\gamma_t \frac{\partial^2 u_B}{\partial t^2}$$

where:

γ_t *unit soil mass*
u *horizontal displacement at depth z from the ground surface*
u_B *horizontal displacement of the bedrock*
C *damping factor*
G *soil shear modulus*

Bedrock and the ground surface are assumed to be fixed and free respectively. Spectrum modal analysis was performed for the first eigenvalue, assuming $C = 0$, then the maximum horizontal displacement at ground surface u_{max} is given in equation (3.6.26).

$(3.6.26)$
$$u_{max} = \frac{4}{\pi}\overline{S_d} = \frac{2}{\pi^2}\overline{S_v}T_s$$

where:

u_{max} *maximum horizontal displacement at the ground surface by shear wave*
T_s *the first natural period at the ground surface*
$\overline{S_d}$ *displacement spectrum at the bedrock*
$\overline{S_v}$ *velocity spectrum at the bedrock ($= 2\pi\overline{S_d}/T_s$)*

Equation (3.6.26) is the basis for the displacement from equation (3.20) in chapter 3.6.2.3.

T_s is given by the equation $T_s = 1.25T_0$ - see equations. (3.18) and (3.19), where a reduction in the rigidity according to the strain level during earthquake is considered.

$\overline{S_v}$ is evaluated as design velocity spectrum S_v at bedrock surface multiplied by horizontal seismic intensity K_{HB} at bedrock surface. S_v is calculated for 1g seismic intensity at bedrock surface (see Fig. 3.6.4).

$(3.6.27)$ $\overline{S_v} = S_v K_{HB}$

Fig. 3.6.4 is obtained as an envelope of sixteen velocity response spectra, with soil damping ratio 0.2, of strong motion records at the second class (Type 2) grounds (alluvium) normalized to 1g level.
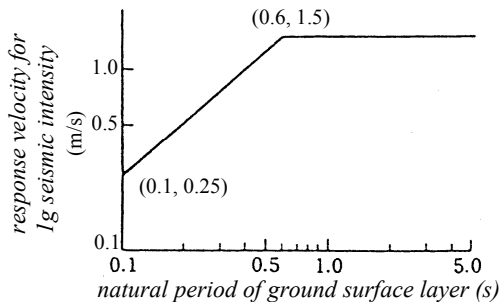

Figure 3.6.4   Velocity spectrum for 1g level

3.7   Design of Cylindrical Metal Shell Wall Against Buckling

3.7.1   Design Stress Criterion

The allowable stress design for both the elastic design and the ultimate strength design is applied. The general design format for the design criterion is given by the following two conditions, eqs. (3.21) and (3.22).

(3.21) $\dfrac{\sigma_c}{_c f_{cr}} + \dfrac{\sigma_b}{_b f_{cr}} \leqq 1$

(3.22) $\dfrac{\tau}{_s f_{cr}} \leqq 1$

where:

σ_c average axial compressive stress = W/A(N/mm^2)

σ_b maximum axial compressive stress caused by the over-turning moment=M/Z(N/mm^2)

τ maximum shear stress caused by the lateral shear force = $2Q/A$(N/mm^2)

W axial compressive force(N)

M overturning moment(Nmm)

Q lateral shear force(N)

A sectional area(mm^2)

Z elastic section modulus(mm^3)

$_c f_{cr}$ allowable axial compressive stress(N/mm^2)

$_b f_{cr}$ allowable bending stress(N/mm^2)

$_s f_{cr}$ allowable shear stress(N/mm^2)

The allowable stresses defined above are composed of ones against the long-term load, ones against the short-term load exclusive of the seismic load, and ones against the seismic load exclusively.

3.7.2   Allowable Stresses Against the Long-Term Load

The allowable stresses against the long-term axial compressive force, overturning moment and lateral shear force are given by the following three terms (1), (2) and (3), respectively, which all depend on both σ_h / F, the ratio of the average circumferential tensile stress caused by the internal pressure σ_h to the basic value for determining the yield stress F, and r/t, the ratio of the cylinder's inside radius of curvature r to the cylinder's wall thickness t.

(1)   Allowable axial compressive stress $_c f_{cr}$ against the long-term vertical force

(3.23)   for $0 \leqq \dfrac{\sigma_h}{F} \leqq 0.3$ $_c f_{cr} = \overline{_c f_{cr}} + \dfrac{0.7 f_{cr0} - \overline{_c f_{cr}}}{0.3}(\dfrac{\sigma_h}{F})$

(3.24)   for $\dfrac{\sigma_h}{F} \geqq 0.3$ $_c f_{cr} = f_{cr0}(1 - \dfrac{\sigma_h}{F})$

where:

σ_h average circumferential tensile stress caused by the internal pressure (N/mm^2)

F basic value for determining the yield stress (N/mm^2)

$_c\overline{f_{cr}}$ allowable axial compressive stress against the long-term load exclusive of internal pressure (N/mm^2)

f_{cr0} basic value for determining the strength of elephant-foot bulge (N/mm^2)

The value of f_{cr0} is given by the following equations according to the value of r/t.

(3.25)   for $\dfrac{r}{t} \leqq 0.069\dfrac{E}{F}$ $f_{cr0} = \dfrac{F}{1.5}$

(3.26)   for $0.069\dfrac{E}{F} \leqq \dfrac{r}{t} \leqq 0.807\dfrac{E}{F}$

$$f_{cr0} = 0.267F + 0.4F\left[\frac{0.807 - \dfrac{r}{t}\dfrac{F}{E}}{0.738}\right]$$

(3.27)   for $0.807\dfrac{E}{F} \leqq \dfrac{r}{t}$ $f_{cr0} = \dfrac{1}{2.25}\sigma_{cr0,e}$

where:
r cylinder's inside radius of curvature (mm)
t cylinder's wall thickness (mm)
E Young's modulus (N/mm^2)
F basic value for determining the yield stresses (N/mm^2)
$\sigma_{cr0,e}$ axially symmetric elastic buckling stress (N/mm^2)

The value of $\sigma_{cr0,e}$ is given by the following equation.

(3.28) $\sigma_{cr0,e} = \dfrac{0.8}{\sqrt{3(1-v^2)}}E\dfrac{t}{r}$

where:
v Poisson's ratio

The value of $_c\overline{f_{cr}}$ is given by the following equations according to the value of r/t.

(3.29)   for $\dfrac{r}{t} \leqq 0.377\left(\dfrac{E}{F}\right)^{0.72}$ $_c\overline{f_{cr}} = \dfrac{F}{1.5}$

(3.30)   for $0.377\left(\dfrac{E}{F}\right)^{0.72} \leqq \dfrac{r}{t} \leqq 2.567\left(\dfrac{E}{F}\right)^{0.72}$

$$_c\overline{f_{cr}} = 0.267F + 0.4F\left[\frac{2.567 - \dfrac{r}{t}\left(\dfrac{F}{E}\right)^{0.72}}{2.190}\right]$$

(3.31)   for $2.567\left(\dfrac{E}{F}\right)^{0.72} \leqq \dfrac{r}{t}$ $\overline{_c f_{cr}} = \dfrac{1}{2.25}{_c\sigma_{cr,e}}$

where:

$_c\sigma_{cr,e}$ the elastic axially asymmetric buckling stress, based on lower bound formula proposed by NASA[3.1].

The value of $_c\sigma_{cr,e}$ is given by the following equation.

(3.32) $_c\sigma_{cr,e} = 0.6E\dfrac{t}{r}\left\{1 - 0.901\left[1 - exp\left[-\dfrac{1}{16}\left(\dfrac{r}{t}\right)^{1/2}\right]\right]\right\}$

(2)   Allowable bending stress $_b f_{cr}$ against the long–term overturning moment

(3.33)   for $0 \leqq \dfrac{\sigma_h}{F} \leqq 0.3$ $_b f_{cr} = \overline{_b f_{cr}} + \dfrac{0.7f_{cr0} - \overline{_b f_{cr}}}{0.3}\left(\dfrac{\sigma_h}{F}\right)$

(3.34)   for $\dfrac{\sigma_h}{F} \geqq 0.3$ $_b f_{cr} = f_{cr0}\left(1 - \dfrac{\sigma_h}{F}\right)$

where:

$\overline{_b f_{cr}}$ allowable bending stress against the long-time overturning moment exclusive of internal pressure (N/mm^2)

f_{cr0} value given by eq. (3.25), (3.26) or (3.27) (N/mm^2)

The value of $\overline{_b f_{cr}}$ is given by the following equations according to the value of r/t.

(3.35)   for $\dfrac{r}{t} \leqq 0.274\left(\dfrac{E}{F}\right)^{0.78}$ $\overline{_b f_{cr}} = \dfrac{F}{1.5}$

(3.36)   for $0.274\left(\dfrac{E}{F}\right)^{0.78} \leqq \dfrac{r}{t} \leqq 2.106\left(\dfrac{E}{F}\right)^{0.78}$

$$\overline{_b f_{cr}} = 0.267F + 0.4F\left[\dfrac{2.106 - \dfrac{r}{t}\left(\dfrac{F}{E}\right)^{0.78}}{1.832}\right]$$

(3.37)   for $2.106\left(\dfrac{E}{F}\right)^{0.78} \leqq \dfrac{r}{t}$ $\overline{_b f_{cr}} = \dfrac{1}{2.25}{_b\sigma_{cr,e}}$

where:

$_b\sigma_{cr,e}$ the elastic bending buckling stress, based on lower bound formula proposed by NASA[3.1].

The value of $_b\sigma_{cr,e}$ is given by the following equation

(3.38) $$_b\sigma_{cr,e} = 0.6E\frac{t}{r}\left\{1 - 0.731\left[1 - exp\left[-\frac{1}{16}\left(\frac{r}{t}\right)^{1/2}\right]\right]\right\}$$

(3) Allowable shear stress $_s f_{cr}$ against the long-time lateral force

(3.39) for $0 \leqq \dfrac{\sigma_h}{F} \leqq 0.3$ $_s f_{cr} = \overline{_s f_{cr}} + \dfrac{\dfrac{F}{1.5\sqrt{3}} - \overline{_s f_{cr}}}{0.3}\left(\dfrac{\sigma_h}{F}\right)$

(3.40) for $\dfrac{\sigma_h}{F} \geqq 0.3$ $_s f_{cr} = \dfrac{F}{1.5\sqrt{3}}$

where:

$\overline{_s f_{cr}}$ allowable shear stress against the long-time lateral load exclusive of internal pressure (N/mm^2)

The value of $\overline{_s f_{cr}}$ is given by the following equations according to the value of r/t.

(3.41) for $\dfrac{r}{t} \leqq \dfrac{0.204\left(\dfrac{E}{F}\right)^{0.81}}{\left(\dfrac{l}{r}\right)^{0.4}}$ $\overline{_s f_{cr}} = \dfrac{F}{1.5\sqrt{3}}$

(3.42) for $\dfrac{0.204\left(\dfrac{E}{F}\right)^{0.81}}{\left(\dfrac{l}{r}\right)^{0.4}} \leqq \dfrac{r}{t} \leqq \dfrac{1.446\left(\dfrac{E}{F}\right)^{0.81}}{\left(\dfrac{l}{r}\right)^{0.4}}$

$$\overline{_s f_{cr}} = \frac{0.267F}{\sqrt{3}} + \frac{0.4F}{\sqrt{3}}\left[\frac{1.446 - \frac{r}{t}\left(\frac{l}{r}\right)^{0.4}\left(\frac{F}{E}\right)^{0.81}}{1.242}\right]$$

(3.43) for $\dfrac{1.446\left(\dfrac{E}{F}\right)^{0.81}}{\left(\dfrac{l}{r}\right)^{0.4}} \leqq \dfrac{r}{t}$ $\overline{_s f_{cr}} = \dfrac{1}{2.25}\,_s\sigma_{cr,e}$

where:

l shear buckling wave length in the axial direction (mm)

$_s\sigma_{cr,e}$ the elastic shear buckling stress, based on 95 percent probability formula introduced by multiplying the Donnel's torsional buckling formula by 0.8

The value of $_s\sigma_{cr,e}$ is given by the following equation.

$$(3.44) \qquad _s\sigma_{cr,e} = 0.8\frac{4.83E}{\left\{\dfrac{l}{r}\left(\dfrac{r}{t}\right)^{1/2}\right\}^2}\frac{t}{r}\left[1+0.0239\left\{\dfrac{l}{r}\left(\dfrac{r}{t}\right)^{1/2}\right\}^3\right]^{1/2}$$

3.7.3 Allowable Stresses against the Short-Term Load

The allowable stresses against the short-term load exclusive of the seismic load should be the values given by multiplying the allowable stresses against the long-term load shown in 3.7.2 by 1.5.

3.7.4 Allowable Stress against the Seismic Load

The allowable axial compressive, bending and shear stresses against the seismic load are given by the following three terms (1), (2) and (3), respectively, which are also depend on both σ_h/F and r/t, and which should be applied to the ultimate strength design.

(1) Allowable axial compressive stress against the seismic load

$$(3.45) \qquad \text{for } 0\leqq\frac{\sigma_h}{F}\leqq0.3 \qquad _cf_{cr}=\overline{_cf_{cr}}+\frac{0.7f_{crs}-\overline{_cf_{cr}}}{0.3}\left(\frac{\sigma_h}{F}\right)$$

$$(3.46) \qquad \text{for } \frac{\sigma_h}{F}\geqq0.3 \qquad _cf_{cr}=f_{crs}\left(1-\frac{\sigma_h}{F}\right)$$

where:

$\overline{_cf_{cr}}$ allowable seismic axial compressive stress exclusive of internal pressure (N/mm^2)

f_{crs} basic value for determining the strength of elephant-foot bulge (N/mm^2)

The value of f_{crs} is given by the following equations according to the value of r/t.

$$(3.47) \qquad \text{for } \frac{r}{t}\leqq0.069\frac{E}{F} \qquad f_{crs}=F$$

$$(3.48) \qquad \text{for } 0.069\frac{E}{F}\leqq\frac{r}{t}\leqq0.807\frac{E}{F}$$

$$f_{crs}=0.6F+0.4F\left[\frac{0.807-\dfrac{r}{t}\dfrac{F}{E}}{0.738}\right]$$

$$(3.49) \qquad \text{for } 0.807\frac{E}{F}\leqq\frac{r}{t} \qquad f_{crs}=\sigma_{cr0,e}$$

where:

$\sigma_{cr0,e}$ value given by eq. (3.28)

The value of $_c\overline{f_{cr}}$ is given by the following equations according to the value of r/t.

(3.50)　　　　for $\dfrac{r}{t} \leqq 0.377 \left(\dfrac{E}{F}\right)^{0.72}$　　$_c\overline{f_{cr}} = F$

(3.51)　　　　for $0.377 \left(\dfrac{E}{F}\right)^{0.72} \leqq \dfrac{r}{t} \leqq 2.567 \left(\dfrac{E}{F}\right)^{0.72}$

$$_c\overline{f_{cr}} = 0.6F + 0.4F \left[\dfrac{2.567 - \dfrac{r}{t}\left(\dfrac{F}{E}\right)^{0.72}}{2.190}\right]$$

(3.52)　　　　for $2.567 \left(\dfrac{E}{F}\right)^{0.72} \leqq \dfrac{r}{t}$　　$_c\overline{f_{cr}} = {_c\sigma_{cr,e}}$

　　　　　　where:

　　　　　　$_c\sigma_{cr,e}$　　value given by eq. (3.32)

(2)　Allowable bending stress against the seismic overturning moment

(3.53)　　　　for $0 \leqq \dfrac{\sigma_h}{F} \leqq 0.3$　　$_bf_{cr} = {_b\overline{f_{cr}}} + \dfrac{0.7f_{crs} - {_b\overline{f_{cr}}}}{0.3}\left(\dfrac{\sigma_h}{F}\right)$

(3.54)　　　　for $\dfrac{\sigma_h}{F} \geqq 0.3$　　$_bf_{cr} = f_{crs}\left(1 - \dfrac{\sigma_h}{F}\right)$

　　　　　　where:

　　　　　　$_b\overline{f_{cr}}$　　allowable seismic bending stress exclusive of internal pressure (N/mm^2)

　　　　　　f_{crs}　　value given by the eq. (3.47), (3.48) or (3.49). (N/mm^2)

The value of $_b\overline{f_{cr}}$ is given by the following equations according to the value of r/t.

(3.55)　　　　for $\dfrac{r}{t} \leqq 0.274 \left(\dfrac{E}{F}\right)^{0.78}$　　$_b\overline{f_{cr}} = F$

(3.56)　　　　for $0.274 \left(\dfrac{E}{F}\right)^{0.78} \leqq \dfrac{r}{t} \leqq 2.106 \left(\dfrac{E}{F}\right)^{0.78}$

$$_b\overline{f_{cr}} = 0.6F + 0.4F \left[\dfrac{2.106 - \dfrac{r}{t}\left(\dfrac{F}{E}\right)^{0.78}}{1.832}\right]$$

(3.57)　　　　for $2.106 \left(\dfrac{E}{F}\right)^{0.78} \leqq \dfrac{r}{t}$　　$_b\overline{f_{cr}} = {_b\sigma_{cr,e}}$

　　　　　　where:

　　　　　　$_b\sigma_{cr,e}$　　value given by eq. (3.38)

(3) Allowable shear stress against the seismic lateral force

(3.58) $\qquad$ for $0 \leqq \dfrac{\sigma_h}{F} \leqq 0.3$ $\qquad$ $_s f_{cr} = {}_s\overline{f_{cr}} + \dfrac{\dfrac{F}{\sqrt{3}} - {}_s\overline{f_{cr}}}{0.3}\left(\dfrac{\sigma_h}{F}\right)$

(3.59) $\qquad$ for $\dfrac{\sigma_h}{F} \geqq 0.3$ $\qquad$ $_s f_{cr} = \dfrac{F}{\sqrt{3}}$

where:

$_s\overline{f_{cr}}$ $\qquad$ allowable seismic shear stress exclusive of internal pressure (N/mm^2)

The value of $_s\overline{f_{cr}}$ is given by the following equations according to the value of r/t.

(3.60) $\qquad$ for $\dfrac{r}{t} \leqq \dfrac{0.204\left(\dfrac{E}{F}\right)^{0.81}}{\left(\dfrac{l}{r}\right)^{0.4}}$ $\qquad$ $_s\overline{f_{cr}} = \dfrac{F}{\sqrt{3}}$

(3.61) $\qquad$ For $\dfrac{0.204\left(\dfrac{E}{F}\right)^{0.81}}{\left(\dfrac{l}{r}\right)^{0.4}} \leqq \dfrac{r}{t} \leqq \dfrac{1.446\left(\dfrac{E}{F}\right)^{0.81}}{\left(\dfrac{l}{r}\right)^{0.4}}$

$$_s\overline{f_{cr}} = \dfrac{0.6F}{\sqrt{3}} + \dfrac{0.4F}{\sqrt{3}}\left[\dfrac{1.446 - \dfrac{r}{t}\left(\dfrac{l}{r}\right)^{0.4}\left(\dfrac{F}{E}\right)^{0.81}}{1.242}\right]$$

(3.62) $\qquad$ for $\dfrac{1.446\left(\dfrac{E}{F}\right)^{0.81}}{\left(\dfrac{l}{r}\right)^{0.4}} \leqq \dfrac{r}{t}$ $\qquad$ $_s\overline{f_{cr}} = {}_s\sigma_{cr,e}$

where:

l $\qquad$ shear buckling wave length in the axial direction (mm)

$_s\sigma_{cr,e}$ $\qquad$ value given by eq. (3.44)

3.7.5 $\qquad$ Remarks on the Evaluation of the Design Shear Stress

(1) The design shear stress can be evaluated by the mean value within the range of the shear bucking wave length in the axial direction.

(2) The cylinder's inside radius of curvature r and wall thickness t can be defined by their mean values within the range of the shear bucking wave length in the axial direction.

(3) In the design of silos containing granular materials, the allowable shear stress can be calculated by setting $l/r = 1$ and $\sigma_h = 0$.

Commentary:

1. Empirical formula for buckling stresses

1.1 Case without internal pressure

The lower bound values of elastic buckling stresses which apply to cylindrical shells without internal pressures are given by the following empirical formula.

(a)   elastic axial compressive buckling stresses (empirical formula by NASA[3.1])

$$(3.7.1) \qquad {}_c\sigma_{cr,e} = 0.6E\left\{1 - 0.901\left(1 - e^{-\frac{1}{16}\sqrt{\frac{r}{t}}}\right)\right\}\Big/\left(\frac{r}{t}\right)$$

(b)   elastic flexural buckling stresses (empirical formula by NASA[3.1])

$$(3.7.2) \qquad {}_b\sigma_{cr,e} = 0.6E\left\{1 - 0.731\left(1 - e^{-\frac{1}{16}\sqrt{\frac{r}{t}}}\right)\right\}\Big/\left(\frac{r}{t}\right)$$

(c)   elastic shear buckling stresses [3.2] [3.3]

$$(3.7.3) \qquad \tau_{cr,e} = \frac{4.83E \times 0.8}{\left(\frac{l}{r}\sqrt{\frac{r}{t}}\right)^2}\sqrt{1 + 0.0239\left(\frac{l}{r}\sqrt{\frac{r}{t}}\right)^3}\Big/\left(\frac{r}{t}\right)$$

Eq.(3.7.3) is given by the torsional buckling stress derived by Donnell multiplied by the reduction factor of 0.8. These formula correspond to the 95 % reliability limit of experimental data.

Based on the elastic buckling stresses, the nonlinearity of material is introduced. In the region where the elastic buckling stresses exceeds 60 % of the yield point stress of material (σ_y or τ_y), the buckling mode is identified to be nonlinear. In Fig.3.7.1, the relationship between the buckling stress and the r/t ratio (the buckling curve) is shown. The buckling curve in the nonlinear range is modified as shown in Fig.3.7.1. $(r/t)_I$ is the (r/t) ratio at which the elastic buckling stress $\sigma_{cr,e}$ reaches 60 % of the yield stress. $(r/t)_{II}$ denotes the (r/t) ratio at which the buckling stress exceeds the yield point stress. In the region of (r/t) ratios less than $(r/t)_{II}$, the buckling stresses are assumed to be equal to the yield point stress. In the region of (r/t) ratios between $(r/t)_{II}$ and $(r/t)_I$, the buckling stresses are assumed to be on a line as shown in the figure. $(r/t)_{II}$ was determined on the condition that the elastic buckling stress at $(r/t)_{II}$ reaches 6.5 times to 7.5 times as large as the yield point stress.
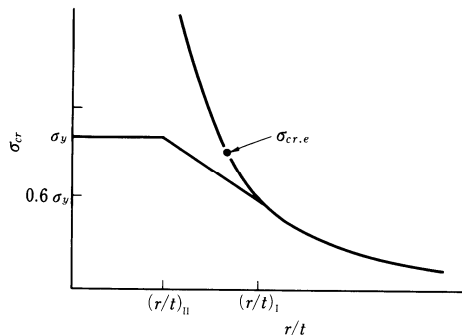

Fig.3.7.1   Buckling curve

(r/t)$_I$ and (r/t)$_{II}$ are determined according to the stress conditions as shown in Table 3.7.1. The occurrence of buckling under combined stresses can be checked by the following criteria

$$(3.7.4) \qquad \left.\begin{array}{c} \dfrac{\sigma_c}{_c\sigma_{cr}} + \dfrac{\sigma_b}{_b\sigma_{cr}} = 1 \\ or \\ \dfrac{\tau}{\tau_{cr}} = 1 \end{array}\right\}$$

Notations:

σ_c *mean axial compressive stress*

σ_b *compressive stress due to bending moment*

τ *shear stress*

Eq.(3.7.4) implies that the axial buckling and the flexural buckling are interactive, while the shear buckling is independent of any other buckling modes. The experimental data are shown in Fig.3.7.2 . Figure (a) shows the data obtained by Lundquist on cylindrical shells made of duralumin all of which buckled in the elastic range[3.4]. Figure (b) indicates the test results on steel cylindrical shells[3.3]. The ordinate indicates $\sigma_c/_c\sigma_{cr} + \sigma_b/_b\sigma_{cr}$ and the abscissa indicates τ/τ_{cr} . The buckling criteria which correspond to Eq.(3.7.4) is shown by the solid lines. Although a few data can not be covered by Eq.(3.7.4), Eq.(3.7.4) should be applied as a buckling criterion under the seismic loading considering that the estimate of D_s-values are made conservatively. For short-term loadings other than the seismic loading, the safety factor of 1.5 is introduced in the estimate of the elastic buckling stresses to meet the scatter of the experimental data.

Table 3.7.1   Limit r/t ratios

Stress Condition	$(r/t)_{II}$	$(r/t)_{I}$
Axial Compression	$0.377\left(\dfrac{E}{F}\right)^{0.72}$	$2.567\left(\dfrac{E}{F}\right)^{0.72}$
Bending	$0.274\left(\dfrac{E}{F}\right)^{0.78}$	$2.106\left(\dfrac{E}{F}\right)^{0.78}$
Shearing	$\dfrac{0.204\left(\dfrac{E}{F}\right)^{0.81}}{\left(\dfrac{l}{r}\right)^{0.4}}$	$\dfrac{1.446\left(\dfrac{E}{F}\right)^{0.81}}{\left(\dfrac{l}{r}\right)^{0.4}}$

| (a) Duralumin cylindrical shell | (b) Steel cylindrical shell |
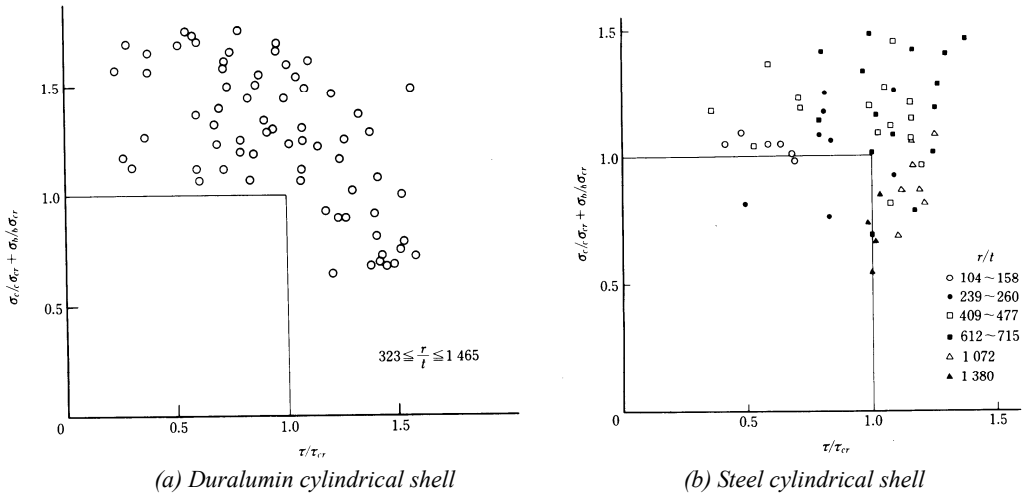
Fig.3.7.2   Comparison between test results and predictions

1.2   Case with internal pressure

The effects of the internal pressure on the buckling of cylindrical shells are twofold :
· The internal pressure constrains the occurrence of buckling.
· The internal pressure accelerates the yielding of shell walls and causes the elephant foot bulge.
The effect of the internal pressure is represented by the ratio of the tensile hoop stress, σ_h, to the yield point stress, σ_y, (σ_h / σ_y) [3.5].

Referring to experimental data, it was made clear that the buckling stresses under axial compression and bending moment can be expressed by the following empirical formula[3.6] [3.7]:

(3.7.5)

$$\left.\begin{array}{l} \text{for } \sigma_h / \sigma_y \leq 0.3, \\[2mm] \sigma_{cr} = \overline{\sigma}_{cr} + \dfrac{(0.7\sigma_{cr0} - \overline{\sigma}_{cr})(\sigma_h / \sigma_y)}{0.3} \\[4mm] \text{for } \sigma_h / \sigma_y > 0.3, \\[2mm] \sigma_{cr} = \sigma_{cr0}\left(1 - \dfrac{\sigma_h}{\sigma_y}\right) \end{array}\right\}$$

Notations:

$\overline{\sigma}_{cr}$ buckling stress in case without internal pressure

σ_{cr0} compressive buckling stress in axi-symmetric mode
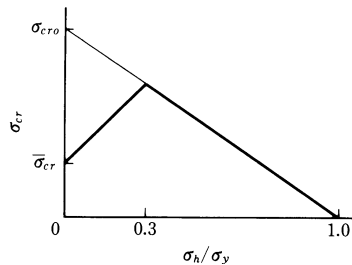
Fig.3.7.3   Influence of internal pressure on buckling stress

Eq.(3.7.5) is shown in Fig.(3.7.3). In the region below $\sigma_h / \sigma_y = 0.3$, the buckling occurs in inextensional mode, whereas beyond $\sigma_h / \sigma_y = 0.3$, the buckling occurs in elephant foot bulge mode. σ_{cr0} for cylinders which buckle elastically was found to be expressed by

$$(3.7.6) \qquad \sigma_{cr0,e} = \frac{0.8E}{\sqrt{3(1-\nu^2)}}\left(\frac{t}{r}\right)$$

Notations:

ν *Poisson's ratio*

Eq.(3.7.6) is the theoretical buckling stress of axially compressed cylinders multiplied by a empirical reduction factor of 0.8. The buckling stress in the inelastic range, σ_{cr0}, can be related to $\sigma_{cr0,e}$, similarly to $_c\sigma_{cr,e}$ and $_b\sigma_{cr,e}$ as follows:

for $\dfrac{r}{t} \leq 0.069\left(\dfrac{E}{F}\right)$

$(3.7.7) \qquad \sigma_{cr0} = \sigma_y$

for $0.807\left(\dfrac{E}{F}\right) \leq \dfrac{r}{t}$

$(3.7.8) \qquad \sigma_{cr0} = \sigma_{cr0,e}$

for $0.069\left(\dfrac{E}{F}\right) < \dfrac{r}{t} < 0.807\left(\dfrac{E}{F}\right)$

σ_{cr0} *is linearly interpolated between the values given by Eq.(3.7.7) and Eq.(3.7.8)*

Fig.3.7.4   Comparison between test results and predictions for axial loading

The applicability of Eq.(3.7.5) is demonstrated in the following:

i) Axially compressed cylinders experimental data and the results of analysis are shown in Fig.3.7.4, together with Eq.(3.7.5) [3.7]. The abscissa indicates the hoop stress ratio, σ_h/σ_y, and the ordinate indicate the ratio of the buckling stress to the classical theoretical buckling stress, σ_{c1}.
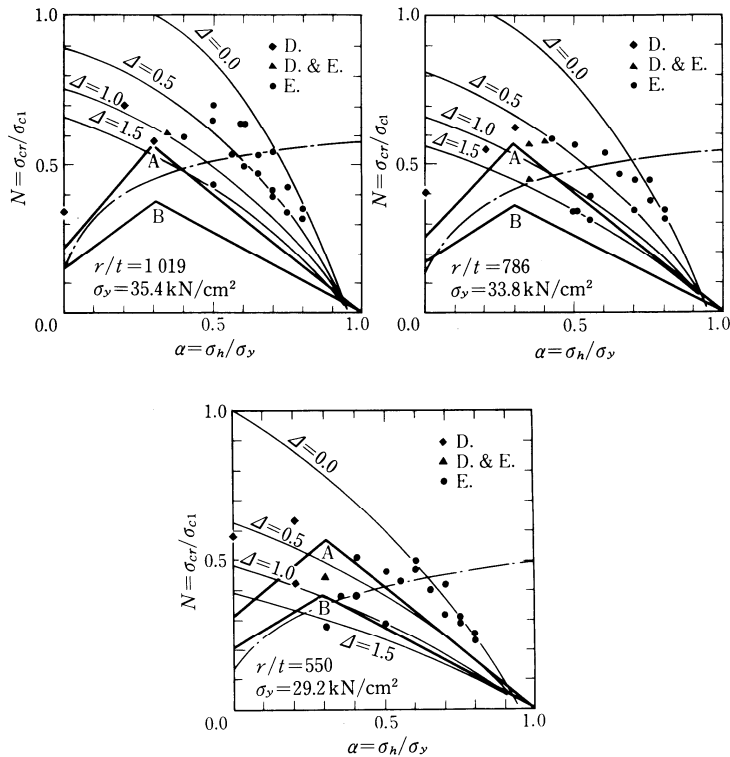
Shell walls were perfectly clamped at both ends. Test data are indicated by the symbols of ◆ that indicates the buckling under diamond pattern, ● that indicates the buckling under elephant foot bulge mode and ▲ that is the case of simultaneous occurrence of diamond pattern and elephant foot bulge mode.

Curves with a specific value of Δ are theoretical values for elephant foot bulge mode. Δ is the initial imperfection divided by the thickness of wall. The chained line going up right-handedly is the theoretical curve of diamond pattern of buckling derived by Almroth[3.8]. The polygonal line A is the design curve for seismic loading given by Eq.(3.7.5). The polygonal line B is the design curve for loading other than the seismic loading.

ii) Cylinders subjected to shear and bending[3.6]

Referring to experimental results on cylindrical shells subjected to shear and bending, it was made clear that the shear buckling pattern becomes easily localized with a faint presence of the internal pressure.

In Fig.3.7.5, a shear buckling pattern under $\sigma_h/\sigma_y = 0.05$ is shown. Thus, it is understood that the internal pressure makes the substantial aspect ratio, ℓ/r in Eq.(3.7.3), reduced drastically. At $\sigma_h/\sigma_y = 0.3$, the shear buckling disappears.

Considering these facts, the shear buckling stress under the internal pressure can be summarized as follows:

(3.7.9) $\quad$ *for $\sigma_h/\sigma_y \leq 0.3$, $\tau_{cr} = \bar{\tau}_{cr} + \dfrac{\left(\tau_y - \bar{\tau}_{cr}\right)\left(\sigma_h/\sigma_y\right)}{0.3}$*

$\qquad\qquad$ *for $\sigma_h/\sigma_y > 0.3$, $\tau_{cr} = \tau_y$*

$\qquad$ *Notations:*

$\qquad$ τ_y $\qquad\quad$ *shear yield-point stress*
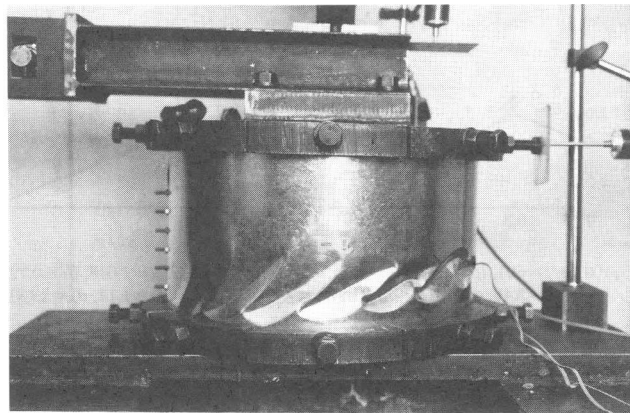
Fig.3.7.5　　Buckling wave pattern of shear buckling
$\sigma_h/\sigma_y = 0.05,\ r/t = 477,\ \ell/r = 1.0,\ \sigma_y = 32.3 kN/cm^2$

$r/t = 477.2$
$l/r = 2.0$
$h/r = 2.56$
$\sigma_y = 33.8\,\mathrm{kN/cm^2}$

$r/t = 477.2$
$l/r = 1.0$
$h/r = 1.57$
$\sigma_y = 33.8\,\mathrm{kN/cm^2}$
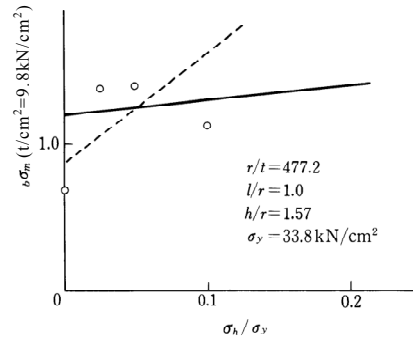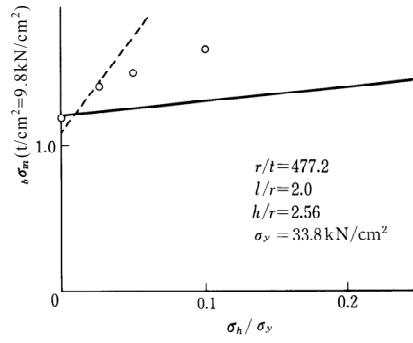
Fig.3.7.6 Influence of internal pressure on buckling
(in case of small internal pressure)

(a) $r/t = 340$, $l/r = 4.65$
$h/r = 5.88$, $\sigma_y = 33.8\,\mathrm{kN/cm^2}$

(b) $r/t = 456$, $l/r = 1.39$
$h/r = 1.95$, $\sigma_y = 26.6\,\mathrm{kN/cm^2}$

(c) $r/t = 691$, $l/r = 1.39$
$h/r = 1.95$, $\sigma_y = 31.2\,\mathrm{kN/cm^2}$

(d) $r/t = 691$, $l/r = 2.89$
$h/r = 3.46$, $\sigma_y = 31.4 \sim 37.2\,\mathrm{kN/cm^2}$

(e) $r/t = 1\,018$, $l/r = 0.72$
$h/r = 1.14$, $\sigma_y = 33.8\,\mathrm{kN/cm^2}$

Fig.3.7.7 Buckling strength under combined internal pressure and flexural-shear loading

In Fig.3.7.6, test results in the range of small values of σ_h / σ_y are compared with the estimate made by Eq.(3.7.5) and Eq.(3.7.9). The ordinate indicates the bending stress at the lower edge of cylinder. Therefore, the shear buckling stress is converted to the equivalent bending stress by the following equation.

$$(3.7.10) \qquad \sigma_{cr} = \tau_{cr} \frac{h}{r}$$

Notations:

h   distance between the lower edge of shell and the point where horizontal load is applied

Eq.(3.7.5) is shown by solid lines and Eq.(3.7.9) is shown by broken lines. As shown in the figure, cylindrical shells subjected to internal pressures are hardly influenced by shear buckling.
In Fig.3.7.7, test data under wider range of parameters are shown, predictions made by Eq.(3.7.5) and Eq.(3.7.9) are shown by solid lines. The point shown by ○ indicates the inextentional mode of buckling, and the point shown by ● indicates the elephant foot bulge mode of buckling.

2.   Safety factor on buckling stresses

Safety factors for various loading conditions are set up as shown in Table 3.7.2. The level of safety factor depends on the probability of occurrence of the specified design loading.

Table 3.7.2 Safety factor for buckling

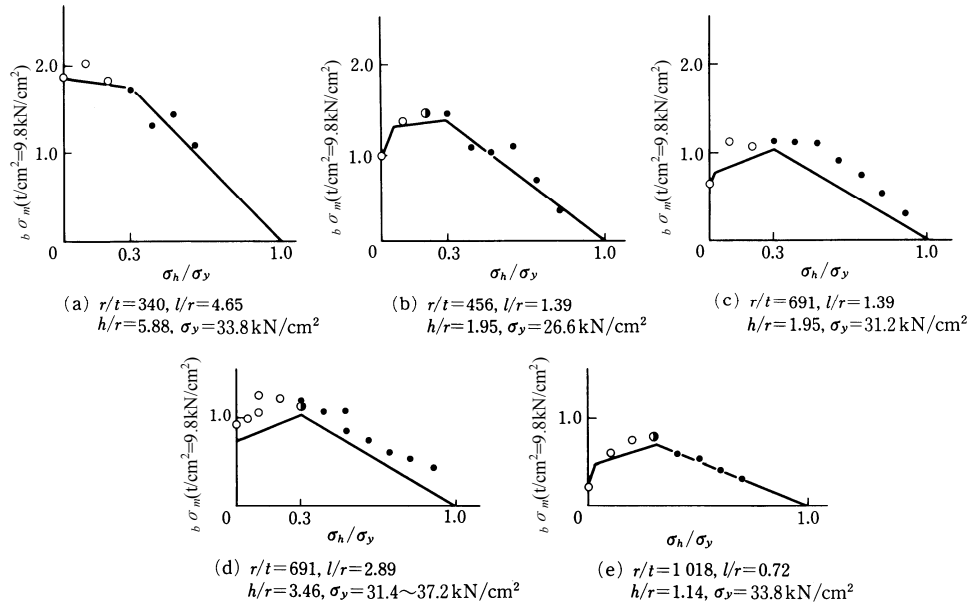| Loading condition	Safety factor for buckling		
	$\dfrac{r}{t} < \left(\dfrac{r}{t}\right)_{\mathrm{II}}$	$\left(\dfrac{r}{t}\right)_{\mathrm{II}} < \dfrac{r}{t} < \left(\dfrac{r}{t}\right)_{\mathrm{I}}$	$\left(\dfrac{r}{t}\right)_{\mathrm{I}} < \dfrac{r}{t}$
Long term	1.5	Linear interpolation	2.25
Short term (except earthquake)	1.0	Linear interpolation	1.5
Earthquake	1.0		

3.   Supplementary comment on shear buckling

When geometrical parameters and structural parameters change within a range of shear buckling length, the mean values of them can be taken according to the usual practice of engineering.
Generally, the buckling strengths of silos containing granular contents are influenced by the internal pressure and stiffness associated with the properties of contents, and the shear buckling length, ℓ / r is considered to be less than unity. Still, the exact estimate of internal pressure under seismic loading is difficult. As a tentative measure of compromise, the constraining effect of internal pressure is to be disregarded on the condition that ℓ / r is fixed to be unity.

4.   Deformation characteristics after buckling

The general load-deformation curve of cylindrical shells subjected to the monotonic horizontal force is schematically shown in Fig.3.7.8. The ordinate indicates the maximum bending stress, $_b\sigma$.
The abscissa indicates the mean inclination angle, θ. In the post-buckling range, the deformation develops with a gradual decrease of resistant force, finally approaching a horizontal asymptote.
The level of the asymptote depends on the level of the axial stress, σ_0. When $\sigma_0 / {_c\sigma_{cr}}$ becomes larger than 0.2, the asymptote disappears, and the resistant force decreases monotonously as the deformation increases.
When $\sigma_0 / {_c\sigma_{cr}}$ remains less than 0.2, cylindrical shells exhibit a stable energy absorption capacity

[3.3] [3.6] [3.10] [3.11].
The hysteretic behavior of cylindrical shells under repeated horizontal forces is shown in Fig.(3.7.9).
The basic rule which governs the hysteretic behavior is described as follows.

- *Definitions to describe the hysteretic rule:*
  a)   *The loading path is defined by $_b\sigma d\theta > 0$.*
  b)   *The unloading path is defined by $_b\sigma d\theta < 0$.*
- *The $_b\sigma - \theta$ relationship under the monotonic loading is defined to be the skeleton curve.*
- *The unloading point is defined to be the point which rests on the skeleton curve and terminates the loading path.*
- *The initial unloading point is defined to be the point at which the buckling starts.*
- *The intermediate unloading point is defined to be the point which does not rest on the skeleton curve and terminates the loading path.*

On the assumption that the loading which reaches the initial loading point has been already made in both positive and negative directions, the hysteretic rule is described as follows.

a)   *The loading path points the previous unloading point in the same loading domain. After reaching the previous unloading point, the loading path traces the skeleton curve.*
b)   *The unloading path from the unloading point points the initial unloading point in the opposite side of loading domain. The unloading path from the intermediate unloading point has a slope same as that of the unloading path from the previous unloading point in the same loading domain.*
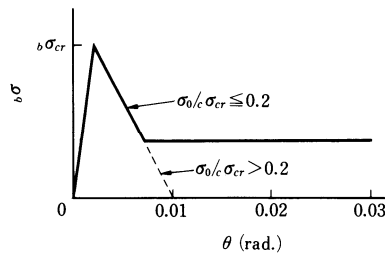*These hysteretic rule has been ascertained to apply even for the case of $\sigma_h / \sigma_y \neq 0$.*

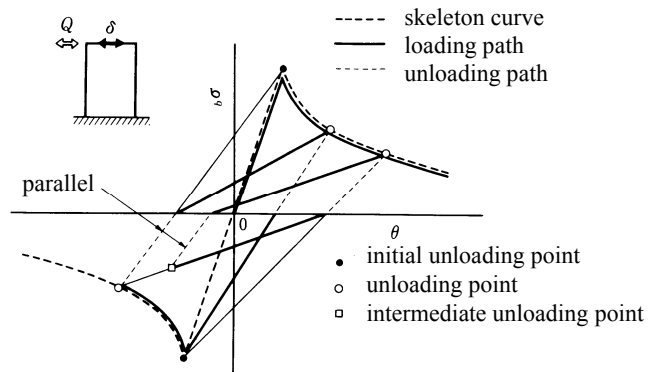*Fig.3.7.8   Load-deformation relationship under monotonic loading*

Fig.3.7.9 Hysteretic rule

5. D_η -values for cylindrical structures

   D_η -values for structures with short natural periods which has been obtained analytically using the load-deformation characteristics shown in Fig.3.7.9 are shown in Fig.3.7.10[3.12].

   Essential points in the analysis are summarized as follows.

5.1 D_η -values in case that uplift of the bottom of the structure is not allowed by restraint of an anchoring system:

1)   Assuming that the structure is one-mass system and equating the structural energy absorption capacity to the energy input exerted by the earthquake, the maximum deformation of the structure is obtained.
2)   The energy input to the structure is obtained by considering the elongation of the vibrational period of structure.
3)   The D_η -values is defined by

   (3.7.11)
   $$D_\eta = \frac{\text{the level of earthquake which causes the buckling deformation}, \delta_{cr}}{\text{the level of earthquake which causes the maximum deformation of } (1+\mu)\delta_{cr}}$$
   Notations:
   $\mu = \dfrac{\delta_m}{\delta_{cr}} - 1$ nondimensionalized maximum deformation

   δ_{cr} buckling deformation

4)   The assumed load-deformation curve in monotonic loading is one that exhibits a conspicuous degrading in strength in the post-buckling range as shown in Fig.3.7.10. q in the figure denotes the nondimensionalized level of the stationary strength in the post buckling range.
   When we select the value of D_η to be 0.5, the pairs of values of (q, μ) are read from Fig.3.7.10 as follows : (0.6, 1.0), (0.5, 2.0), and (0.4, 4.0). See Table 3.7.3.
   These $q - \mu$ relationships which corresponds to $D_\eta = 0.5$ are compared with the nondimentionalized load-deformation curves obtained experimentally in Fig.3.7.11 and Fig.3.7.12. The $q - \mu$ relations are written as white circles in these figures. The experimental curves lie almost above the $q - \mu$ relations for $D_\eta = 0.5$ (see Table 3.7.3). It implies that the actual structures are more abundant in energy absorption capacity than the analytical model equipped with the load-deformation characteristics shown in Fig.3.7.10.
   Thus, to apply the value of 0.5 for D_η -values of cylindrical structures influenced by buckling seems reasonable. When the axial compressive stress becomes large, however, the D_η -values should be kept larger than 0.5 since the strength decreases drastically in the post buckling range.
   Consequently, the value of D_η is determined as follows:
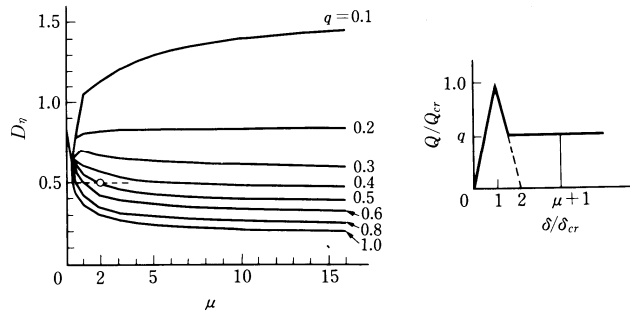
Fig.3.7.10 D_η -values

for $\sigma_0/{}_c\sigma_{cr} \leqq 0.2$,

(3.7.12) $D_\eta = 0.5$

for $\sigma_0/{}_c\sigma_{cr} > 0.2$,

(3.7.13) $D_\eta = 0.7$

Table 3.7.3 $q(=Q/Q_{cr})$ and $\mu(=[\delta - \delta_{cr}]/\delta_{cr})$ relationship (in case of $\delta_0/\delta_{cr} \leqq 0.2$, $D_\eta = 0.5$)

q	μ
0.6	1.0
0.5	2.0
0.4	4.0

(a) $104 \leqq r/t \leqq 239$
$1.10 \leqq l/r \leqq 8.56$

(b) $r/t = 477$
$1.42 \leqq l/r \leqq 5.2$

(c) $r/t = 715$
$1.02 \leqq l/r \leqq 4.28$

(d) $r/t = 1\,072$
$0.88 \leqq l/r \leqq 2.87$
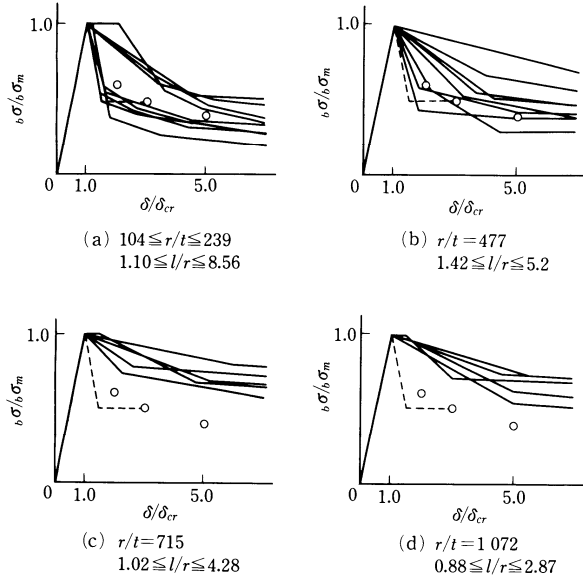
Fig.3.7.11   Load-deformation relationship
which corresponds to $D_\eta = 0.5$

$(\sigma_h/\sigma_y = 0)$
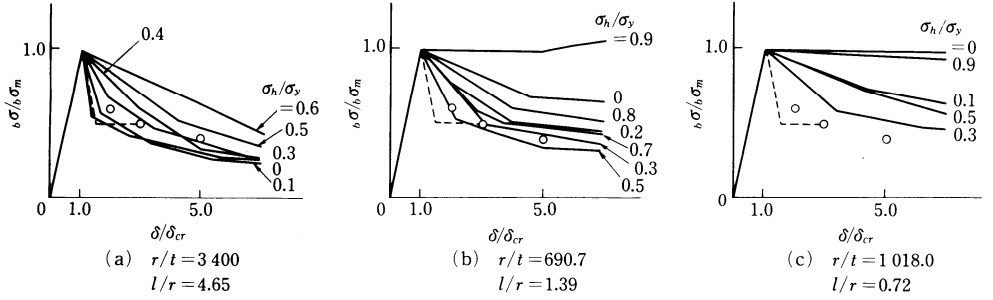
Fig.3.7.12 Load-deformation relationship
which corresponds to $D_\eta = 0.5$
$(\sigma_h / \sigma_y \neq 0)$

5.2 D_η -values in case that uplift of the bottom of the structure is allowed without an anchoring system:

The D_η -value defined in Eq. (3.6.15) of sec. 3.6 should be expressed as follows:

(3.7.14) $D_\eta = \dfrac{1}{\sqrt{1 + \left(\dfrac{W_p}{W_e}\right)}}$

The cumulative plastic strain energy W_p induced by buckling of the shell plate is as indicated in Eq. (3.6.7). However, the elastic vibration energy W_e should be of the strain energy of the cylindrical shell added by the strain energy due to the uplift of the bottom of the shell. In case that uplift of the bottom of the structure is not allowed, replacing D_η and W_e with $D_{\eta f}$ and W_{ef}, respectively, Eq. (3.7.14) should be expressed as follows:

(3.7.15) $D_{\eta f} = \dfrac{1}{\sqrt{1 + \left(\dfrac{W_p}{W_{ef}}\right)}}$

In case that uplift of the bottom of the structure is considered, Eq. (3.6.8) should be expressed as follows:

(3.7.16) $W_e = \dfrac{Q_y \delta_y}{2}$

Whilst in case that uplift of the bottom of the structure is not considered, W_{ef} should be expressed as follows:

(3.7.17) $W_{ef} = \dfrac{Q_y \delta_y}{2}\left(\dfrac{T_f}{T_e}\right)^2$

From (3.7.14) to (3.7.17) D_η value, in case that uplift of the bottom of the structure is allowed, should be given in Eq. (3.7.18).

(3.7.18) $D_\eta = \dfrac{1}{\left[1 + \left(\dfrac{1}{D_{\eta f}{}^2} - 1\right)\left(\dfrac{T_f}{T_e}\right)^2\right]^{1/2}}$

$D_{\eta f}, W_{ef}$ D_{η}, W_e *in case that uplift of the bottom of the structure is not allowed.*

T_f *natural period in case that uplift of the bottom of the structure is not allowed.*

T_e *natural period in case that uplift of the bottom of the structure is considered.*

In general as $T_e > T_f$, $D_{\eta} > D_{\eta f}$.

6. *B-value for cylindrical structures*

In thin steel cylindrical structures, the buckling starts when the maximum stress reaches the buckling stress, σ_{cr} .

Therefore, the stress redistribution due to yielding is hardly considered. Thus, the value of B for steel cylindrical shells should be set as follow:.
for $r/t \geqq (r/t)_{II}$,

(3.7.19)   *B=1.0*

Notations:

$(r/t)_{II}$ *: refer to Table 3.7.1*

3.8 Earth Pressures

3.8.1 Earth Pressure in Normal Condition

Earth pressure in normal condition should be determined according to "Recommendations for Design of Building Foundations, 2001 - Architectural Institute of Japan ".

Commentary:

Earth pressures in the normal condition for sand and clay shall be calculated in accordance with the "Recommendations for design of building foundations (2001)" compiled by the Architectural Institute of Japan (AIJ).

3.8.2 Earth Pressure during Earthquakes

Earth pressures which act on the underground walls of tanks during earthquakes may be considered to be either active or passive and should be calculated in accordance with equations (3.63) and (3.64) for active earth pressures, and (3.65) and (3.66) for passive earth pressures.

(a) Active earth pressure

(3.63) $P_{EA} = (1 - K_V)(\gamma z + \dfrac{\omega}{cos\,\theta}) K_{EA}$

(3.64) $K_{EA} = \dfrac{cos^2(\phi - \theta)}{cos\,\theta\,cos(\delta + \theta)\left[1 + \left\{\dfrac{sin(\phi + \delta)\,sin(\phi - \theta)}{cos(\delta + \theta)}\right\}^{1/2}\right]^2}$

(b)   Passive earth pressure

(3.65) $$P_{EP} = (1 - K_V)(\gamma z + \frac{\omega}{cos\,\theta})K_{EP}$$

(3.66) $$K_{EP} = \frac{cos^2(\phi - \theta)}{cos\,\theta\,cos(\delta + \theta)\left[1 - \left\{\frac{sin(\phi + \delta)\,sin(\phi - \theta)}{cos(\delta + \theta)}\right\}^{1/2}\right]^2}$$

where:

P_{EA} horizontal active earth pressure during earthquakes acting on vertical wall at depth z (N/mm^2) - refer also to Figure 3.1,

K_V vertical underground seismic intensity given in chapter 3.6.2.2,

γ unit weight of soil (N/mm^3),

z depth from the ground surface (mm),

ω load pressure (N/mm^2), - refer also to Figure 3.1,

θ $tan^{-1}K$,

K combined seismic coefficient, see equation (3.67)

(3.67) $$K = \frac{K_H}{1 - K_V}$$

K_H horizontal underground seismic intensity given in chapter 3.6.2.2,

K_{EA} coefficient of active earth pressure during earthquakes,

ϕ internal friction angle of soil,

δ wall friction angle,

P_{EP} horizontal passive earth pressure during earthquakes acting on vertical wall at depth z (N/mm^2), - refer also to figure 3.1

K_{EP} coefficient of passive earth pressure during earthquakes.

Fig.3.1 Definition of symbols

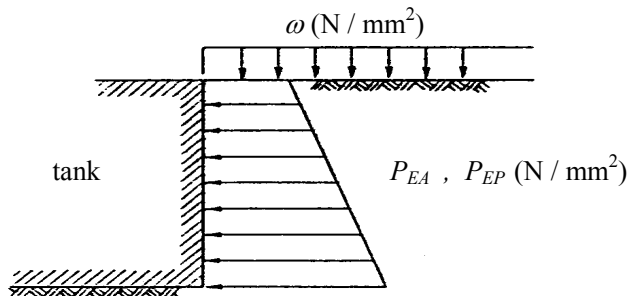*Commentary:*

Although the actual mechanism of soil pressure during earthquakes is complicated and unknown to some extent, Mononobe and Okabe presented their formula for earth pressure during earthquakes using seismic intensity and Coulomb's earth pressure theory of ultimate slip. Vertical tank wall and horizontal ground surface are assumed in equations (3.8.1) and (3.8.2) for simplicity.

(a)   Seismic active earth pressure resultant

$$(3.8.1) \qquad P_{EA}{}' = (1 - K_V)(\frac{\gamma}{2} + \frac{\omega}{H\cos\theta})K_{EA}H^2$$

(b)   Seismic passive earth pressure resultant

$$(3.8.2) \qquad P_{EP}{}' = (1 - K_V)(\frac{\gamma}{2} + \frac{\omega}{H\cos\theta})K_{EP}H^2$$

where:

$P_{EA}{}'$	*seismic active earth pressure resultant acting on the wall with depth H (N/mm)*
K_{EA}	*see eq. (3.64) in chap. 3.8.2*
K_V	*see eq. (3.15) in chap. 3.6.2.2*
γ	*unit weight of soil (N/mm³)*
H	*depth from the ground surface to the tank bottom (mm)*
ω	*imposed loads (N/mm²)*
θ	*seismic composite angle (=$tan^{-1}K$)*
$P_{EP}{}'$	*seismic passive earth pressure resultant acting on the wall with depth H (N/mm)*
K_{EP}	*see equation (3.66) in chap. 3.8.2*

As shown above, Mononobe and Okabe's formula gives the resultant acting on the tank wall for a unit width soil wedge above the slip surface. For convenience, this recommendation transforms equations (3.8.1) and (3.8.2) to pressures per unit area of the tank wall as in equations (3.63) and (3.65). If these equations are integrated in the interval z = 0~H, equations (3.8.1) and (3.8.2) will be obtained.

Equations (3.63) ~ (3.66) give pressures acting in the inclined direction with angle δ from the horizontal plane. But the angle of friction between the wall and the soil may be neglected, and the pressures may be regarded as acting in the normal direction to the wall.

The equations in this chapter give ultimate earth pressure, but they have limitations in that their basis is static equilibrium and they depend on assumed seismic intensity. Therefore additional methods, such as response displacement, seismic intensity, or dynamic analysis methods should also be used in the design for seismic loads.

References:

[3.1]   NASA SP-8007: Buckling of Thin-walled Circular Cylinders, Aug. 1968
[3.2]   Donnell, L. H.: Stability of Thin-walled Tubes under Torsion, NACA, TN479, 1933
[3.3]   Akiyama, H., Takahashi, M., Hashimoto, S.: Buckling Tests of Steel Cylindrical Shells Subjected to Combined Shear and Bending, Trans. of Architectural Institute of Japan, Vol. 371, 1987
[3.4]   Lundquist, E. E.: Strength Test of Thin-walled Duralumin Cylinders in Combined Transverse Shear and Bending, NACA, TN523, 1935
[3.5]   Yamada, M.: Elephant's Foot Bulge of Cylindrical Steel Tank Shells JHPI, Vol. 18, No. 6, 1980
[3.6]   Akiyama, H., Takahashi, M., Nomura, S.: Buckling Tests of Steel Cylindrical Shells Subjected to Combined Bending, Shear and Internal Pressure, Trans. of Architectural Institute of Japan, Vol. 400, 1989
[3.7]   Yamada, M., Tsuji, T.: Large Deflection Behavior after Elephant's Foot Bulge of Circular Cylindrical Shells under Axial Compression and Internal Pressure
Summaries of Technical Papers of Annual Meeting, AIJ, Structure-B, pp. 1295-1296, 1988
[3.8]   Almroth Bo O., Brush D. O.: Postbuckling Behavior of Pressure Core-Stabilized Cylinders under Axial Compression. AIAA J., Vol. 1, pp.2338-2441, 1963

[3.9]   Yamada, M.: Elephant's Foot Bulge of Circular Cylindrical Shells
         The Architectural Reports of the Tohoku University, Vol. 20, pp. 105-120, 1980
[3.10]   Shibata, K., Kitagawa, H., Sampei, T. Misaji, K: The Vibration Characteristics and Analysis of After
         Buckling in Metal Silos, Trans. of Architectural Institute of Japan, Vol. 367, 1986
[3.11]   Kitagawa, H., Shibata, K.: Studies on Comparison of Earthquake - Proof of Metal and FRP Silos,
         Summaries of Technical Papers of Annual Meeting, AIJ, Structure - B, 1988
[3.12]   Akiyama, H.: Post Buckling Behavior of Cylindrical Structures Subjected to Earthquakes, 9th SMiRT,
         Lausanne, 1987
[3.13]   Kato, B., Akiyama, H.: Energy Input and Damages in Structures Subjected to Severe Earthquakes,
         Trans. of Architectural Institute of Japan, Vol. 235, 1975

4   Water Tanks

4.1   Scope

4.1.1   General

This chapter is applicable to the design of potable water storage tanks and their supports.

4.1.2   Materials

Potable water storage tanks are normally constructed using reinforced concrete, pre-stressed concrete, carbon steel, stainless steel, aluminium, FRP, timber, or any combination of these materials.

4.1.3   Notations

B ratio of the horizontal load-carrying capacity to the short term allowable strength.
h_i height of the i-th mass from ground level (m).
Q_{ei} design storey shear force for designing allowable stresses (N).
W design weight imposed on the base of the structure exclusive of convective mass (N). See chap. 4.2.4.4.

4.2   Structural Design

4.2.1   Design Principles

4.2.1.1   Potable water storage tanks should be located such that the contents are not subject to insanitary pollution. They should also be located to enable easy access for inspection, maintenance, and repair.

4.2.1.2   The shape of a water tank should be as simple as possible, be symmetrical about its axis, and mechanically clear of any unnecessary obstructions.

4.2.1.3   Due consideration should be given to stress concentrations at openings or penetrations for pipework.

4.2.1.4   Suitable measures should be taken to prevent a sudden internal pressure drop caused by any uncontrolled release of water.

4.2.1.5   The foundations for water tanks should be designed such that the total forces of the overall structure are transferred to the ground as smoothly as possible.

4.2.2   Allowable Stresses and Material Constants

Allowable stresses and material constants used in the construction of water tanks and their support structures should be in accordance with the applicable codes and standards, and as indicated below.

(1) Long term allowable stresses of reinforcing bars in a reinforced concrete structure should be properly defined after taking into account the allowable cracking width.

(2) Allowable stresses of stainless steel should be defined in accordance with the "Design Standard for Steel Structures – Based on Allowable Stress Concept -" - AIJ 2005. The standard *F* value should be taken as 0.2% strength as stipulated by JIS.

(3) The standard value *F*, which defines yielding stress of all welded aluminium alloy structure, should be defined in accordance with the "Aluminum Handbook – Japan Aluminium Association (2001)" etc.

(4) Allowable stresses and constants of FRP structures should be defined by reference to the material characteristics obtained from tensile and flexural strength tests, ("Method of tension test for FRP" - JIS K 7054, and "Method of flexural test of FRP" - JIS K 7055), after taking into account degradation due to aging, etc.

4.2.3   Loads

4.2.3.1   Loads for structural design should be as shown in chapter 3 in addition to the provisions of 4.2.3.2 below and so on.

4.2.3.2   Water tanks should be considered as being full for the design calculations. However, a partial load for the tank contents may be considered when there is a dangerous combination of loads that would increase the overall loading.

4.2.4   Seismic Design

4.2.4.1   Seismic design of water tanks should be classified below in accordance with 3.6.1.7:

  -    Small water tanks used at private houses   I
  -    Essential water tanks for public use   III
  -    Others   II

4.2.4.2   Design seismic loads should be obtained from the simplified seismic coefficient method or the modal analysis which are shown in 3.6.1.2, 3.6.1.3 and 4.2.4.5 except for 4.2.4.3.

4.2.4.3   Design yield shear forces should be determined based on the horizontal seismic coefficient of 1.5 for the water tanks placed on the roof.

4.2.4.4   Contents in the water tank should be considered in two different masses, i.e. the impulsive mass of the tank contents that moves in unison with the tank and the other convective mass of the tank contents that acts as sloshing liquid. See the commentary of chap. 7.1 and 7.2 for more information.

4.2.4.5   Calculation of design shear forces based on Simplified Seismic Coefficient Method:

(1) The design yield shear force, Q_d, at the ground base of the water tank should be calculated by the equations (3.1) by use of the simplified seismic coefficient method.

Where:

W = design weight imposed on the base of the structure exclusive of convective mass (N)

D_s = structural characteristic coefficient, as is given on Table 4.1

<div align="center">

Table 4.1 D_s Value

(a) Elevated Water Tanks

</div>

Structure	Type of Structure	D_s
Metallic Structure	Moment Frame	0.40
	Truss/Bracing	0.40
	Plate/Shell	0.5~0.7
Reinforced Concrete Structure Steel Reinforced Concrete Structure Pre-stressed Concrete Structure	Moment Frame	0.40
	Plate	0.45

<div align="center">

(b) Water Tanks Installed Directly on the Foundation or Ground

</div>

Structure	D_s
Other than below	0.55
Reinforced Concrete Structure Pre-stressed Concrete Structure	0.45

4.3   Reinforced Concrete Water Tanks

The design of reinforced concrete water tanks should be as indicated in 2.2, 2.3, 2.4 and 4.2, and the "Standard for Structural Calculation of Reinforced Concrete Structures" - AIJ 2010. However, the following provisions should also be taken into consideration.

(1) Concrete for water tanks should be as specified in Chapter 23: Watertight Concrete - JASS 5, AIJ 2009.

(2) The minimum ratio of reinforcing bars of side walls and bottom slab should be more than 0.3% in both orthogonal directions.

(3) The minimum concrete covering of reinforcing bars should be as given in Chapter 3.11: Cover - JASS 5, AIJ 2009.

(4) Any required water proofing should be applied to the surface that is in contact with the stored water.

(5) The minimum concrete covering of reinforcing bars to the surface in contact with stored water should be 30mm, and in the case of light duty water proof finishing, e.g., mortar, or in cases where no water proof finishing is applied, the minimum cover of reinforcing bars should be 40mm and 50mm respectively.

4.4 Pre-stressed Concrete Water Tanks

Pre-stressed concrete water tanks should be as stipulated in 2.2, 2.4, and 4.2 of this document, and the "Standard for Structural Design and Construction of Pre-stressed Concrete Structures" - AIJ 1998. Reinforced concrete components should be as noted in 4.3.   In addition, the following provisions should be taken into consideration.

(1) For usual use conditions, cross sections of members should be designed in full pre-stressing condition. Stresses from water pressure should be considered as live loads.

(2) The additional loads and stresses caused by pre-stressing should also be taken into consideration.

(3) Thermal stresses and additional stresses caused by dry shrink strain should be considered.

4.5 Steel Water Tanks

The design of steel water tanks should conform to the "Design Standard for Steel Structures - Based on Allowable Stress Concept - " 2005 edited by the Institute, and the following items.

(1) Cylindrical shell design of the water tanks should give investigation on the buckling of the cylindrical shell conforming to section 3.7.

(2) The water tanks and pipeline design should give full preventative measures to corrosion.

4.6 Stainless Steel Water Tanks

The design of stainless steel water tanks should conform to the "Guideline of Anti-Seismic Design and Construction of Building Equipments (2005)" edited by the Building Center of Japan (BCJ) etc. The design of stainless steel water tanks support section should conform to the "Design and Construction Standard on the Stainless Steel Building Structure, and the Explanation (2001)" edited by the Stainless Steel Japanese Society of Steel Construction, and the following items.

(1) Cylindrical shell design of the water tanks should give investigation on buckling of the cylindrical shell conforming to section 3.7

(2) The water tanks and pipeline design should give full preventative measures to corrosion.

4.7   Aluminium Alloy Water Tanks

The design of aluminium alloy structure should conform to section 2.5, 4.2 and the "Commentary, Design and Calculation Examples of Technical Standard on the Aluminium Alloy Building Structure (2003) by BCJ etc.", and to the following items.

(1) Cylindrical shell design of the water tanks should give investigation on buckling of the cylindrical shell conforming to section 3.7

(2) The water tanks and pipeline design should give full preventative measures to corrosion.

(3) When the stored water is potable water, adequate lining should be applied to the inner wall surface of the tank.

4.8   FRP Water Tanks

The acceleration response of the story at which FRP water tanks is installed should be taken into consideration on the seismic design of the tank. They are usually installed at a higher elevation.

The pipe connections and the anchoring system should be designed with carefulness. Both of them are known to be relatively easily suffered damages during earthquakes. Consideration should also be given to the sloshing response of the water during earthquake which may cause to damage the ceiling panels.

Materials used in the manufacture of FRP water tanks should meet the requirements of paragraphs, 2.6 and 4.2, and should be designed in accordance with a recognised code, e.g., the Japan Reinforced Plastics Society "Structural Calculation Method for FRP Water Tanks (1996)".

However, the following precautions should be always considered.

(1) The wall thickness of the tank should be more than 3mm except for the manhole cover plate.

(2) The design should give consideration to the anisotropic physical properties of the proposed FRP materials.

(3) The design should give consideration to the thermal properties of the proposed materials in case the tank contains the hot water.

(4) The design should give consideration to the corrosion prevention in case the tank is reinforced with metals.

(5)   The design should give consideration to the measure to prevent formation of algae due to the transmission of light.

(6)   Materials selected for potable water tanks should be of the ones not impair the quality of the stored water, and should be resistant to the chemicals used for cleaning the tank.

(7)   The structural design should give consideration to the expected loads and the physical characteristics of the proposed FRP materials.

4.9   Wooden Water Tanks

This section is omitted in this English version.

Commentary:

In addition to designing for structural integrity, the design of FRP water tanks should include all hygiene requirements for potable water.

The following points should be given due consideration in the design of FRP water tanks:

(1)   With disregard to the calculated strength requirements and the derived wall thickness requirements, a minimum wall thickness of 3mm should be applied to all FRP water tank designs.

(2)   The orientation of glass fibre has a significant effect on the strength and stiffness of FRP. Therefore, due consideration should be given to the anisotropy of the glass fibre reinforcement in the design of FRP water tanks.

(3)   The effect of temperatures between - 40°C and + 40°C on the material characteristics of FRP is minimal. As the normal temperature range of potable water is + 4°C to + 30°C the effect of temperature on FRP materials is therefore insignificant. However, at temperatures above + 60°C the strength and stiffness of FRP is impaired, therefore the design of water tanks for use at high temperatures should take into account this loss of strength and stiffness.

(4)   In cases where a combination of FRP and other materials is necessary, e.g., galvanised steel or stainless steel reinforcement, preventative measures should be taken to prevent corrosion of the non FRP reinforcement by contaminants or other chemicals, e.g., chlorine, in the water .

(5)   In order to prevent the formation of algae inside water tanks, and therefore to maintain water quality, the intensity ratio of illumination (the ratio of intensity of light between the inside and outside of the water tank), should not exceed 0.1%. Care should therefore be taken in the design and placement of manholes, air vents, roof panels, etc., which may provide points of ingress for light.

(6)   Materials used in the construction of potable water tanks should meet the relevant hygiene standards. Particular attention should be paid to the prevention of materials being used in the manufacturing process which may be soluble in water and which can affect the quality of potable water. As the inside of water tanks are washed with an

aqueous solution of sodium hypochlorite, only materials which are known to be resistant to this cleansing agent should be selected for water tanks.

(7)   *FRP does not have the distinct yield point, and neither does it have the ductility similar to metallic materials. Therefore the structural design should take into account this deformation and strength characteristics of the FRP structure.*

5.   Silos

5.1   Scope

5.1.1   This chapter covers the structural design of upright containers and their supports (silos) for storing granular materials.

5.1.2   Definitions

silos   the generic name for upright containers used for storing granular materials and their supports.
containers   tanks for storing granular materials.
silo wall   the upright wall of the containers.
hopper   the inclined wall of the containers.

Note: The term granular materials is taken to include "fine particles".

5.1.3   The structural materials of the silos which are considered in this chapter are reinforced concrete and steel.

5.1.4   Notations

A horizontal area of the silo (m^2)
B ratio of the horizontal load-carrying capacity of the structure to the short-term allowable yield strength
C design yield shear force coefficient at the base of silo
C_d overpressure factor, used to consider increases of pressure occurring during discharge, converting from static pressure to design pressure
C_f safety factor of friction force, used to long term design friction force between silo wall and granular materials
C_i impact factor, used to consider pressure increase due to sudden filling, converting from static pressure to design pressure
C_L ratio of the local pressure to the design horizontal pressure
d diameter (inside) of silo (see Fig.5.1) (m)
H height of the silo (see Fig.5.1) (m)
h_m effective height of material above bottom of hopper assuming top of stored material is levelled (see Fig.5.1) (m)
K_s ratio of P_h to P_v
l_c perimeter of horizontal inside cross section of container (or hopper) (m, cm)
dN_m vertical design force per unit length of silo wall horizontal section (N/mm)
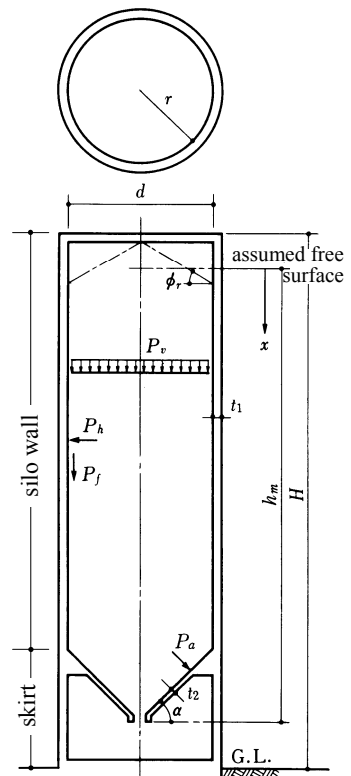P_f friction force of unit area of silo wall surface

Fig.5.1 Silo Section

at depth x (N/mm^2)

P_h	horizontal pressure of unit area at depth x due to stored material (N/mm^2)
P_v	vertical pressure of unit area at depth x due to stored material (N/mm^2)
P_a	pressure normal to the surface of inclined hopper wall (N/mm^2)
dP_h	design horizontal pressure of unit area (N/mm^2)
dP_L	design local horizontal pressure of unit area (N/mm^2)
dP_v	design vertical pressure of unit area (N/mm^2)
dP_a	design normal pressure of unit area to hopper wall (N/mm^2)
r_w	hydraulic radius of horizontal cross section of storage space (m)
x	depth from surface of stored material to point in question (m)
α	angle of hopper from horizontal (°)
γ	weight per unit volume for stored material (N/mm^3)
μ_f	coefficient of friction between stored material and wall or hopper surface
ϕ_i	internal friction angle of stored material (°)
ϕ_r	repose angle of stored material (°)

5.2   Structural Design

5.2.1   General

5.2.1.1   Silos and their supports should be designed to contain all applicable loads taking into account the properties of stored materials, the shape of the silos, methods of material handling, etc.

5.2.1.2   The shape of the silo should be as simple as possible, be symmetrical about its axis, and should have structural members which are proportioned to provide adequate strength.

5.2.1.3   The foundations for silos should be designed to support stresses from the upper structural members of the silos and their supports.

5.2.1.4   The design should include measures to prevent dust or gas explosions and exothermic reaction of stored materials.

5.2.1.5   In the event that fumigation with insecticides is required, the silo should be air tight in accordance with the applicable regulations.

5.2.1.6   The internal surfaces of silos which are used for storing food materials or feed stock should meet the relevant food safety and sanitary regulations.

5.2.1.7   Physical property tests using actual granular materials are expected to find weight per unit volume γ , internal friction angle ϕ_i ; and deformation characteristics (dependency of rigidity and damping ratio on strain level)

5.2.2   Loads

5.2.2.1   General

With the exception of loads for structural design shown in this chapter, all other loadings should, in principle, be based on chapter 3.

(1) Silos, hopper walls, and bottom slabs should be designed to resist all applicable loads, and should include forces from stored materials, static pressures, dynamic over-pressure and under-pressure during charge and discharge, arch, collapse of arch, aeration and eccentric discharge.

(2) Design for group silos should take into account the varying operational scenarios. e.g., some silos are full, others are empty, and some are in the process of being filled or emptied.

(3) In the case that the characteristics of the stored material may be subject to change during storage, the design should consider the most severe load conditions.

(4) The designer may use an alternative method for calculating pressures if it can be verified by experiments etc.

5.2.2.2   Pressures and friction forces of static stored materials

Static pressures exerted by stored material at rest should be calculated using the following methods.

(1) The vertical pressure, P_v, at depth x below the surface of the stored material is calculated using equation (5.1).

(5.1) $$P_v = \frac{\gamma \cdot r_w}{\mu_f \cdot K_s} \cdot \left(1 - e^{-\mu_f \cdot K_s \cdot x / r_w} \right)$$

in which K_s and r_w are obtained from equations (5.2) and (5.3).

(5.2) $$K_s = \frac{1 - \sin \phi_i}{1 + \sin \phi_i} \quad \text{where}: \ K_s \geqq 0.3$$

(5.3) $$r_w \quad = \quad A/l_c$$

(2) The horizontal pressure, P_h, of a unit area at depth x from the free surface is obtained from equation (5.4).

(5.4) $$P_h = K_s \cdot P_v$$

(3) The friction force, P_f, of a unit area of silo wall at depth x from the assumed free surface should be computed from equation (5.5).

(5.5) $$P_f = \mu_f \cdot P_h$$

(4) The static unit pressure P_a normal to the surface inclined at angle α to the horizontal at depth x below the surface of stored material is obtained form equation (5.6).

(5.6) $\qquad P_a = P_h \cdot \sin^2 \alpha + P_v \cdot \cos^2 \alpha$

5.2.2.3 Design pressures and forces exerted by stored materials

(1) Design pressures should be obtained by multiplying the static pressures by the overpressure correction factor C_d or impact factor C_i in accordance with the appropriate equations (5.7), (5.8), or (5.9).

(5.7)
$$\left. \begin{array}{l} dP_v = C_i \cdot P_v \qquad \text{for silo wall.} \\[1em] \left. \begin{array}{l} dP_v = C_i \cdot P_v \\ dP_v = C_d \cdot P_v \end{array} \right\} \text{ for hopper, whichever is greater.} \end{array} \right.$$

(5.8) $\qquad dP_h = C_d \cdot P_h$

(5.9) $\qquad \left. \begin{array}{l} dP_a = C_i \cdot P_a \\ dP_a = C_d \cdot P_a \end{array} \right\}$ whichever is greater.

(2) The impact factor, C_i, should be used to consider the material properties, the charging method and the charging rates, and should be taken a value between the 1.0 and 2.0.

(3) The minimum required values of overpressure factor C_d are given in Figure 5.2.

for $h_m/d \geqq 4.0$
$\qquad C_d=2.0$
for $4.0 > h_m/d > 1.0$
$\qquad C_d=4/3+h_m/6d$
for $1.0 \geqq h_m/d$
$\qquad C_d=1.5$
h_0 : *hopper height*
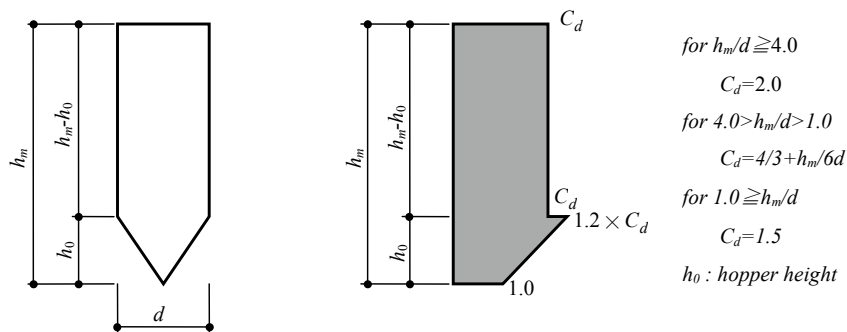
Fig.5.2 Minimum Required Values of Overpressure Factor C_d

(4) For small scale and $1.5 \geqq h_m/d$ silos, minimum required factor may be $C_d =1.0$, however P_v is taken as $P_v = \gamma \cdot x$.

(5) The long - term local pressure shown below should be taken into account, as well as above discussed C_i and C_d, to consider the increase and decrease of pressure by arching and collapse of the arch etc. in stored materials.

1) The design pressure $C_d \cdot P_h$ is multiplied by C_L, which ranges from 0.15 to 0.4 and depends on eccentricity of the discharge outlet, and this local pressure dP_L (= $C_L \cdot C_d \cdot P_h$) is applied to the partial area of the silo wall of 0.1d width. A set of pressures, compressive directions or tensile ones both, is applied to any point - symmetric locations of silo wall, as shown in Figure 5.4. The eccentricity "e" is defined in Figure 5.3.

2) C_L=0.15 when e=0, and C_L=0.4 when e=0.5d, the case where the outlet is just on the wall. For other values of "e", C_L is given by C_L=0.15+0.5 (e/d).

3) For cases where "e" is less than or equal to 0.1d, the local pressure for the upper part of the silo wall may be reduced. The C_L is given by C_L=0.15+0.5(e/d) if the height of the location from the bottom end of the silo walls is less than 1.5d, and takes zero at the top. Between the 1.5d height and the top, a linear function of height gives the C_L value. See equation (5.10) and Figure 5.5.
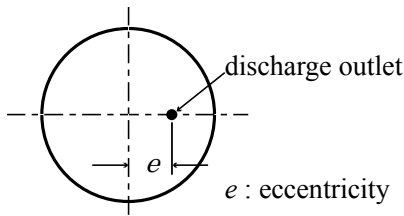
Fig.5.3   Definition of Eccentricity   Fig.5.4   Local Pressure
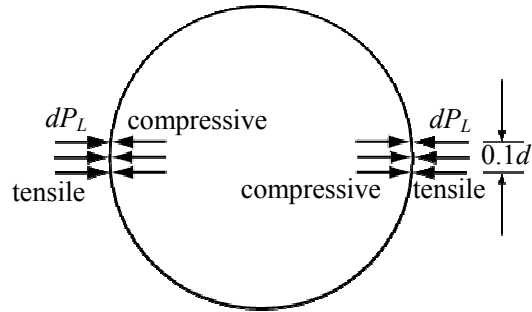
(5.10)
$$\left. \begin{array}{l} dP_L = C_L \cdot C_d \cdot P_h \\ C_L = 0.15 + 0.5(e/d) \end{array} \right\}$$

(6) Vertical long-term design force dN_m per unit length of silo wall horizontal section, at depth x from free surface, should be computed as shown in equation (5.11).

(5.11) $dN_m = (\gamma \cdot x - P_v) \cdot r_w \cdot C_f$

where C_f is taken both 1.0 and more than 1.5, because either case may generate the larger stress.

(7) Vertical short-term design force dN_m by the seismic force should be calculated by equation.5.12

(5.12) $dN_m = (\gamma \cdot x - P_v) \cdot r_w$

(8) The axial force in the direction of generator on the hopper wall horizontal section per unit length, N_ϕ, and the tensile force in the circumferential direction, N_θ, are calculated using equations (5.13) and (5.14) respectively. See Figure 5.6.

(5.13) $N_\phi = \dfrac{(W_h + W_s)}{l_c \cdot \sin \alpha} + \dfrac{dP_v \cdot d'}{4 \cdot \sin \alpha}$

$$(5.14) \qquad N_\theta = \frac{dP_a \cdot d'}{2 \cdot \sin \alpha}$$

Where :

W_h	weight of the contents of the hopper beneath the section (N)
W_s	weight of the hopper beneath the section (N)
l_c	perimeter of the hopper at the section level (mm)
d'	diameter of the hopper at the section level (mm)
α	slope of the hopper (°)
dP_v	design vertical pressure of unit area at the section level (N/mm²)
dP_a	design normal pressure of unit area to hopper wall at the section level (N/mm²)

For design of the connection of the hopper and the silo wall, however, an additional case where N_ϕ is assumed to be zero should be considered.
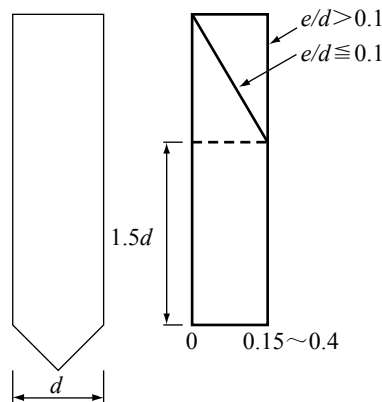
Fig.5.5 Local Pressure Factor C_L

Fig.5.6 Force Acting on the Hopper

5.2.2.4   Mixing by Stirring and Rotation

The effect of mixing materials by stirring and rotation, in which stored materials are discharged to other silos and simultaneously charged from other silos, should be considered for both dynamic overpressure and impact pressure.

5.2.2.5   Eccentric discharge

The design should take into account the effect of asymmetric flow, the local pressure given by equation (5.10), caused by concentric or eccentric discharge openings. If a silo has mobile discharge openings, the maximum value of eccentricity should be adopted.
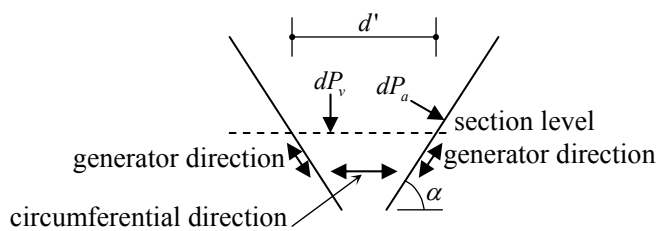
5.2.2.6   Pressure increase due to aeration

In the case of aeration in a silo and pneumatic conveyance, the possibility of pressure increase should be considered.

5.2.2.7   Flushing phenomenon

The possibility of flushing phenomenon should be considered where there is the possibility that the silos could be mis-operated, or where it is likely that material fluidity could be a contributing factor in any seismic event.

5.2.2.8   Thermal stresses

Consideration should be given to thermal stresses generated in the walls of silos in which hot materials are stored.

Commentary:

5.2.2.2   Pressures and friction forces of static stored materials
Foreign standards[5.1)~5.3)] may be referred to for better understanding of this chapter. Janssen's equation[5.4)] and Rankine's earth pressure (equations (5.1) and (5.2)) are used for static pressures. To obtain design pressures, overpressure factor C_d , impact factor C_i and local pressure dP_L should be considered.
5.2.2.3   Design pressures and forces exerted by stored materials
1) Local pressure
Although large pressures of stored materials to silo walls had been observed in many cases, the actual effect of them on the wall stress (strain) was regarded as unclear. Recently simultaneous measurements of wall strain and pressure were made to make clear the effect of the pressure to the strain as well as to discriminate between bending and membrane strains [5.5), 5.6)]. Simulation analyses of the measured results assuming local pressure were carried out [5.6)]. Dependency of the magnitude and fluctuation of the local pressure on the eccentricity of the discharge outlet was also studied [5.5)]. The local pressure given by the equation (5.10) is determined with due regard to above references and other design and accident examples.
2) Local stress coefficient
Based on parametric studies and for approximate estimations, equations below are made to calculate bending stresses.
2-1) The maximum bending moment for a simple ring loaded with a pair of normal local force at opposite sides is given by the equation below.
(5.2.1) $M_0 = 0.318 \cdot 0.1d \cdot dP_L \cdot (d/2)$
Where M_0 is the bending moment per unit width of the ring calculated using simple ring model.
If a 3D cylindrical model with high rigidity bottom and top boundaries is considered instead of the simple ring, the bending moment will be smaller.
2-2) For steel silos, approximate estimation of the maximum bending stress (moment) is given by multiplying the coefficient " k " below into the " M_0 " above in some cases defined below. High rigidity boundary cases, with stiffening beams at the boundary, roofs, hoppers e.g., are assumed.

i)   The local stress coefficient " k " is applicable when $h_m/d \leqq 5$, $d \leqq 10m$ and $t \leqq 20mm$

ii) For each plate thickness of the silo wall, the location (height) where the bending stress is maximum should be checked.

iii) The local stress coefficient " k " is given by the equation below.

$$(5.2.2) \qquad k = 0.1 + 0.05(h_m/d - 2)$$

2-3) The bending moment M_b is given by the equation below.

$$(5.2.3) \qquad M_b = kM_0$$

where M_b is the bending moment per unit width of the silo wall for which the effect of rigid boundaries is approximately considered.

2-4) For reinforced concrete silos, another local stress coefficient is defined below, similarly to steel silos. High rigidity boundary cases are assumed.

$$(5.2.4) \qquad k = 0.25 + 0.2(h_m/d - 1)$$

In case h_m/d is smaller than 1, k is fixed at 0.25. In many cases, the rigidity of the top end is not sufficient to ensure the accuracy of the equation (5.2.4). Therefore, the bending moment for the silo wall near the top end is modified. From the top surface of the stored material to $0.2\,h_m$ depth, the bending moment at the $0.2\,h_m$ depth is fixed for this region.

3) In silos with mobile discharge openings or a large number of discharge outlets, the bottom region is flat compared to single hopper cases. Therefore, large pressure to the bottom region is probable and should be designed with due regard.

4) Large pressure and stress are expected at the connection of the silo wall and the hopper because of the hopper weight, the pressure and the frictional force on the hopper, etc. Sufficient margin is necessary in structural design.

5) Equations (5.13) and (5.14) are derived from the membrane shell theory [5.7], and the equation (5.13) can also be derived from equilibrium of forces. In the equation (5.14), only the normal pressure is considered and the effect of the frictional force is neglected.

5.2.3   Seismic Design

5.2.3.1   The importance factor is determined in accordance with the classification of the seismic design I, II and IV given in Table 5.1 below.

Table 5.1 Classification of Seismic Design and Essential Facility Factor

Seismic Design Classification	Silos	Importance Factor I
I	Small silos - the height of which is below 8.0m	0.6 and over
II	Other silos not included in Classification I and IV	0.8 and over
IV	Silos used for the storage of hazardous or explosive materials	1.2 and over

5.2.3.2   The design seismic loads are obtained from the modified seismic coefficient analysis or the modal analysis which are shown in 3.6.1.2 and 3.6.1.3.

5.2.3.3   In case that the first natural period, T, is unknown, T should be taken as 0.6s for the purposes of the silo design. In this case, the modified seismic coefficient analysis should be used.

5.2.3.4   Using the modified seismic coefficient analysis, the design yield shear force of the silo at the ground base of the silo Q_d should be taken from equations (3.1).

Notations:

      C design yield shear force coefficient at the base of the silo

      W design weight imposed on the base of silo

      I importance factor, given in Table 5.1

      D_η a value obtained from the plastic deformation property of the structure, given in Table 5.2

      D_h a value obtained from the radiation damping of the silo basement, given in Table 5.3

Table 5.2 D_η Value

Structure	D_η
Reinforced concrete	0.45
Steel or aluminium alloy	0.5 ~ 0.7

Table 5.3 D_h Value

Short length of silo foundation	Area of silo foundation	D_h
$\leqq 25$m	$\leqq 2000$m^2	1.0
25m ~ 50m	2000m^2 ~ 4000m^2	1.0 ~ 0.9
$\geqq 50$m	$\geqq 4000$m^2	0.9

5.2.3.5   Assessment of Seismic Capacity

The seismic capacity of the silo design should be assessed using equation.(3.10) given in paragraph 3.6.1.8. The acceptable ratios of the horizontal load-carrying capacity of the silo structure to the short-term allowable yield strength are:

      Reinforced concrete silos: $B = 1.5$.

      Metal silos: $B = 1.0$.

5.2.3.6   When calculating seismic forces on silos by the modified seismic coefficient or modal analysis, the lateral forces can be reduced due to, other than the radiation

damping of silo structures, energy loss caused by the internal friction between the stored materials or between the materials and the silo walls. The weight of the stored material can be reduced for this purpose. Similarly, when calculating seismic forces for group silos which are not always fully loaded, a reduction of material weight can be considered. But in neither case should the reduced weight of stored material be less than 80% of the maximum stored material weight.

5.2.3.7   Dynamic analysis considering the deformation characteristics of the stored material

In case large ground motion of the design earthquake is assumed, or for some kinds of stored material and silo configuration, effect of the deformation characteristics of the stored material is very large. In such cases, dynamic response analysis for seismic design has an advantage because the energy absorption by the stored material friction and slip can be taken into consideration when the silo response and load are estimated.

5.2.3.8   Group silo

Due consideration should be given to group silo design because loads and stresses are different from single silo cases.

5.3   Reinforced Concrete Silos

The design of reinforced concrete silos should conform to the requirements of the "Standard for Structural Calculation of Reinforced Concrete Structures (2010) - Architectural Institute of Japan", together with the provisions of the following paragraphs.

5.3.1   Both the membrane stress and the out-of-plane stress should be given due consideration in the design of silo walls and hoppers. Incidental stress and stress transmission at connection of shells and plates should be taken into consideration especially of group silos and silos with unusual configurations.

5.3.2   Design allowable crack width should be appropriately determined considering necessary margin against deterioration of reinforcing bars and leakage.

5.3.3   The cross-sectional shape and the quality of the concrete parts and the arrangements of steel bars should be carefully considered when using the slip form construction method.

5.4   Steel Silos

The design of steel silos should conform to section 2.2, the "Design Standard for Steel Structure – Based on Allowable Stress Concept - (2005) - Architectural Institute of Japan" and the recommendations given below.

5.4.1   Design of Cylindrical Walls

The guidelines given in section 3.7.1 should be followed when examining the buckling stress of cylindrical walls.

The calculation of stresses on the parts of the silo during earthquakes should be based on the requirements of section 3.7.4.

The calculation of short-term stresses on parts caused by other than earthquakes should be based on section 3.7.3.

5.4.2   Design of Hopper Walls

The axial stress on the section of the hopper wall in the direction of generator, σ_ϕ, and the tensile stress in the circumferential direction, σ_θ, are calculated using equations (5.15) and (5.16) respectively.

(5.15) $$\sigma_\phi = \frac{(W_h + W_s)}{l_c \cdot t_2 \cdot \sin\alpha} + \frac{dP_v \cdot d'}{4 \cdot t_2 \cdot \sin\alpha} \leq f_t$$

(5.16) $$\sigma_\theta = \frac{dP_a \cdot d'}{2 \cdot t_2 \cdot \sin\alpha} \leq f_t$$

where:

W_h	weight of the contents of the hopper beneath the section (N)
W_s	weight of the hopper beneath the section (N)
t_2	wall thickness of the hopper (mm)
l_c	perimeter of the hopper at the section level (mm)
d'	diameter of the hopper wall at the section level (mm)
α	inclination of the hopper wall (degree)
dP_v	vertical design pressure per unit area at the section level (N/mm^2)
dP_a	perpendicular design pressure per unit area on the hopper wall at the section level (N/mm^2)
f_t	allowable tensile stress (N/mm^2)

5.4.3 Design of Supports

Local bending stresses should be considered in design procedure that may act on the connections between the hopper or machines and their supports or other similar parts.

References:

[5.1]   *International Standard : ISO 11697, Bases for Design of Structures – Loads due to Bulk Materials, 1995.6*
[5.2]   *American Concrete Institute : Standard Practice for Design and Construction of Concrete Silos and Stacking Tubes for Storing Granular Materials (ACI 313-97) and Commentary—ACI 313R-97, 1997.1*
[5.3]   *Australian Standard : Loads on Bulk Solids Containers (AS 3774-1996), 1996.10*
[5.4]   *Janssen, H.A. : Versuche Über Getreidedruck in Silozellen : VID Zeitschrift (Dusseldorf) V. 39, pp. 1047～1049, 1885.8*
[5.5]   *Naito, Y., Miyazumi, K., Ogawa, K., Nakai, N. : Overpressure Factor Based on a Measurement of a Large - scale Coal Silo during Filling and Discharge, Proceedings of the 8th International Conference on Bulk Materials Storage, Handling and Transportation (ICBMH'04), pp. 429 – 435, 2004.7*
[5.6]   *Ishikawa, T., Yoshida, J. : Load Evaluation Based on the Stress Measurement in a Huge Coal Silo (in Japanese), Journal of Structural and Construction Engineering (Transactions of AIJ), No.560, pp. 221 – 228, 2002.10*

[5.7]   S.P. Timoshenko and S.W. Kreiger : Theory of Plates and Shells, McGraw-Hill, 1959

[5.8]   G.E. Blight : A Comparison of Measured Pressures in Silos with Code Recommendations, Bulk Solids Handling Vol. 8, No. 2, pp. 145〜153, 1988.4

[5.9]   J.E. Sadler, F. T. Johnston, M. H. Mahmoud : Designing Silo Walls for Flow Patterns, ACI Structral Journal, March-April 1995, pp. 219〜228 (Title No. 92-S21), 1995

[5.10]   A.W. Jenike: Storage and Flow of Solid, Bulletin No. 123 of the Utah Engineering Experiment Station, University of Utah, 1964.11

6. Seismic Design of Supporting Structures for Spherical Tanks

6.1 Scope

6.1.1 This chapter is applicable to the seismic design of supporting structures for spherical steel tanks. Other general requirements for designing structures should be in accordance with the applicable codes and standards.

6.1.2 In general, the supporting structures should be composed of steel pipe columns with bracings made of steel pipes or solid round bars. However, other steel sections may be used and designed in accordance with this chapter.

6.1.3 Notations

d external diameter of the supporting pipe column (mm)
$f(\xi)$ weight ratio of the effective mass of the tank contents
F_y short-term allowable lateral force of the supporting structure (kN)
N_C short-term allowable compressive strength of bracings (kN)
N_T short-term allowable tensile strength of the bracings (kN)
t_1 wall thickness of the supporting pipe column (mm)
V_I usable liquid volume (m^3)
V_D volume of the spherical tank (m^3)
W design weight imposed on the base of structure (kN)
W_D dead weight of the structure (kN)
W_I weight of the stored contents (kN)
δ_m horizontal displacement of the column head when a supporting column reaches the short-term allowable strength (m)
δ_y horizontal displacement of the column head when a bracing reaches the short-term allowable strength (m)
ξ ratio of the usable liquid volume to the volume of spherical tank $= V_I / V_D$
η mean cumulative plastic deformation rate of the supporting structure

----

Commentary:
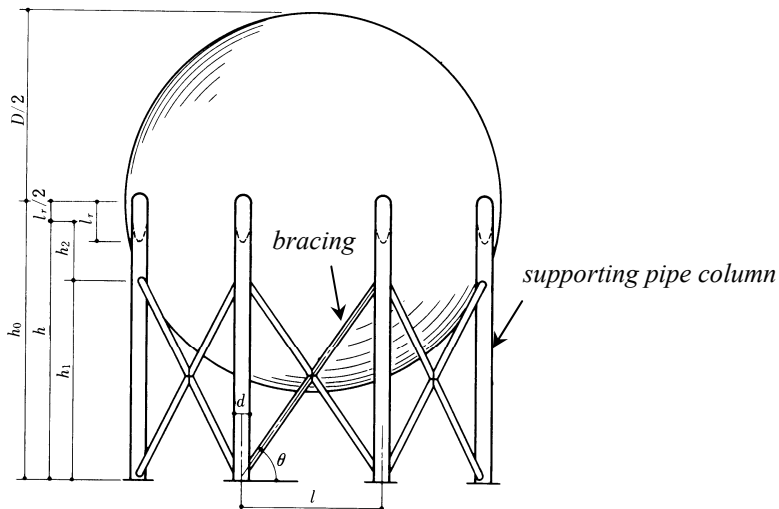
Fig.6.1.1 General View of Spherical Tank

Steel spherical tanks are usually supported on steel pipe columns where steel pipe bracings reinforce the column structures as illustrated in Figure 6.1.1. The intention of this chapter is to provide seismic design recommendations for this type of structure.

6.2   Material Properties and Allowable Stresses

6.2.1   Materials for the structures should be in accordance with section 2.2 of this recommendation.

6.2.2   Table 6.1 gives the physical properties of steel materials.

Table 6.1 Physical Properties of Steel Materials

Materials	Young's Modulus (N/mm^2)	Shear Modulus (N/mm^2)	Poisson's Ratio	Expansion Coefficient (1/°C)
Steel Plates, Pipe and Cast Steel	2.05 x 10^5	7.9 x 10^4	0.3	12 x 10^{-6}

6.2.3   Allowable stresses should be determined as follows:

(1)   Allowable stresses for steel materials should be determined by use of the *F* value and in accordance with Chapter 5, Design Standard for Steel Structures – Based on Allowable Stress Concept – (2005), Architectural Institute of Japan.

(2)   *F* values of steel plates and pipe should be as shown in Table 6.2. *F* values for hard steel wires should be taken to be the value either 70% of tensile strength or yield strength whichever is lesser.

Table 6.2 *F*-Values

Type of steel	Grade	F(N/mm^2)		
		≦40mm thick	> 40mm thick and ≦ 75mm thick	> 75mm thick and ≦ 100mm thick
Rolled Steels for General Structure (JIS G 3101), Rolled Steels for Welded Structure; (JIS G 3106), Rolled Steel for Building Structure; (JIS G 3136)	SS400, SM400, SN400	235	215	
	SM490	315	295	
	SN490	325	295	
	SM490Y	343	335	325
	SM520	355	335	325
	SM570	399	339	
Carbon Steel Tubes for General Structural Purposes; (JIS G 3444)	STK400	235	215	
	STK490	315	295	

Carbon Steel Square Pipes for General Structural Purposes; (JIS G 3466)	STKR400	245	215	
	STKR490	325	295	

		> 6mm thick and ≦ 50mm thick	> 50mm thick and ≦ 100mm thick	> 100mm thick and ≦ 200mm thick
Steel Plates for Pressure Vessels for Intermediate Temperature Service; (JIS G 3115)	SPV235	235	215	195
	SPV315	315	295	275
	SPV355	355	335	315
	SPV450	399	399	399
	SPV490	427	427	427
Mn-Mo and Mn-Mo-Nickel Alloy Steel Plates Quenched and Tempered for Pressure Vessels; (JIS G 3120)	SQV1A, 2A, 3A	345		
	SQV1B, 2B, 3B	434		
Carbon Steel Plates for Pressure Vessels for Low Temperature Service; (JIS G 3126)	SLA235	≦ 40mm thick 235		> 40mm thick 215
	SLA325	308		
	SLA365	343		

6.3 Seismic Design

6.3.1   Seismic Loads

6.3.1.1   Seismic loads should be determined in accordance with section 3.6 of chapter 3.

6.3.1.2   Design seismic loads should be determined by the modified seismic coefficient method in par. 3.6.1.2.

(1)   Design yield shear force, Q_d, should be calculated by the equations (6.1) and (6.2) below.

(6.1) $Q_d = C \cdot W$

(6.2) $C = Z_s \cdot I \cdot D_s \cdot \dfrac{S_{a1}}{g}$

Where : $C \geqq 0.3 Z_s \cdot I$

Notations:

Q_d design yield shear force (kN)
C design yield shear force coefficient
W design load imposed on the base of the structure, (kN), which is equal to the sum of dead weight of structure and weight of impulsive mass of liquid content = $W_D + f(\xi) W_I$ (kN)
W_D dead weight of the structure (kN)

W_I	weight of the stored contents (kN)
$f(\xi)$	weight ratio of the impulsive mass of the tank contents – refer to Fig. 6.1 below.
ξ	ratio of the usable liquid volume to the volume of spherical tank i.e., V_I/V_D
V_I	usable liquid volume (m^3)
V_D	volume of the spherical tank (m^3)
S_{a1}	design acceleration response spectrum, (m/s^2), corresponding to the first natural period, given in par. 3.6.1.6
g	acceleration of gravity (9.8m/s^2)
Z_s	seismic zone factor, which is the value as per the Building Standards Law, or the local government
I	importance factor, given in par. 3.6.1.7
D_s	structural characteristic coefficient, which is the value specified in par. 6.3.1.2.(2)
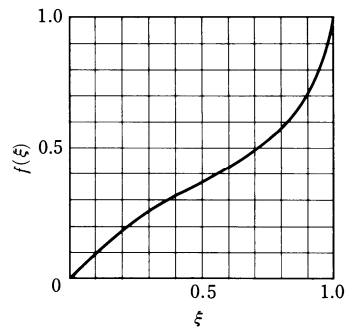
Fig.6.1   Weight Rtio of the Impulsive Mass of the Tank Contents

(2) The structural characteristic coefficient, D_s, should be calculated using equations (6.3) and (6.4) below.

(6.3)
$$D_s = \frac{1}{\sqrt{1+4a\eta}}$$

(6.4)
$$\eta = \frac{\delta_m - \delta_y}{\delta_y}$$

where: $a\eta \le 3.0$

Notations:

η	mean cumulative plastic deformation ratio of the supporting structure
a	correction factor for η considered the reduction of the strength of the bracings
	$a=1.0$ for $N_T \geqq 2N_C$
	$a=0.75$ for $N_T < 2N_C$
N_C	short-term allowable compressive strength of bracings (kN)

N_T short-term allowable tensile strength of the bracings (kN)

δ_m horizontal displacement of the column head when a supporting column reaches the short-term allowable strength (m)

δ_y horizontal displacement of the column head when a bracing reaches the short-term allowable strength (m)

6.3.2   Evaluation for Seismic Resistance of Supporting Structures

Evaluation for seismic resistance of supporting structures should be calculated by using equation (6.5).

(6.5) $F_y \geq Q_d$

where:

F_y *short*-term allowable lateral force of the supporting structures (kN), provided that the lateral force of the compressive bracings should be ignored where $N_T \geq 2N_C$

6.3.3   Design of Supporting Structure Components

Design of supporting structure components and bases should be performed in accordance with "Design Standard for Steel Structures – Based on Allowable Stress Concept – (2005) " and "Recommendations for Design of Building Foundations (2001)" both published by Architectural Institute of Japan. In addition, the following requirements should be satisfied.

(1) The slenderness ratio of the supporting columns, should be, $\leqq 60$. The ratio of diameter to thickness of the steel supporting columns is determined in accordance with equation (6.6) using F value (N/mm^2).

(6.6) $\dfrac{d_1}{t_1} \leq \dfrac{19{,}600}{F}$

where:

d_1 external diameter of the pipe supporting column (mm)

t_1 thickness of the pipe supporting column (mm).

(2) The ratio of diameter to thickness of the steel pipe bracings, should be, ≤ 40.

(3) The strength of the joints in the bracings should be greater than the tensile yield force of the bracing members.

(4) Bracings should be installed without slackness.

Commentary:

As the structure discussed in this chapter is considered to be the vibration system of a mass, the seismic force is obtained by the modified seismic coefficient method given in 3.6.1.2. The design

weight imposed on the base of the structure W is calculated as the sum of W_D, and f(ξ) W_I. The weight ratio of the impulsive mass of the tank contents, f(ξ), is determined with reference to experimental data of the vibration of a real scale structure [6.1] [6.2].

The structural characteristic coefficient, D_s, is obtained from equation (6.3) which is based on the mean cumulative plastic deformation ratio of the supporting structure, η, (see Commentary 3.6.1), which is obtained from equation (6.4). This equation assumes that δ_m is the horizontal displacement of the column head when a supporting column reaches the short-term allowable strength, that δ_y is the horizontal displacement of the column head when a bracing reaches the short-term allowable strength, and δ_m - δ_y is the mean cumulative plastic deformation. When the allowable strength of the bracing is governed by a buckling, i.e., when $N_T < 2N_C$, the energy absorption capacity (deformation capacity) is lowered due to the lower strength of the structure after the structure becomes plastic. Considering this lowering, equation (6.3) adopts "a" value for lowering the deformation capacity by 25%. Seismic design is evaluated by reference to equation (6.5) assuming that the short-term allowable strength F_y is considered to be the lateral retaining strength [6.3].

1. *The calculation method of η and the design method to obtain the plastic deformation capacity of bracings is given in the following paragraphs.*

1.1 *Elastic analysis of the structure (when $N_T < 2N_C$)*

When the horizontal section of the supporting structure is a regular polygon with n equal sides as shown in Figure 6.3.1, the maximum stress takes place in the side which is parallel (or is the closest to parallel) to the direction of the force. The shearing force in the side is obtained from equation (6.3.1).
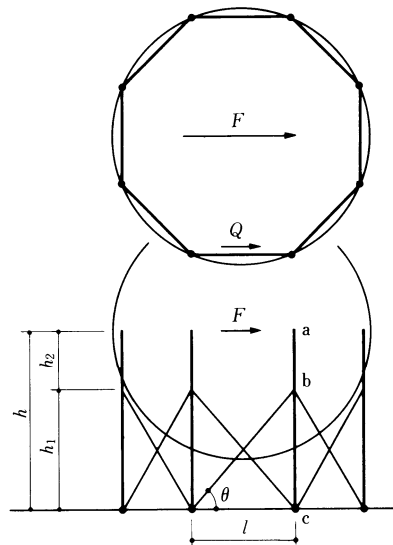

Fig.6.3.1 Modelling

(6.3.1) $$Q = \frac{2F}{n}$$

      where:
      F   is the lateral force imposed on the supporting structure,
      n   is the number of columns = the number of the sides.

Although it should be sufficient that an analysis of the side which receives the in-plane shear force is carried out, and as such can be considered to represent the total design, it should be noted that the adjacent bracings to the sides at point "b" have both a tensile force and a compressive force respectively. The compressive strength of the bracing is generally smaller than the short-term allowable tensile strength, and the compressive force due to the adjacent bracing is generally smaller than the force in the bracing being analysed as the compressive force is not in the analysed plane. To simplify the analysis, the design force acting at point "b" is considered as being twice the horizontal component of the tensile bracing force at point "b"

The analysis should proceed under the following conditions:

i)   *In Figure 6.1.1, $h = h_o - l_r/2$ as demonstrated by experimental data and where l_r is obtained from equation (6.3.2).*

(6.3.2) $l_r = \sqrt{\dfrac{Dd}{2}}$

            where:
            D   *diameter of spherical tank*
            d   *diameter of supporting column*

ii)   *An elastic deformation and a local deformation of the sphere can be neglected as the rigidity of the sphere is relatively large.*

iii)   *To simplify the analysis, the conservative assumption is made that the sphere-to-column joint is considered to be a fixed joint in the plane tangent to the sphere, and a pinned joint in the plane perpendicular to the tangential plane and including the column axis.*

iv)   *The column foot is considered to be a pinned joint.*

v)   *Column sections are considered uniform along their entire length.*

vi)   *Column deformation in the axial direction is neglected.*

The column head "a", shown in Figure 6.3.2 (a), displaces with δ, [as shown in equation (6.3.3)] due to the lateral force Q.

(6.3.3) $\delta = \delta_1 + \delta_2 + \delta_3$

            where:
            δ_1 *displacement due to an elongation of the bracing*
            δ_2 *column displacement at b-point due to the horizontal component 2S of the bracing*
            δ_3 *relative displacement between "a"point and b-point when the joint translations angle of the column is assumed*
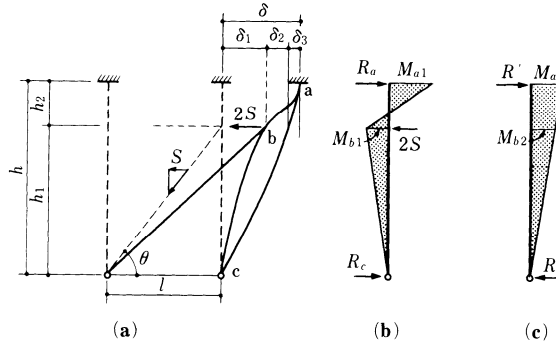
Fig.6.3.2 Stresses in Supporting Column

From the elasticity theory of bars, δ, δ_1, and δ_2 may be calculated in accordance with equations (6.3.4), (6.3.5), and (6.3.6).

(6.3.4)
$$\delta = \frac{2h^3}{3h^2 h_1 - h_1^3}(\delta_1 + \delta_2)$$

(6.3.5)
$$\delta_1 = \frac{Sh_1}{A_b E \cos^2 \theta \cdot \sin \theta}$$

(6.3.6)
$$\delta_2 = \frac{Sh_1^2 h_2^3 (4h_1 + 3h_2)}{6EIh^3}$$

Equation (6.3.7) is obtained from the above three equations:

(6.3.7)
$$\delta = \frac{2h^3}{(3h^2 h_1 - h_1^3)}\left[\frac{h_1^2 h_2^3 (4h_1 + 3h_2)}{6EIh^3} + \frac{h_1}{A_b E \cos^2 \theta \cdot \sin \theta}\right]S$$

where:
A_b cross sectional area of the bracing
I moment of inertia of the supporting column
E Young's modulus of the steel

Figure 6.3.2 (b) shows a stress diagram of a supporting column with a force of 2S exerted by the bracing when the column head "a" does not displace. The reacting forces and moments at points "a", "b", and "c" are obtained from the following equation (6.3.8).

(6.3.8)

$$R_c = \frac{Sh_2^2}{h^3}(3h_1 + 2h_2)$$

$$R_a = \frac{Sh_1}{h^3}(2h_1^2 + 6h_1 h_2 + 3h_2^2)$$

$$M_{a1} = \frac{Sh_1 h_2}{h^2}(2h_1 + h_2)$$

$$M_{b1} = -\frac{Sh_1 h_2^2}{h^3}(3h_1 + 2h_2)$$

$$|M_a| > |M_b| \text{ when } h_2 < \sqrt{2}h_1$$

Figure 6.3.2 (c) shows a stress diagram of the supporting column when the column head "a" displaces by δ. The reacting forces and moments at points, "a", "b", and "c", are obtained from the following equation (6.3.9).

(6.3.9)

$$\left.\begin{aligned}
R' &= \frac{M_{a2}}{h} \quad R' = \frac{M_{a2}}{h} \\
M_{a2} &= \frac{3EI}{h^2}\delta = \frac{1}{(3h^2h_1 - h_1^3)}\left[\frac{h_1^2 h_2^3(4h_1 + 3h_2)}{h^2} + \frac{6Ihh_1}{A_b \cos^2\theta \cdot \sin\theta}\right]S \\
M_{b2} &= \frac{1}{(3h^2 - h_1^2)}\left[\frac{h_1^2 h_2^3(4h_1 + 3h_2)}{h^3} + \frac{6Ih_1}{A_b \cos^2\theta \cdot \sin\theta}\right]S
\end{aligned}\right\}$$

The lateral force Q is calculated using equation (6.3.10).

(6.3.10) $\quad Q = R_a + R'$

The reacting force at the supporting column foot, R, is calculated using equation (6.3.11).

(6.3.11) $\quad R = R' - R_c$

The bending moments at points a, and b, M_a and M_b, are given in equations (6.3.12), and (6..3.13) respectively.

(6.3.12) $\quad M_a = M_{a1} + M_{a2}$

(6.3.13) $\quad M_b = M_{b1} + M_{b2}$

1.2 Elastic analysis of the structure (when $N_T \geqq 2N_C$)

In this case, the compressive force due to the bracing is neglected. Therefore, the horizontal force 2S acting at point "b" shown in Figure 6.3.2 is converted to S, and equations (6.3.14) ~ (6.3.17) are given instead of equations (6.3.6) ~ (6.3.9). Equations (6.3.1) ~ (6.3.5) and equations (6.3.10) ~ (6.3.13) have no modification except the definition of δ_2, the displacement due to S in this case instead of 2S.

(6.3.14)

$$\delta_2 = \frac{Sh_1^2 h_2^3(4h_1 + 3h_2)}{12EIh^3}$$

(6.3.15)

$$\delta = \frac{2h^3}{(3h^2h_1 - h_1^3)}\left[\frac{h_1^2 h_2^3(4h_1 + 3h_2)}{12EIh^3} + \frac{h_1}{A_b E \cos^2\theta \cdot \sin\theta}\right]S$$

(6.3.16)

$$\left.\begin{aligned}
R_c &= \frac{Sh_2^2}{2h^3}(3h_1 + 2h_2) \\
R_a &= \frac{Sh_1}{2h^3}(2h_1^2 + 6h_1 h_2 + 3h_2^2) \\
M_{a1} &= \frac{Sh_1 h_2}{2h^2}(2h_1 + h_2) \\
M_{b1} &= -\frac{Sh_1 h_2^2}{2h^3}(3h_1 + 2h_2)
\end{aligned}\right\}$$

$$(6.3.17) \quad \left\{ \begin{aligned} M_{a2} &= \frac{3EI}{h^2}\delta = \frac{1}{(3h^2 h_1 - h_1^3)}\left[\frac{h_1^2 h_2^3 (4h_1 + 3h_2)}{2h^2} + \frac{6Ihh_1}{A_b \cos^2 \theta \cdot \sin \theta}\right]S \\ M_{b2} &= \frac{1}{(3h^2 - h_1^2)}\left[\frac{h_1^2 h_2^3 (4h_1 + 3h_2)}{2h^3} + \frac{6Ih_1}{A_b \cos^2 \theta \cdot \sin \theta}\right]S \\ R' &= \frac{M_{a2}}{h} \end{aligned} \right\}$$

1.3 Yield strength F_y and yield deformation δ_y of supporting structures

When $N_T < 2N_C$, the yield strength of supporting structures should be equal to the strength of which the maximum stress element of a bracing in compression becomes yielding, i.e., $S = S_y = 1.5 A_b f_c \cos\theta$ (where f_c is the allowable compressive stress) is input into equation R_a of (6.3.8), and in the equation R' of equation (6.3.9). Q_y is obtained as $Q = Q_y = R_a + R'$ in (6.3.10) and the yield strength (short-term allowable strength) of the supporting structure F_y is obtained from (6.3.1).

The yield deformation δ_y is similarly obtained by inputting $S = S_y = 1.5 A_b f_c \cos\theta$ into (6.3.7).

On the other hand, when $N_T \geqq 2N_C$, the yield strength of supporting structures should be equal to the strength of which the maximum stress element of a bracing in tension becomes yielding, i. e., $S = S_y = 1.5 A_b f_t \cos\theta$ (where f_t is the allowable tensile stress) is input into equation R_a of (6.3.16), and in the equation R' of (6.3.17). Q_y is obtained as $Q = Q_y = R_a + R'$ in (6.3.10) and the yield strength (short- term allowable strength) of the supporting structure F_y is obtained from (6.3.1).

The yield deformation δ_y is similarly obtained by inputting $S = S_y = 1.5 A_b f_t \cos\theta$ into (6.3.15).

The spring constant k can be calculated from equation (6.3.18) as follows:

$$(6.3.18) \quad k = \frac{F_y}{\delta_y}$$

1.4 Critical deformation of a frame δ_m

When the lateral displacement of the column head increases after the bracing reaches its elastic limit, points "a" and "b" reach their yield point. In this situation, M_{a1} and M_{b1} do not increase as the bracing is already in yielding condition, but M_{a2} and M_{b2} increase so that eventually the column reaches its yield point. It is noted that point "a" at the column head reaches its yield point first as long as h_2 is relatively short as shown in equation (6.3.8).

Because the rigidity of the sphere-to-column joint, $\pm l_r / 2$ distance region from point "a", is large, the bending moment diagram of the column at this joint is not linear function of the height as shown in Figure 6.3.3. Figure 6.3.3 shows that the critical bending moment, $_eM_a$, should be calculated by the Equation (6.3.19) at a distance of $l_r/4$ below point "a".
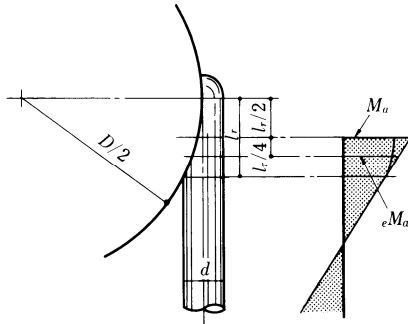
Fig.6.3.3 Modelling of the Top Part of Supporting Column

(6.3.19) $$_eM_a = M_a - \frac{l_rQ}{4}$$

Values for the lateral force Q, and the bending moment $_eM_a$ are obtained from equations (6.3.10), and (6.3.12) respectively.

The yielding moment of the column M_y is calculated using equation (6.3.20) as follows:

(6.3.20) $$M_y = Z\left(\sigma_y - \frac{N}{A}\right)$$

$$N = (W_D + W_I)/n$$

Notations:

Z   *section modulus of the column*
N   *axial compressive force in the column*
A   *sectional area of the column*
σ_y *short-term allowable tensile stress (yield stress)*
n   *number of columns*

The surplus in the critical bending at the $-l_r/4$ distant location from point "a", ΔM, is obtained from equation (6.3.21) as follows:

(6.3.21) $$\Delta M = M_y - (_eM_a)_y$$

where: $(_eM_a)_y$ is equal to $_eM_a$ when the supporting structure reaches the yield strength F_y

The increment in the virtual bending moment at point "a" is shown in equation (6.3.22).

(6.3.22) $$\Delta M_a = \Delta M \left(\frac{h}{h - l_r/4}\right)$$

This equation is necessary to obtain the increment in displacement at point "a".

The increment in displacement, Δδ, at point "a" is given in equation (6.3.23).

(6.3.23) $$\Delta \delta = \delta_m - \delta_y = \frac{\Delta M_a h^2}{3EI}$$

η is obtained from (6.4) by use of (6.3.23) and δ_y, as follows.

(6.3.24) $$\eta = (\delta_m - \delta_y)/\delta_y$$

Note that buckling is not considered in equation (6.3.20) in the evaluation of a supporting column. The overall length of the supporting column, h, should be considered in assessing out-of-plane buckling as no restraint is provided at joint "b" of the bracings in terms of out-of-plane deformation. On the other hand, in-plane buckling between points "a" and "b" need not be considered as the length is relatively short, and if the effect of buckling is considered between points "b" and "c", the evaluation at point "a" by (6.3.20) governs. Out-of-plane buckling may be considered as Euler Buckling, and as such a suitable evaluation method is given in equation (6.3.25).

(6.3.25)
$$\frac{\sigma_c}{f_c} + \frac{{}_c\sigma_b}{f_t} \leq 1$$

However, steel pipe columns need not checking of flexural-torsional buckling, no out-of-plane secondary moments due to deflection and axial forces. Therefore, equation (6.3.25) has little meaning for pipe columns. As the equation (6.3.25) is based on a pipe column, it is assumed that $f_b = f_t$.

Taking the above observations into consideration, equation (6.3.20) is adopted as an acceptable evaluation method on condition that the slenderness ratio is less than 60 and on the assumption that the buckling length is h. The effective slenderness ratio is approximately 42 (0.7 ×60) for out-of-plane buckling and the column will never buckle before yielding at the extremity of point "a".

Although the above summary assumes that the bracing yields first, such design that point "a" of the column yields first is allowable. However, this is not a practical solution in anti-seismic design, as the energy absorption by the plastic elongation of the bracing cannot be utilised. As the supporting ability against lateral seismic load decreases when the bracing which is in compression stress buckles, the yield strength of the frame will be reduced, and the restoring force characteristics after yielding will become inferior. However, experimental data[6.4] show that in supporting structures which use pipe bracings, the lateral retaining strength is reduced by approximately 25% of the yield strength even when a comparatively large plastic deformation takes place in the bracing.

Typical examples of the joint design between the pipe column and bracing are shown in Figures 6.3.4 to 6.3.7 [6.5].

In Figure 6.3.4 the design force at the joint should be determined by the 130% of the yield strength of the bracing [6.6].

In Figure 6.3.5(b) the short-term allowable force P_{a1} at the bracing cross is obtained in equation (6.3.26);

(6.3.26)
$$P_{a1} = \frac{29t_1{}^2F}{\sin\varphi_1} = \frac{29t_1{}^2F}{\sin 2\theta} \quad (N)$$

Where $P_{a1} > A_\rho F$ (where A_ρ is the sectional area of pipe bracing), equation (6.3.27) is used.

(6.3.27)
$$t_1 > \frac{\sqrt{A_\rho \sin\varphi_1}}{5.5} \quad (mm)$$

In case the requirements of the above equation cannot be satisfied, either the thickness of the pipe wall should be increased at the joint, refer to Figure 6.3.6(a), or the joint should be reinforced with a rib as indicated in Figure 6.3.6(b).

In Figure 6.3.5(c) the short-term allowable force, P_{a2}, at the joint between the column and bracing is obtained from equation (6.3.28) below:

(6.3.28) $P_{a2} = 5.35\left[1+4.6\left(\dfrac{d_1}{d_2}\right)^2\right]\dfrac{f(n)}{\sin\varphi_2}\cdot t_2{}^2 F$ (N)

where:

$\sin\varphi_2 = \cos\theta$

$f(n)$ $= 1.0$ (when $n \geqq -0.44$)

$f(n)$ $= 1.22 - 0.5\left|n\right|$ (when $n < -0.44$)

$n = N/A_c F =$ ratio of the axial force in the column to the yielding force.

Notations:

F yield strength of column (refer to Table 6.2 for appropriate value)

N axial force in the column (compression is expressed with minus (-))

A_c sectional area of the column

P_{a2} should satisfy the condition given below.

(6.3.29) $P_{a2} > A_\rho F_1$

where: F_1 is the yield strength of the bracings, (refer to Table 6.2 for the appropriate value)

In case the requirements of equation (6.3.29) cannot be satisfied, either the thickness of the column wall should be increased at the joint, or the joint should be reinforced with a rib, refer to Figure 6.3.7.

gusset plate

rib
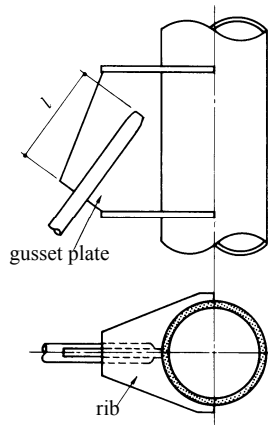
Fig.6.3.4 Reinforcement at the Column to Bracing Joint (Solid round bar)

(a)   (b)   (c)
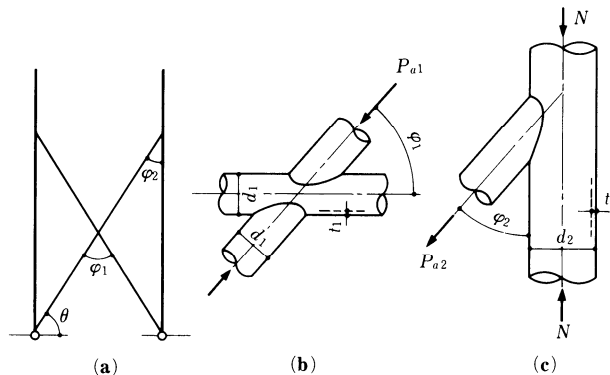
Fig.6.3.5 Joint Detail of Steel Pipe Bracings

(a)

(b)
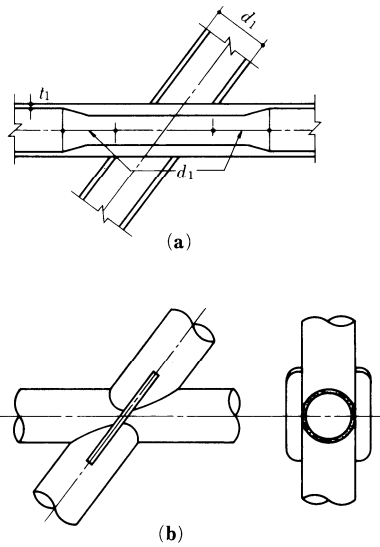
Fig.6.3.6 Reinforcement at the Bracing Joint (Steel pipe)

ring stiffener

rib
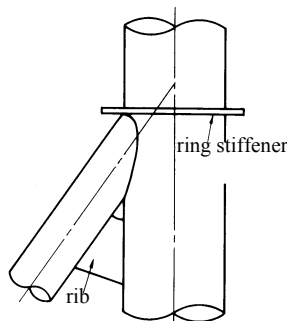
Fig.6.3.7 Reinforcement at the Column to Bracing Joint (Steel pipe)

References:

[6.1]   Akiyama, H. et al.: Report on Shaking Table Test of Spherical Tank, LP Gas Plant, Japan LP Gas Plant Association, Vol. 10, (1973) (in Japanese)

[6.2]   Akiyama, H.: Limit State Design of Spherical Tanks for LPG Storage, High Pressure Gas, The High Pressure Gas Safety Institute of Japan , Vol.13, No.10 (1976), (in Japanese)

[6.3]   Architectural Institute of Japan: Lateral Retaining Strength and Deformation Characteristics on Structures Seismic Design, Ch. 2 Steel Structures (1981), (in Japanese)

[6.4]   Kato, B. & Akiyama, H: Restoring Force Characteristics of Steel Frames Equipped with Diagonal Bracings, Transactions of AIJ No.260, AIJ (1977), (in Japanese)

[6.5]   Architectural Institute of Japan: Recommendation for the Design and Fabrication of Tubular Structures in Steel, (2002), (in Japanese)

[6.6]   Plastic Design in Steel, A Guide and Commentary, 2nd ed. ASCE, 1971

7. Seismic Design of Above-ground, Vertical, Cylindrical Storage Tanks

7.1 Scope

7.1.1 This chapter covers the seismic design of above-ground vertical cylindrical tanks for liquid storage. General structural design are regulated by the relevant standards.

7.1.2 Notations

C_e	design shear force coefficient
D	diameter of the cylindrical tank (m)
H_l	depth of the stored liquid (m)
P_s	design dynamic pressure of the convective mass - the sloshing mass (N/mm^2)
P_{so}	reference dynamic pressure of the convective mass - the sloshing mass (N/mm^2)
P_w	design dynamic pressure of the impulsive mass - the effective mass of the tank contents that moves in unison with the tank shell (N/mm^2)
P_{wo}	reference dynamic pressure of the impulsive mass - the effective mass of the tank contents that moves in unison with the tank shell (N/mm^2)
η_s	height of sloshing wave (m)
Q_y	design yield shear force of the storage tank (kN)
Q_{dw}	design shear force of the impulsive mass vibration - the effective mass of the tank contents that moves in unison with the tank shell (kN)
Q_{ds}	design shear force of the convective mass vibration - the effective mass of the first mode sloshing contents of the tank (kN)

Commentary:

There are two main types of above-ground cylindrical tanks for liquid storage; one is for oil storage and the other is for liquefied gas. Many oil storage tanks are generally placed on earth foundations with a concrete ring at periphery. They are usually not equipped with anchoring devices. In case of oil storage tanks having floating roofs, the roof moves up and down following the movements of the oil surface. (See Fig.7.1.1) Whilst, liquefied gas storage tanks is usually a double container type tank which consists of an inner tank having a fixed-dome roof and an outer tank also having a domed roof. They are usually placed on concrete slab foundations. The gas pressure in the inner tank, in which the liquefied gas is contained, is resisted by the inner dome roof and with anchoring devices provided at the bottom of the inner shell not to lift up the bottom plate (See Fig.7.1.2).
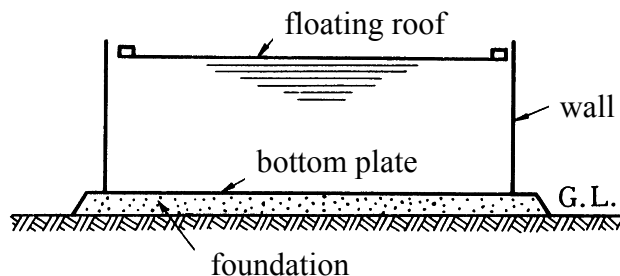
Fig.7.1.1 Oil storage tank
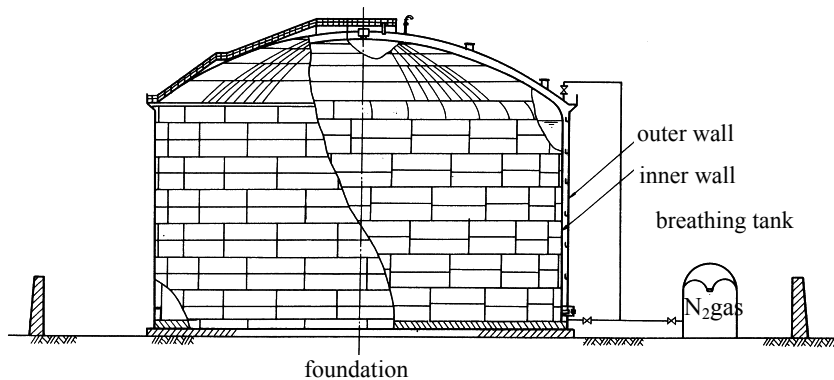
Fig.7.1.2 Liquefied gas storage tank

These two different structures give different seismic response characteristics.

The rocking motion, accompanied by an uplifting of the rim of the annular plate or the bottom plate, is induced in oil storage tanks by the overturning moment due to the horizontal inertia force. In this case, particular attention should be paid to the design of the bottom corner(ⓐ) of the tank as shown in Fig.7.1.3, because this corner is a structural weak point of vertical cylindrical storage tanks.
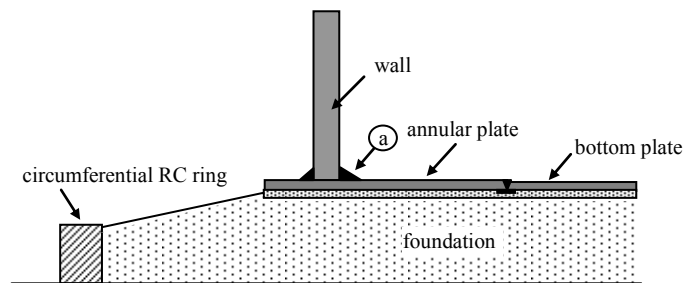
Fig.7.1.3   Bottom corner of tank

On the other hand the rocking motion in the liquefied gas storage tank caused by the overturning moment induces pulling forces in anchor straps or anchor bolts in place of uplifting the annular plate. In this case, the stretch of the anchor straps or anchor bolts which are provided at the bottom course of the tank, should be the subject of careful design.

Figure 7.1.4 shows several examples of tank damages observed after the Hanshin-Awaji Great Earthquake in Japan in 1995 [7.1]. Figure 7.1.4(a) shows an anchor bolt that was pulled from its concrete foundation. Figure 7.1.4(b) shows an anchor bolt whose head was cut off. Figure 7.1.4(c) shows the bulge type buckling at the bottom course of tank wall plate, (Elephant's Foot Bulge - E.F.B.). Figure 7.1.4(d) shows diamond pattern buckling at the second course of tank wall plate. Figure 7.1.4(e) shows an earthing wire that has been pulled out when the tank bottom was lifted due to the rocking motion.

The type and extent of this damage shows the importance of seismic design for storage tanks. Especially the rocking motion which lifts up the rim of the tank bottom plate, buckles the lower courses of tank wall, and the pulls out the anchor bolts or straps from their foundations.

The contained liquid, which exerts hydrodynamic pressure against the tank wall, is modelled into two kinds of equivalent concentrated masses: the impulsive mass m_1 that represents impulsive dynamic pressure, and the convective mass m_s that represents convective dynamic pressure, (Housner) [7.2].

(a) Pulled out of anchor bolt

(b) Cut off of anchor bolt

(c) Elephant foot bulge type buckling of tank wall

(d) Diamond pattern buckling of tank wall

(e) Pulled out of earthing wire

Fig.7.1.4 Tank damage mode at Hanshin-Awaji Earthquake

The short-period ground motion of earthquakes induce impulsive dynamic pressure. Impulsive dynamic pressure is composed of two kinds of dynamic pressures (Velostos)[7.3], as shown in Fig.7.1.5. That is, the impulsive dynamic pressure in rigid tanks, p_r, and the impulsive dynamic pressure in flexible tanks, p_f. The ordinates are for the height in the liquid with $z/H_l=1.0$ for the surface, and D/H_l is the ratio of the tank diameter to the liquid depth. The long-period ground motion of earthquakes induce convective dynamic pressure to tank walls as the result of the sloshing response of the contained liquid in the tank. Moreover, the sloshing response causes large loads to both floating and fixed roofs.

The effect of long-period ground motion of earthquakes has been noticed since the 1964 Niigata Earthquake. As well as this earthquake, the 1983 Nihonkai-chubu earthquake and the 2003 Tokachioki Earthquake caused large sloshing motion and damage to oil storage tanks. Particularly, the Tokachioki Earthquake (M8.0) caused damage to oil storage tanks at Tomakomai about 225km distant from the source region. Two tanks fired (One was a ring fire and the other was a full surface fire.) and many floating roofs submerged. Heavy damage of floating roofs was restricted to single-deck type floating roofs. No heavy damage was found in the double-deck type floating roofs.

(a) Distribution in flexible tank   *(b) Distribution in rigid tank*
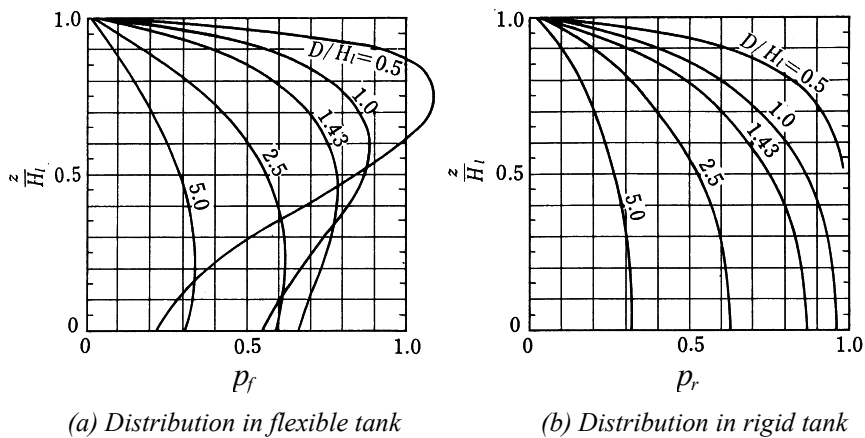
Fig.7.1.5 Impulsive pressure distribution along tank wall

These two kinds of dynamic pressures, impulsive and convective, to the tank wall cause a rocking motion which accompanies a lifting of the rim of the annular plate or bottom plate by their overturning moments for unanchored tanks. Wozniak [7.5] presented the criteria for buckling design of tanks introducing the increment of compressive force due to the rocking motion with uplifting in API 650 App.E [7.6] . Kobayashi et al. [7.7] presented a mass-spring model for calculating the seismic response analysis shown as Fig.7.1.6.   The Disaster Prevention Committee for Keihin Petrochemical Complex established, A Guide for Seismic Design of Oil Storage Tanks which includes references to the rocking motion and bottom plate lifting [7.8].

(a) Uplift region   *(b) Rocking model*   *(c) Spring mass system*
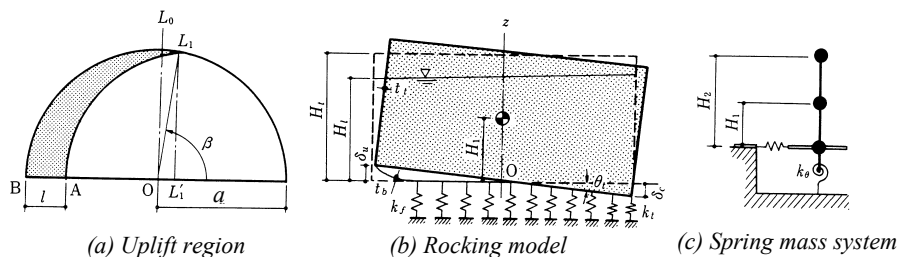
Fig.7.1.6   Rocking model of tank

This recommendation presents the seismic design criteria that takes into account both the rocking motion with uplifting of bottom plate for unanchored tanks, and the elasto-plastic stretch behaviour of anchor bolts or anchor straps for anchored tanks.

7.2 Seismic Loads

7.2.1 Seismic loads for vertical cylindrical tanks used for liquid storage should be calculated using the procedure described in section 3.6.1. However, in case sloshing response is taken into consideration, the velocity response spectrum shown in section 7.2.3. should be used.

7.2.2 Design dynamic pressure of the impulsive mass should be calculated using the modified seismic coefficient method in 3.6.1.2.

(1) Design dynamic pressure of the impulsive mass P_w is calculated using equations (7.1) and (7.2). Design shear force of the impulsive mass vibration Q_{dw} is obtained by integrating the component in seismic force direction of P_w around the inside of tank shell.

(7.1) $\qquad P_w = C_e \cdot P_{wo}$

(7.2) $\qquad C_e = Z_s \cdot I \cdot D_s \cdot S_{a1}/g$

where,

$C_e \geqq 0.3 Z_s \cdot I$

Notations:
C_e design shear force coefficient
P_{wo} reference dynamic pressure of the impulsive mass (the effective mass of the tank contents that moves in unison with the tank shell) (N/mm^2)
Z_s seismic zone factor
I importance factor
D_s structural characteristic coefficient
S_{a1} acceleration response spectrum of the first natural period obtained from equations (3.8) or (3.9) (m/s^2)
g acceleration of gravity; 9.8 m/s^2

(2) Structural characteristic coefficient, D_s , should be calculated using one of the following two methods:

a) For unanchored tanks, D_s is obtained from equations (7.3), (7.4) and (7.6),

In the case that the yield ratio of the annular plate, Y_r , is smaller than 0.8, D_s is:

(7.3) $\qquad D_s = \dfrac{1.42}{1+3h+1.2\sqrt{h}} \cdot \dfrac{1}{\sqrt{1+84\left(\dfrac{T_1}{T_e}\right)^2}}$

In the case that Y_r is greater than 0.8, D_s is:

$$(7.4) \qquad D_s = \frac{1.42}{1+3h+1.2\sqrt{h}} \cdot \frac{1}{\sqrt{1+24\left(\dfrac{T_1}{T_e}\right)^2}}$$

b) For anchored tanks, D_s is obtained from equations.(7.5) and (7.6).

$$(7.5) \qquad D_s = \frac{1.42}{1+3h+1.2\sqrt{h}} \cdot \frac{1}{\sqrt{1+\dfrac{3.3\ t\sigma_y^2}{l_a p_a \sigma_y}\left(\dfrac{T_1}{T_e}\right)^2}}$$

c) Buckling of tank wall plate should be examined with D_s in equation (7.6).

$$(7.6) \qquad D_s = \frac{1.42}{1+3h+1.2\sqrt{h}} \cdot \frac{1}{\sqrt{1+3\left(\dfrac{T_f}{T_e}\right)^2}}$$

Notations:
h damping ratio
T_1 natural period of the storage tank when only the bottom plate and anchor bolts (or anchor straps) deform (s)
T_e modified natural period of the storage tank considering deformation of the wall plate as well as the bottom plate and anchorage (s)
σ_y yield stress of the bottom plate (N/mm^2)
$_a\sigma_y$ yield stress of anchor bolt or anchor strap (N/mm^2)
l_a effective length of anchor bolt or anchor strap (mm)
t thickness of the bottom plate (mm)
p static pressure imposed on the bottom plate (N/mm^2)
Y_r the ratio of yield stress to ultimate tensile strength of annular plate
T_f fundamental natural period related to tank wall deformation without uplifting of bottom plate.

7.2.3   Design seismic loads of the convective mass should be calculated using the procedure described in section 3.6.1.

However, in case sloshing response by long-period ground motion of earthquakes is taken into account, the velocity response spectrum shown in equation (7.7) in item (1) should be used for periods longer than 1.28s. This spectrum depends on the damping ratio of sloshing response shown in item (2).

(1) Velocity response spectrum for the first mode of sloshing is obtained from equation (7.7) in case the damping ratio is 0.5%.

$$(7.7) \qquad \begin{cases} IS_v = 2(m/s) & 1.28s \leqq T \leqq 11s \\ IS_v = \dfrac{22}{T}(m/s) & 11s \leqq T \end{cases}$$

Notations : T period (s)

For cases of other damping ratio than 0.5%, the velocity response is varied according to the damping ratio. However, when the sloshing response of higher mode, higher than the 1st, is calculated, 2m/s should be adopted at the minimum for the velocity response even if less velocity is obtained in accordance with the larger damping ratio. This velocity response includes an importance factor, I, and therefore means IS_v.

The seismic zone factor, Z, should be 1.0 except there is special reason and basis. The velocity response spectrum for cases of $Z=1.0$ are shown in figure 7.2.7 in commentary.

(2) The damping ratio for the 1st mode sloshing should be less than 0.1% for fixed roof tanks, 0.5% for single-deck type floating roof tanks and 1% for double-deck type floating roof tanks. For the higher modes, the damping ratio should be less than the 1st mode damping ratio multiplied by the frequency ratio, the ratio of the frequency of the mode to the 1st mode frequency. The 1st mode damping ratios are shown in table 7.2.1 and the damping ratios for higher modes are shown in figure 7.2.8 in commentary.

(3) Predicted strong motions considering precisely the source characteristics and path effects can be used as design seismic ground motions according to the judgment of the designer instead of the velocity response spectrum shown in equation (7.7).

(4) Design dynamic pressure of the convective mass P_s is calculated by using equation (7.8). Design shear force of the convective mass vibration Q_{ds} for sloshing is obtained by integrating P_s around the inside of tank shell.

$$(7.8) \qquad P_s = \frac{\eta_s \cdot P_{so}}{D}$$

(5) Height of sloshing wave η_s is calculated by using equation.(7.9).

$$(7.9) \qquad \eta_s = 0.802 \cdot Z_s \cdot I \cdot S_{v1} \sqrt{\frac{D}{g} \tanh\left(\frac{3.682 H_l}{D}\right)}$$

Notations:

η_s height of sloshing wave (m)
D diameter of the cylindrical tank (m)
P_{so} reference dynamic pressure of the convective mass (N/mm^2)
H_l depth of the stored liquid (m)
S_{v1} design velocity response spectrum of the first natural period in the sloshing mode as calculated by equations (7.7) (m/s)

7.2.4   Stress and Response of Floating Roofs

Concerning floating roof type tanks, overflow of contained liquid and damage of floating roofs by sloshing should be checked at design stage. When stresses in floating roofs by sloshing response are calculated, higher modes response as well as the 1st mode response should be taken into consideration.

7.2.5   Sloshing Pressure on Fixed Roofs

Impulsive pressure and hydrodynamic pressure by sloshing on fixed roofs should be taken into consideration for the seismic design of fixed roof tanks.

Commentary:

7.2.2 1. Design dynamic pressure

The response magnification factor of tanks is approximately 2, when the equivalent damping ratio of a tank is estimated to be 10% [7.9]. The reference dynamic pressure of the impulsive mass P_{wo} is calculated as follows:

The impulsive mass m_f is obtained by integrating equation (7.2.1) over the whole tank wall.

(7.2.1)
$$P_{wo} = \sqrt{p_f{}^2 + \frac{1}{4}\left(p_r - p_f\right)^2}\ \cos\varphi$$

Base shear S_B is obtained from equations (7.2.2) and (7.2.3).

(7.2.2)
$$m_f = \iint \left(P_{wo}/g\right)\cos\varphi\, rd\varphi dz = f_f \cdot m_l$$

where, m_l is total mass of contained liquid, and f_f is given in Fig.7.2.1.

(7.2.3)
$$S_B = C_e \cdot g \cdot m_f$$

Reference dynamic pressure of the convective mass P_{so} and natural period of sloshing response T_s are calculated as shown in equations (7.2.4) and (7.2.5).

(7.2.4)
$$P_{so} = \gamma \cdot g \cdot D\cosh\left(3.682\frac{Z}{D}\right)\cos\varphi\ \Big/ \cosh\left(3.682\frac{H_l}{D}\right)$$

(7.2.5)
$$T_s = 2\pi\sqrt{\frac{D}{3.682g\tanh\left(3.682H_l/D\right)}}$$

> *where:*
> D *diameter of the cylindrical tank*
> H_l *depth of the stored liquid*
> γ *density of the contained liquid.*

2.   *Coefficient determined by the ductility of tank D_η*

 2.1   *Unanchored tank*

As the failure modes of the unanchored tank are the yielding of the bottom corner due to uplifting, and the elephant foot bulge type buckling on the tank wall, D_η can be obtained from equation (7.6) applying $D_{\eta f} = 0.5$ in equation (3.7.18) .

The following paragraphs show how to derive D_η for the uplifting tank.

The elastic strain energy W_e stored in the uplifting tank is as shown in equation (7.2.6),

(7.2.6)
$$W_e = \frac{k_e\delta_e^2}{2}$$

where, k_e is the spring constant of tank wall - including the effect of uplifting tank, and δ_e is the elastic deformation limit of uplifting tank.

The relation of the uplifting resistance force, q, and the uplifting displacement, δ , per unit circumferential length of tank wall in the response similar to that shown in Fig.7.1.6(b) is given as the solid line in Fig.7.2.2.
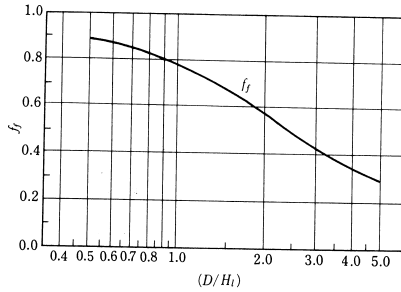
Fig.7.2.1 Effective mass ratio   Fig.7.2.2 q vs δ relation
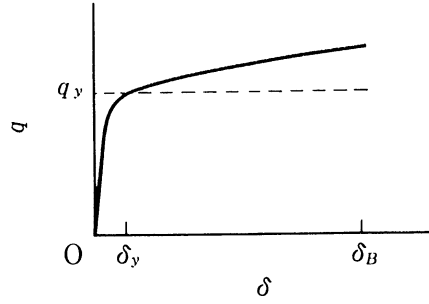
The rigid plastic relation as shown by the dotted line is introduced for simplifying, the plastic work W_{p1} for one cycle of horizontal force is as shown in equation (7.2.7)

(7.2.7) $W_{p1} = 2\pi r q_y \delta_B$

where:
r   radius of the cylindrical tank
q_y yield force of the bottom plate
δ_B the maximum uplifting deformation,

Cumulative plastic strain energy W_p is given as twice W_{p1} (Akiyama [7.10]) as shown in equation (7.2.8).

(7.2.8) $W_p = 2W_{p1} = 4\pi r q_y \delta_B$

When the bottom plate deforms with the uplifting resistance force, q, and liquid pressure, p, as shown in Fig.7.2.3, the equilibrium of the bottom plate, as the beam, is given in (7.2.9)

(7.2.9) $EIy'''' + p = 0$

Deformation y is resolved in equation (7.2.10) under boundary conditions $y = y' = 0$ at x=0, $y' = y'' = 0$ at x=l.

(7.2.10) $y = \dfrac{1}{EI}\left(- px^4/24 + plx^3/9 - pl^2x^2/12\right)$

where, EI is bending stiffness.

The uplifting resistance force q, the bending moment at the fixed end M_c and the relationship between q and δ are obtained as follows:

q   =   2pl/3

M_c = $pl^2/6$

δ   = $9q^4/128EI\,p^3$.

When M_c comes to the perfect plastic moment, M_c is equal to $\sigma_y\,t^2/4$. In this condition, the yielding force of the bottom plate q_y, the uplifting deformation for the yielding force δ_y, and the radius direction uplifting length of bottom plate l_y are obtained from equations (7.2.11).

(7.2.11)
$$q_y = 2t\sqrt{1.5 p\sigma_y}\,/3$$
$$\delta_y = 3t\sigma_y^2\big/8Ep$$
$$l_y = t\sqrt{3\sigma_y/2p}$$
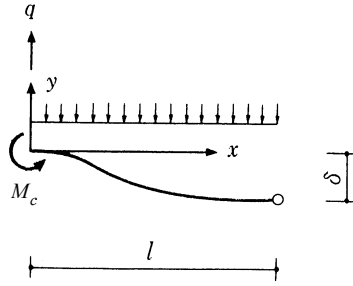
Fig.7.2.3 Bottom plate deformation
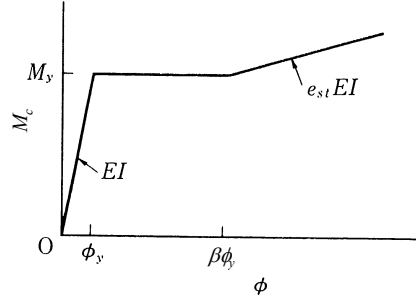
Fig.7.2.4 M_c vs ϕ relation in bottom plate

When the relationship between the bending moment M_c and the curvature φ of elasto-plastic beam is as indicated in Fig.7.2.4, the relationship between q and δ, and M_c and δ are obtained by numerical calculation, refer to Fig.7.2.5. In these figures, β denotes the ratio of the curvature at the beginning of strain hardening to that at the elastic limit, and e_{st} denotes the ratio of the stiffness at the beginning of strain hardening to that at the elastic limit.

The values β = 1.0 and e_{st} = 0.005 are applied for high tensile steel, and β = 1.0 to 11.0, and e_{st} = 0.03 are applied for mild steel. Equation.7.2.12 is a reasonable approximation of the relationship between M_c and δ, which is shown with dot-dash line in Fig.7.2.5(b).

$$(7.2.12) \qquad \frac{\delta}{\delta_y} = 1 + 32\left(\frac{M_c}{M_y} - 1\right)$$

(a) q vs δ relation

(b) M_c vs δ relation
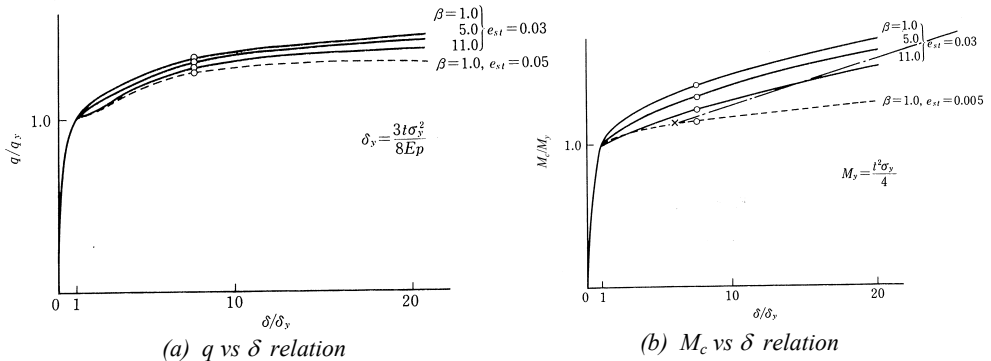
Fig.7.2.5 Wall reaction and bending moment at bottom corner

As the bottom plate failure is considered to be caused when M_c reaches the fully plastic moment M_y, which is obtained from the tensile strength of bottom plate material, the maximum value of M_c / M_y is given as

$$(7.2.13) \qquad (M_c / M_y)_{max} = \sigma_B / \sigma_y$$

where, σ_B is the tensile strength of bottom plate material and is defined as (σ_B / σ_y) being equal to 1.45 for materials of which the ratio of yield stress to ultimate tensile strength of annular plate Yr is smaller than 80%, or 1.10 for materials of which Yr is greater than 80%.

By substituting the relationships in equation (7.2.12), the limit uplift displacement δ_B is obtained as shown in equation (7.2.14).

$$(7.2.14) \quad \left. \begin{array}{l} \delta_B = 14\sigma_y \quad \text{for } Y_r \leq 80\% \\ \delta_B = 4\sigma_y \quad \text{for } Y_r \geq 80\% \end{array} \right\}$$

The spring constant of unit circumferential length for uplifting resistance k_1 is defined as the tangential stiffness at the yield point of q-δ relation, and is shown in equation (7.2.15).

$$(7.2.15) \quad k_1 = \frac{q_y}{\delta_y} = \frac{16pE}{9\sigma_y}\sqrt{\frac{1.5p}{\sigma_y}}$$

The overturning moment M can be derived as the function of the rocking angle of tank θ as shown in equation (7.2.16),

$$(7.2.16) \quad \begin{array}{l} M = \int_0^{2\pi} k_1 r \theta (1+\cos\varphi) \; r \; (1+\cos\varphi) \; rd\varphi = K_M \theta \\ K_M = 3\int_0^{2\pi} k_1 r^2 \sin^2\varphi \; rd\varphi = 3k_1\pi \; r^3 \end{array}$$

where, K_M is the spring constant that represents the rocking motion of tank. The spring constant K_1 as the one degree of freedom system that represents the horizontal directional motion of tank is given as,

$$(7.2.17) \quad K_1 = M \big/ (0.44H_l)^2 \, \theta = 48.7 r^3 k_1 \big/ H_l^2$$

where $0.44H_l$ is the gravity centre height of impulsive mass.

Then the natural period of the storage tank when only the bottom plates deform, T_1, is derived form equation (7.2.18).

$$(7.2.18) \quad T_1 = 2\pi\sqrt{m_t / K_1}$$

where, m_t is the effective mass which is composed of the roof mass m_r, m_f and the mass of wall plate m_w.

The modified natural period of the storage tank considering deformation of both the wall plate and the bottom plate, T_e, can be written as equation (7.2.19).

$$(7.2.19) \quad T_e = \sqrt{T_f^2 + T_1^2}$$

In this equation, T_f is the fundamental natural period related to tank wall deformation without uplifting of bottom plate (JIS B8501[7.4] , MITI [7.9]), and is given as

$$(7.2.20) \quad T_f = \frac{2}{\lambda}\sqrt{m_0 \big/ \pi \; E \; t_{1/3}}$$

where, $t_{1/3}$ is the wall thickness at $H_l/3$ height from the bottom, m_0 is the total mass of tank which is composed of m_l, m_w and the mass of roof structure m_r, and λ is given as following equation,

$$\lambda = 0.067(H_l/D)^2 - 0.30(H_l/D) + 0.46 \, .$$

As the equivalent spring constant considering deformation of both the wall plate and the bottom plate, k_e, can be derived from equation (7.2.21),

$$(7.2.21) \quad K_e = K_1(T_1/T_e)^2$$

the elastic deformation of the centre of gravity of the tank, δ_e, is determined by using the design yield shear force of the storage tank, Q_y, which is further described in section 7.3 below, and equation (7.2.22).

$$(7.2.22) \quad \delta_e = Q_y / k_e$$

By substituting equations (7.2.21) and (7.2.22) into equation (7.2.6), W_e can be calculated, and from equation (7.2.14), W_p can be calculated.

D_η, in equation (3.6.15), can then be written as equation (7.2.23).

(7.2.23)
$$D_\eta = \frac{1}{\sqrt{1 + W_p/W_e}}$$

Then, the coefficient determined by the ductility of the bottom plate uplifting, D_η, is obtained in accordance with the equations (7.2.24).

(7.2.24)
$$\left. \begin{array}{ll} D_\eta = \dfrac{1}{\sqrt{1 + 84(T_1/T_e)^2}} & \text{for } Y_r \leq 80\% \\[4mm] D_\eta = \dfrac{1}{\sqrt{1 + 24(T_1/T_e)^2}} & \text{for } Y_r \geq 80\% \end{array} \right\}$$

Finally, the structural characteristic coefficient D_s is determined as shown in equations (7.3) and (7.4) by multiplying D_h and D_η.

2.2   Anchored tank

The yield force of anchor straps for unit circumferential length $_a q_y$ is given as equation (7.2.25)

(7.2.25)
$$_a q_y = \frac{A_a \cdot _a \sigma_y - \pi\, r^2 P_i}{2\pi\, r}$$

where:

$_a \sigma_y$	*yield stress of anchor straps*
A_a	*sectional area of anchor straps*
P_i	*internal pressure of tank.*

From Hook's low, the anchor strap deformation for yield point, $_a\delta_y$, and the spring constant of anchor straps for unit circumferential length, $_a k_1$, are calculated in accordance with equations (7.2.26) and (7.2.27).

(7.2.26) $_a \delta_y = l_a \cdot _a \sigma_y / E$

(7.2.27) $_a k_1 = \dfrac{_a q_y}{_a \delta_y} = \dfrac{_e A_a \cdot E}{2\pi\, r l_a}$

where:
l_a is the effective length of anchor bolt or anchor strap,
and $_e A_a = A_a(1 - \pi\, r^2 P_i / A_a \cdot _a \sigma_y)$.

When the deformation limit of the anchor is set to be δ_B, the mean deformation of anchor strap $\overline{\delta}_B$ is calculated as $\overline{\delta}_B = (2 + \pi)\delta_B / 2\pi$. By referring to Fig.7.2.6, δ_B is determined as one half of the bottom plate displacement at which point the second plastic hinge occurs in the bottom plate. The white circles in Fig.7.2.5 show the second plastic hinge, and δ is approximately $7\delta_y$. Then $\overline{\delta}_B$ can be rewritten as equation (7.2.28).
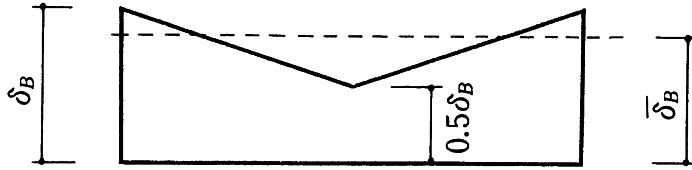
Fig.7.2.6 Average elongation of anchor strap

$$(7.2.28) \qquad \overline{\delta}_B = \frac{(2+\pi)\,\delta_B}{2\pi} = \frac{1.08\ t\sigma_y^2}{Ep} = \frac{1.08\ t\sigma_y^2 \cdot_a \delta_y}{l_a p \cdot_a \sigma_y}$$

By referring to equation(7.2.7), the plastic work W_p becomes

$$W_p = 2\pi\ r\cdot_a q_y \cdot \overline{\delta}_B .$$

Then, the coefficient determined by the ductility of the anchor strap elongation, D_η, and the spring constant K_1 are determined in accordance with equations (7.2.29) and (7.2.30) respectively.

$$(7.2.29) \qquad \left.\begin{array}{l} D_\eta = \dfrac{1}{\sqrt{1+\dfrac{3.3\ t\sigma_y^2}{l_a p \cdot_a \sigma_y}\left(\dfrac{T_1}{T_e}\right)^2}} \\[2em] T_e = \sqrt{T_f^2 + T_1^2} \\[1em] T_1 = 2\pi\sqrt{\dfrac{m_t}{K_1}} \end{array}\right\}$$

$$(7.2.30) \qquad K_1 = 48.7 r_a^3 k_1 \big/ H_l^2$$

Finally, the structural characteristic coefficient, D_s, is determined as equation (7.5) by multiplying D_h and D_η.

2.3 Elephant foot type buckling of wall (E.F.B.)

When the uplifting of bottom plate is caused due to the overturning moment, the coefficient determined by the ductility of the wall plate of the cylindrical tank, D_η is given as equation (7.2.31) from equation (3.7.18).

$$(7.2.31) \qquad D_\eta = \frac{1}{\sqrt{1+3(T_f/T_e)^2}}$$

Then, the structural characteristic coefficient, D_s, is determined as equation (7.6) multiplying D_h and D_η.

7.2.3
1. Damping ratio of sloshing
  Concerning the damping ratios of sloshing for oil storage tanks, experimental data with actual and model tanks are obtained and published [7.12), 7.13)]. Damping ratios for the 1st mode are determined based on mainly earthquake observations and forced vibration tests. Although there are few questions to support the 0.1% or less damping ratio for fixed roof tanks (free surface), neither experimental nor observational data is sufficient to support the 0.5% damping ratio for single-deck type floating roofs and the 1.0% damping ratio for double-deck type.

Table7.2.1 Damping Ratio for the 1st Mode Sloshing

Surface (Roof) Condition	Damping Ratio
Free Surface (Fixed Roof)	0.1%
Single-deck (Floating Roof)	0.5%
Double- Deck (Floating Roof)	1.0%

Concerning the damping ratios for higher modes, some data for actual and model tanks show 5% or more damping ratio on the one hand, but other data show that the same damping ratio as the 1st mode gives the best simulation of the earthquake response of actual tanks.

Therefore, the damping ratios given for the higher modes have not much safety margin, and enough margin for the 1st mode seismic design is recommended. Figure 7.2.8 shows the upper limits of the higher mode damping ratios.

2. Velocity response spectrum for sloshing response

Simple spectrum is regarded as preferable. Therefore, 1.0m/s uniform velocity spectrum for engineering bedrock is assumed for 5% damping response with coefficient 1.2 for importance factor, modification coefficient 1.29 for 0.5% damping response and 1.29 for large scale wave propagation and bi-directional wave input effects. For damping ratios other them 0.5%, $1.10/(1+3h+1.2\sqrt{h})$ should be multiplied as below and Figure 7.2.7.

$$(7.2.32) \qquad IS_v = 2 \cdot \frac{1.10}{1+3h+1.2\sqrt{h}} \ [m/s]$$

Bi-directional effect is considered because tank structures are usually axisymmetric and the maximum response in some direction usually different from given X-Y direction occurs without fail. If the earthquake waves for X and Y directions are identical, the coefficient for this effect is $\sqrt{2}$, but usually it ranges from 1.1 to 1.2.

As explained above, importance factor, 1.2, is already considered. Seismic zone factor Z_s is fixed at 1.0 with the exception of particular basis because there are insufficient data for long-period ground motion.

In case velocity response spectrum for periods shorter than 1.28s is necessary, to obtain higher mode sloshing response, the velocity response spectrum is calculated from the 9.8m/s^2 uniform acceleration response spectrum if the damping ratio is 0.5% or more. In case the damping ratio is less than 0.5%, the same modification as equation (7.2.32) is necessary.
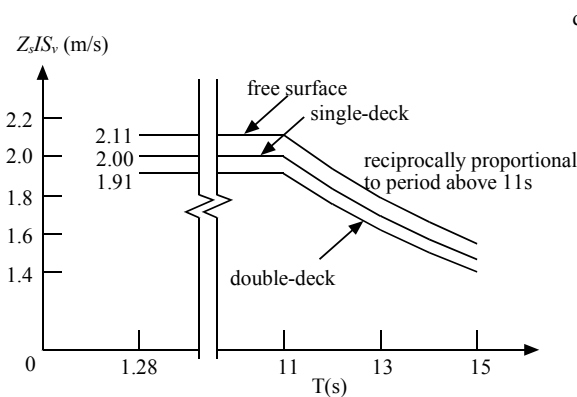
Fig.7.2.7   Velocity Response Spectrum for the 1st Mode Sloshing
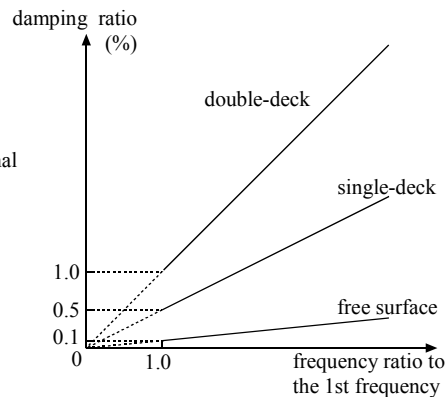
Fig.7.2.8   Upper Limits for the Higher Mode Damping Ratios

Figure 7.2.9 shows the spectrum with typical observed and predicted long period earthquake ground motions[7.13]. Compared with the observed earthquakes and considering the bi-directional effect, the proposed spectrum shows appropriate relations in magnitude to the observed. On the other hand, some of the predicted earthquake spectra exceed the 2.0m/s level in magnitude.

3. Natural period of higher mode sloshing

    The i-th natural period of free liquid surface sloshing in cylindrical tank is calculated by the equation below.

(7.2.33)
$$T_i = \frac{2\pi\sqrt{D}}{\sqrt{2g\varepsilon_i \tanh(2\varepsilon_i \frac{H_l}{D})}}$$

Where :
T_i i-th natural period of sloshing (s)
g acceleration of gravity (m/s^2)
D diameter of the cylindrical tank (m)
ε_i i-th positive root of the equation, $J'_1(\varepsilon_i) = 0$.

J_1 is Bessel function of the first kind. $\varepsilon_1 = 1.841$, $\varepsilon_2 = 5.33$, $\varepsilon_3 = 8.54$

    In case the tank has a single-deck type floating roof, the natural sloshing periods are calculated by equation (7.2.33), in other words, the effect of the roof is negligible. In double-deck type floating roof cases, only the effect to the 1st mode is negligible.

7.2.4. Response and Stress Analysis of sloshing in a tank with a floating roof

    Stress in peripheral pontoon and roof is calculated by recently proposed analysis methods and simplified approximate calculation methods. In these analysis methods, nonlinear FEM for liquid and elastic body, velocity potential theory, calculus of variation, boundary integral, and Bessel function expansion of the roof modes are used.
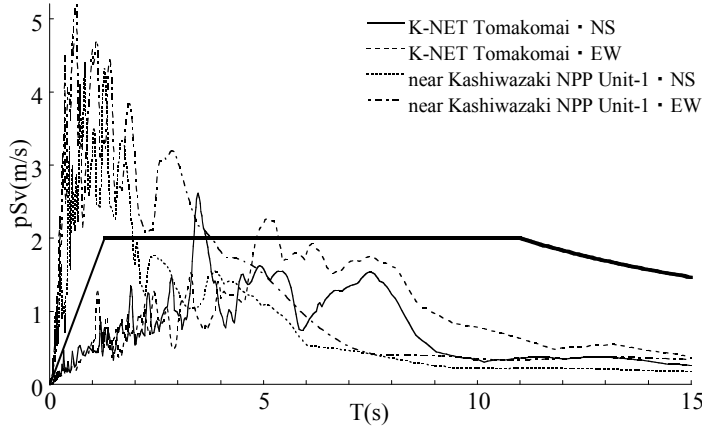
comparison with observed earthquakes (26 Sep. 2003 Tokachi-oki (Tomakomai) and 16 Jul. 2007 Niigataken Chuetsu-oki (Kashiwazaki))
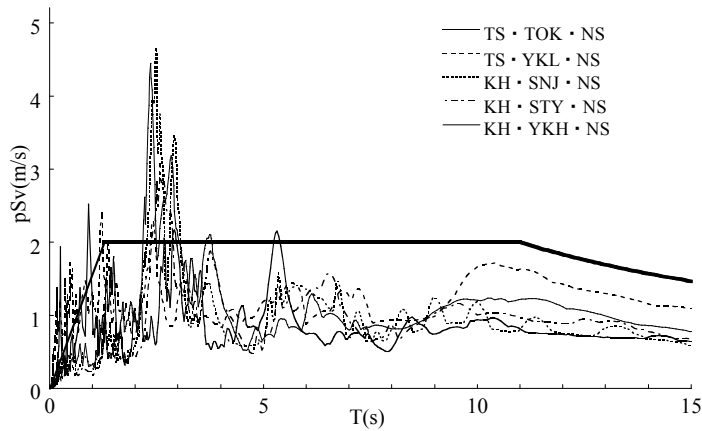
comparison with predicted earthquakes for Tokyo and Yokohama region
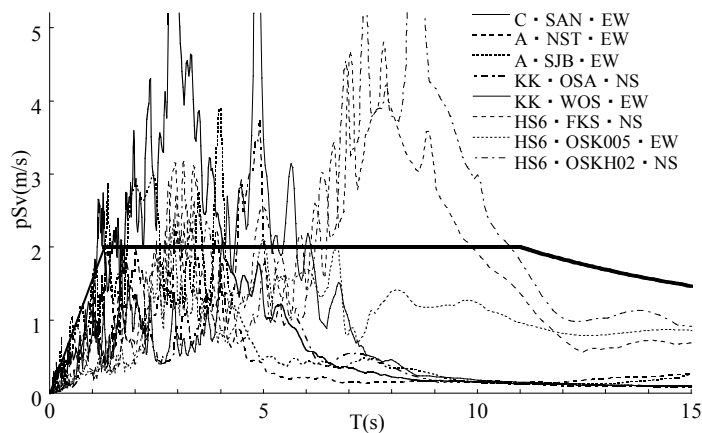
comparison with predicted earthquakes for Nagoya and Osaka

Fig.7.2.9   Comparison of the Velocity Response Spectrum with Typical Observed and Predicted Long Period Earthquakes

7.2.5 Sloshing force acting on the fixed roof of the tank

When the sloshing is excited in the tank with the fixed roof subjected to the earthquake motion, the contained liquid hits the fixed roof as shown in Fig.7.2.10 in the case that the static liquid surface is close to the fixed roof. Figure 7.2.11 sketches the typical time evolution of the dynamic pressure acting on the point A of the fixed roof [7.14]. The impulsive pressure P_i acts on the fixed roof at the moment that the sloshing liquid hits it, and the duration of acting of the impulsive pressure is very short [7.14), 7.15)]. The hydrodynamic pressure P_h acts on the fixed roof after impulsive pressure diminishes as the sloshed contained liquid runs along the fixed roof [7.14)]. Since the duration of acting of the hydrodynamic pressure is long, the hydrodynamic pressure can be regarded as the quasi static pressure.
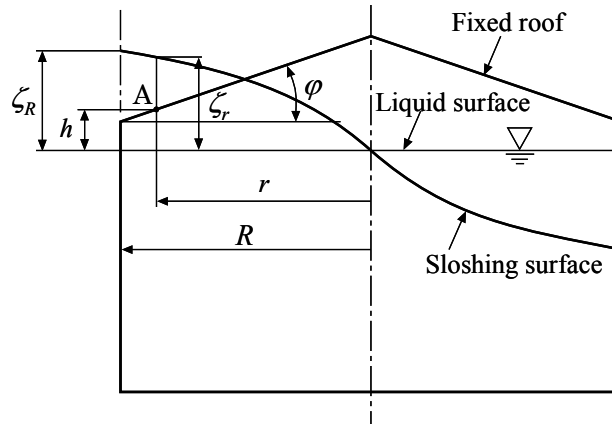
Fig.7.2.10   Fixed roof and sloshing configuration
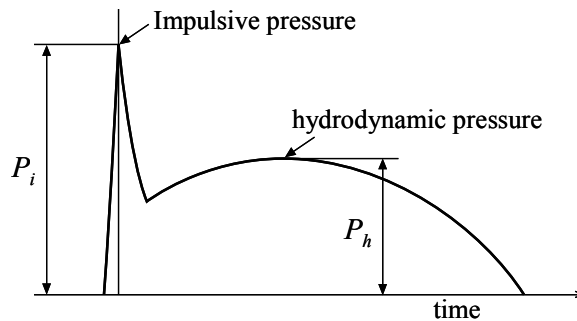
Fig.7.2.11   Impulsive and hydrodynamic pressure

The behavior of the sloshed liquid depends on the shape of the fixed roof. When the roof angle φ is large, the restraint effect from the roof on sloshing is small as shown in Fig. 7.2.12. Then the sloshed liquid elevates along the roof with small resistance from the fixed roof, and yields the hydrodynamic pressure P_h. When the roof angle φ is small, the restraint effect on sloshing is large and the sloshing liquid hardly increases it's elevation at all as shown in Fig. 7.2.13. Then small hydrodynamic pressure P_h yields on the fixed roof of which angle φ is small [7.14), 7.16), 7.17)].

The impulsive pressure P_i acting on the point A of a cone roof tank is given by Yamamoto [7.15] as

(7.2.34) $$P_i = \frac{\pi}{2}\rho\cot\varphi\left(\dot{\varsigma}_r^A\right)^2 \quad [N/m^2],$$

where $\dot{\varsigma}_r^A$ is the sloshing velocity at the point A. ς_r is the sloshing height at the radial distance r from the center of the tank [7.15)]. The first sloshing mode is enough to evaluate the sloshing velocity and the magnitude of the impulsive pressure. According to Yamamoto [7.15], Eq. (7.2.34) is applicable to the roof angle $\varphi \geq 5°$.
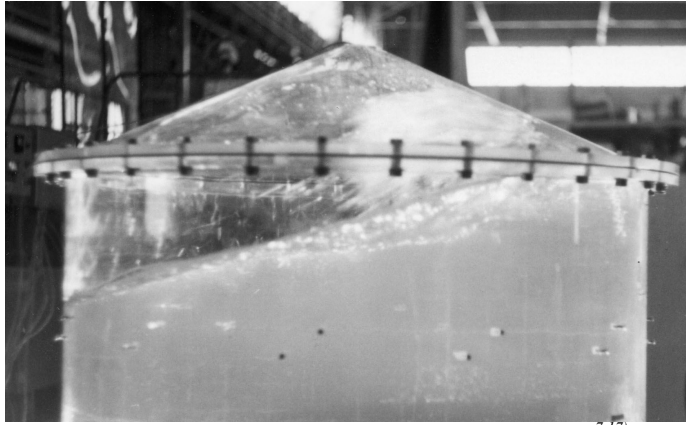
Fig.7.2.12   Sloshing at cone roof with 25deg slope [7.17)]
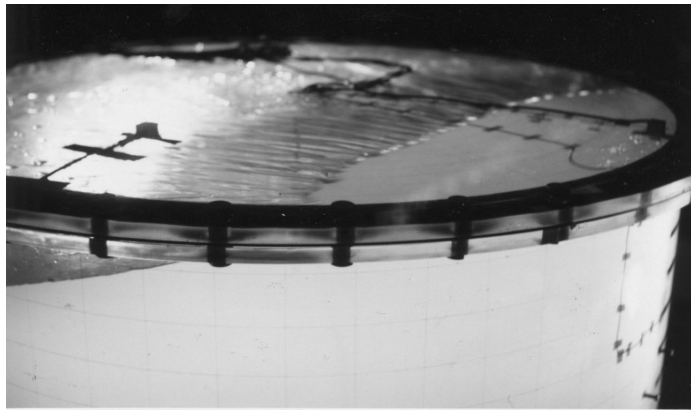
Fig.7.2.13   Sloshing at plate roof [7.17)]

Kobayashi [7.14] presented that the impulsive pressure P_i acting on the dome and cone roof tank can be estimated by Eq. (7.2.34), using the maximum sloshing velocity response without the fixed roof subjected to the sinusoidal input of which the period coincides with the sloshing natural period and three waves repeat. Transforming the impulsive pressure shown in the literature [7.14] represented by the gravimetric unit to SI unit, the following relation is obtained;

$$(7.2.35) \qquad P_i = 34.97 \rho \left(\dot{\varsigma}_r^A \right)^{1.6} \qquad [N/m^2].$$

Since the sloshing response is sinusoidal, the sloshing velocity $\dot{\varsigma}_r^A$ at the point A is approximately given as Eq. (7.2.36) using the distance h from the static liquid surface to the fixed roof;

$$(7.2.36) \qquad \dot{\varsigma}_r^A = \varsigma_r \omega_s \cos\left(\sin^{-1} \frac{h}{\varsigma_r} \right) \qquad [m/s]$$

where ω_s is the circular natural frequency of the sloshing.

From these discussions, the impulsive pressure and the hydrodynamic pressure at a point oriented an angle θ to the exciting direction is given as follows;

1. in the case of $\varphi \geq 5^{\circ}$

Impulsive pressure:

$$(7.2.37) \qquad P_i = \frac{\pi}{2} \rho \cot\varphi \left(\dot{\varsigma}_r^A \cos\theta \right)^2 \qquad [N/m^2]$$

hydrodynamic pressure:

(7.2.38) $P_h = \rho g (\varsigma_r - h) \cos \theta \quad [N/m^2]$

2. *in the case of $\varphi < 5°$*

   Impulsive pressure:

(7.2.39) $P_i = 34.97 \rho \left(\dot{\varsigma}_r^A \cos \theta \right)^{1.6} \quad [N/m^2]$

   hydrodynamic pressure: excluded

   Since the hydrodynamic pressure varies slowly according to the natural period of the sloshing, the earthquake resistance of the fixed roof can be examined by integrating the hydrodynamic pressure along the wetted surface of the roof statically.

   Since the magnitude of the impulsive pressure is high and the duration of action is very short, the earthquake resistance examination of the fixed roof by the impulsive pressure should take the dynamic response of the fixed roof into account [7.17]. For example, if the fixed roof is assumed to be a single degree of freedom system and the impulsive pressure is approximated as the half-triangle pulse shown in Fig.7.2.14, the transient response of the system is obtained from the response to the half-triangle pulse load in the very short period Δt. Thus the impulse response of the fixed roof can be calculated using the load f_s which is obtained by integrating the impulsive pressure along the wetted surface of the roof.

   When the equation of motion of a single degree of freedom system is given as Eq. (7.2.40);

(7.2.40) $m_r \ddot{x} + c_r \dot{x} + k_r x = f(t)$,

where m_r, c_r and k_r are the equivalent mass, the equivalent damping coefficient and the equivalent stiffness of the fixed roof, the response x to the half-triangle pulse under the initial conditions $x = 0, \dot{x} = 0$ is obtained as following using the Duhamel integral;

(7.2.41) $x(t) = \dfrac{4I}{k_r \omega_n \Delta t^2} \left\{ 2 \sin \omega_n \left(t - \dfrac{\Delta t}{2} \right) - \sin \omega_n (t - \Delta t) - \sin \omega_n t \right\}$,
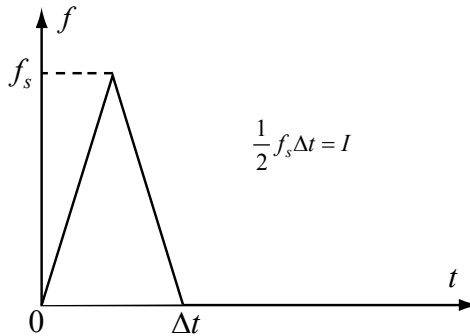
Fig.7.2.14   Pressure shape of half-triangle pulse

where ω_n is the natural circular frequency of the fixed roof, $I=(1/2)f_s\Delta t$ is the magnitude of the impulse during the small time interval Δt and $t>0$.

   In the case that ω_n is sufficiently smaller than $2\pi/\Delta t$, the impulse is assumed to be a delta function of magnitude $I=(1/2)f_s\Delta t$ and Eq. (7.2.41) is simplified into Eq. (7.2.42).

(7.2.42) $x(t) = \dfrac{1}{2} \Delta t \omega_n \cdot \dfrac{f_s}{k_r} \sin \omega_n t$.

From Eq. (7.2.42), multiplying the magnitude of response $(1/2)\Delta t \omega_n$ by pressure given as Eqs. (7.2.37) and (7.2.39) gives the equivalent pressure. The resultant force yielded by the equivalent pressure is obtained from

integrating along the wetted surface of the fixed roof. Stresses in the fixed roof due to the resultant force can be obtained using the resultant force as the static force.

Since the rising time of impulsive pressure is commonly shorter than 0.01s [7.17], it is recommended to set Δt as 0.02s on the safe side. ω_n should be calculated according to the actual structural characteristics of the fixed roof. For example, if Δt is 0.02s and ω_n is 12rad/s, the magnitude of response is reduced to 12% of that obtained on the assumption of static f_s itself acting. This result is obtained, from Eq. (7.2.42), on the assumption that the envelope of the maximum value of the impulsive pressure obtained by Eqs. (7.2.37) or (7.2.39) acts simultaneously over the wetted surface of the fixed roof.

The maximum impulsive pressures, actually, never act simultaneously all over the fixed roof, because the contact point, where the impulsive pressure yields, moves as the cap of the sloshing wave moves. Though this assumption seems too safe side to design, it is recommended to keep a margin of an unpredictable response magnification due to such as the moving force effect.

A guide to estimate the resultant force by applying Eq. (7.2.42) is that the natural frequency of the fixed roof is less than 15Hz when Δt is 0.02s. When the natural frequency of the fixed roof is more than 15Hz, the maximum response during $0 \le t \le \Delta t$ can be estimated using Eq. (7.2.41) and the magnitude of response to the static force can be obtained. Alternatively, the magnitude of response can be estimated by interpolating linearly between 15Hz to 45Hz of the natural frequency of the fixed roof, assuming the magnitude of response $(1/2)\Delta t \omega_n$ is 1.0 in the case of 15Hz and $(1/2)\Delta t \omega_n$ is 1.5 in the case of 45Hz.

7.3   Evaluation of Seismic Capacity

7.3.1   Checking of Seismic Capacity of Whole Tank

Design shear force of the impulsive mass vibration should satisfy equation (7.10).

(7.10) $_f Q_y \geqq Q_{dw}$

Design shear force of the convective mass vibration should satisfy equation (7.11).

(7.11) $_s Q_y \geqq Q_{ds}$

Notations:
$_f Q_y$ yield shear force of the storage tank at the impulsive mass vibration (kN)
$_s Q_y$ yield shear force of the storage tank at the convective mass vibration (kN)
Q_{dw} design shear force of the impulsive mass vibration (kN)
Q_{ds} design shear force of the convective mass vibration (kN)

7.3.2   Checking of Seismic Capacity for Tank

Checking of seismic capacity for tank parts should be conducted by comparing working stresses and strains at corresponding parts in the storage tank with the allowable values. Working stresses and strains should be obtained by combining seismic load and ordinary operation load.

Commentary:

1   Design shear force

The design shear force of the impulsive mass vibration Q_{dw} is given by the equation (7.3.1)

(7.3.1) $Q_{dw} = D_s \cdot S_B = Z_s \cdot I \cdot D_s \cdot S_{a1} \cdot m_f$

The design hoop stress at the bottom course of tank wall $_Q \sigma_{hd}$ is given by the equation (7.3.2)

(7.3.2) $_Q \sigma_{hd} = Q_{dw}/2.5 H_l t_0 + m_l g / \pi r t_0$

where, t_0 is the wall thickness at the bottom.

The design shear force of the convective mass vibration Q_{ds} is given by the equation (7.3.3)

(7.3.3) $Q_{ds} = Z_s \cdot I \cdot S_{a1} \cdot m_s$

The yield shear force of the storage tank at the convective mass vibration, $_sQ_y$, is approximately given as shown in equation (7.3.4)

(7.3.4) $_sQ_y = 0.44 \, _fQ_y.$

2   Design yield shear force

The design yield shear force of the storage tank, Q_y, is determined in accordance with equation (7.3.5).

(7.3.5) $Q_y = 2\pi r^2 q_y / 0.44 H_l$

This formula is modified as shown in equation (7.3.6), when elephant's foot bulge type buckling is evaluated,

(7.3.6) $_eQ_y = \pi r^2 \cdot _e\sigma_{cr} t_0 / 0.44 H_l$

where, $_e\sigma_{cr}$ is the critical stress for the elephant foot bulge type buckling.

It can be further modified as shown in equation (7.3.7), when the yield of the anchor strap is evaluated,

(7.3.7) $_aQ_y = 2\pi r^2 \cdot _a q_y / 0.44 H_l$

3   Evaluation flow

Figures 7.3.1 and 7.3.2 summarise the evaluation procedure for anchored and unanchored tanks respectively.

References:

[7.1]   Kobayashi, N. and Hirose, H.: Structural Damage to Storage Tanks and Their Supports, Report on the Hanshin-Awaji Earthquake Disaster, Chp.2, Maruzen (1997) pp353-378, (in Japanese)
[7.2]   Housner, G.W.: Dynamic Pressures on Accelerated Containers, Bull. Seism. Soc. Amer., Vol47, (1957) pp15-35
[7.3]   Velestos, A. S.: Seismic Effects in Flexible Liquid Storage Tanks, Proc. 5th World Conf. on Earthquake Engineering, Session 2B (1976)
[7.4]   Japanese Industrial Standards Committee: Welded Steel Tanks for Oil Storage, JIS B8501, (1985), (in Japanese)
[7.5]   Wozniak, R. S. and Mitchel, W. W.: Basis of Seismic Design Provisions for Welded Steel Storage Tanks, API Refinery Department 43rd Midyear Meeting, (1978)
[7.6]   API: Welded Steel Tanks for Oil Storage, App.E, API Standard 650, (1979)
[7.7]   Ishida, K and Kobayashi, N.: An Effective Method of Analyzing Rocking Motion for Unanchored Cylindrical Tanks Including Uplift, Trans., ASME, J. Pressure Vessel Technology, Vol.110 No.1 (1988) pp76-87
[7.8]   The Disaster Prevention Committee for Keihin Petrochemical Complex, A Guide for Seismic Design of Oil Storage Tank, (1984), (in Japanese)
[7.9]   Anti-Earthquake Design Code for High Pressure Gas Manufacturing Facilities, MITI (1981), (in Japanese)
[7.10]   Akiyama, H.: No.400, AIJ (1989), (in Japanese)
[7.11]   Akiyama, H. et al.: Report on Shaking Table Test of Steel Cylindrical Storage Tank, 1st to 3rd report, J. of the High Pressure Gas Safety Institute of Japan, Vol.21, No.7 to 9   (1984) (in Japanese)

[7.12]   H. Nishi, M. Yamada, S. Zama, K. Hatayama, K. Sekine : Experimental Study on the Sloshing Behaviour of the Floating Roof using a Real Tank, JHPI Vol. 46 No.1, 2008

[7.13]   AIJ (Architectural Institute of Japan) : Structural Response and Performance for Long Period Seismic Ground Motions, 2007.12, (in Japanese)

[7.14]   Nobuyuki Kobayashi: Impulsive Pressure Acting on The Tank Roofs Caused by Sloshing Liquid, Proceedings of 7th World Conference on Earthquake Engineering, Vol.5, 1980, pp. 315-322

[7.15]   Yoshiyuki Yamamoto: in Japanese, Journal of High Pressure Institute of Japan, Vol.3, No.1, 1965, pp. 370-376

[7.16]   Chikahiro Minowa: Sloshing Impact of a Rectangular Water Tank : Water Tank Damage Caused by the Kobe Earthquake, Transaction of JSME, Ser. C, Vol.63, No. 612, 1997, pp. 2643-2649, in Japanese

[7.17]   Yoshio Ochi and Nobuyuki Kobayashi: Sloshing Experiment of a Cylindrical Storage Tank, Ishikawajima-Harima Engineering Review, Vol.17, No. 6, 1977, pp. 607-615

```
 ┌───┐            ╭──────────────────╮
 │ 1 │ ─────────▶│   Design Spec.    │
 └───┘            ╰──────────────────╯
                           │
              ┌────────────────────────────┐
              │  Checking for impulsive mass │
              └────────────────────────────┘
                           │
              ┌────────────────────────────┐
              │  Checking of buckling capacity│
              └────────────────────────────┘
```

Calculate K_1 by Eq. (7.2.17)

Calculate T_e by Eq. (7.2.19)

Calculate $_e\sigma_{cr}$ and $_Q\sigma_{hd}$ by Eqs. (3.54) and (7.3.2)

Calculate D_s of buckling by Eq. (7.6)

Calculate $_eQ_y$ by Eq. (7.3.6)

Calculate Q_{dw} by Eqs. (7.3.1)

$_eQ_y > Q_{dw}$ — No → 1

Yes

Checking of bottom plate capacity

Calculate D_s of bottom plate by Eq. (7.3) or (7.4)

Calculate q_y by Eq. (7.2.11)

Calculate Q_{dw} by Eq. (7.3.1)

Calculate Q_y by Eq. (7.3.5)

$Q_y > Q_{dw}$ — No → 1

Yes

Checking for convective mass

Calculate Q_{ds} by Eq. (7.3.3)

Calculate $_sQ_y$ by Eq. (7.3.4)

Pressure to fixed roof by Eq.7.2.37 ~ 39

$_sQ_y > Q_{ds}$ — No → 1

Yes

Finish

Fig.7.3.1 Evaluation flow for unanchored tanks

1 → Design Spec.

Checking for impulsive mass

Checking of buckling capacity

Calculate D_s of buckling by Eq. (7.6)

Calculate $_e\sigma_{cr}$ and $_Q\sigma_{hd}$ by Eqs. (3.54) and (7.3.2)

Calculate Q_{dw} by Eqs. (7.3.1)

Calculate $_eQ_y$ by Eq. (7.3.6)

$_eQ_y > Q_{dw}$ — No → 1

Yes

Checking of anchor strap capacity

Calculate K_1 by Eq. (7.2.30)

Calculate T_e by Eq. (7.2.29)

Calculate $_aq_y$ by Eq. (7.2.25)

Calculate D_s of anchor strap by Eq. (7.5)

Calculate $_aQ_y$ by Eq. (7.3.7)

Calculate Q_{dw} by Eq. (7.3.1)

$_aQ_y > Q_{dw}$ — No → 1

Yes

Checking for convective mass

Calculate Q_{ds} by Eq. (7.3.3)

Calculate $_sQ_y$ by Eq. (7.3.4)

Pressure to fixed roof by Eq.7.2.37 ~ 39

$_sQ_y > Q_{ds}$ — No → 1

Yes

Finish

Fig.7.3.2 Evaluation flow for anchored tanks

8 Seismic Design of Under-ground Storage Tanks

8.1 Scope

This chapter covers the seismic design of water tanks, cylindrical tanks, etc., which are either completely buried, or have a considerable part of the outside surface below ground level. For the purposes of this recommendation, the general structural design is assumed to be regulated by the relevant codes and standards.

Commentary:

1. General

The seismic advantage of under-ground tanks is that they are not subjected to the same vibration amplification as above-ground structures. However, as the surrounding soil has a significant influence on the seismic behaviour, this, together with the inertia force of the stored material, should be taken into account when designing for seismic loads.

2. Definition of an under-ground tank

For the purposes of this recommendation, an under-ground storage tank may be defined as a storage tank which is for the most part covered by earth or similar materials and whose seismic response depends on the surrounding soil. Figure 8.1.1 illustrate the general concept of under-ground tanks.
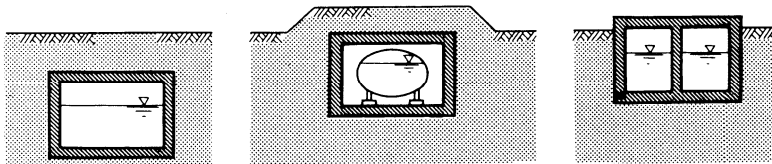
Figure 8.1.1 Conceptual examples of under-ground tanks

Although under-ground tanks may be constructed from steel, concrete, wood, FRP, or other combinations of materials, the outer part of them which is in contact with soil is generally of concrete, e.g., under-ground steel tanks usually have outer under-ground containers of concrete. In view of this generally accepted method of construction, only concrete and pre-stressed concrete structures are considered in this chapter.

8.2 Seismic Design

8.2.1 Under-ground tanks should be constructed in satisfactory and stable ground. Soft ground, or inclined ground which is subject to sliding and slope failure should be avoided, as should ground with abrupt changes in contours or materials, or at connecting sections with different structures where significant deformation and stress can be expected. However, when construction on unstable ground is unavoidable, it is preferable that suitable soil improvement measures, piled foundations, or other methods are adopted for higher seismic safety.

8.2.2   The seismic intensity method, response displacement method or a dynamic analysis may be used in the seismic design of under-ground tanks. A dynamic analysis is preferable when the tank has an interface with other structures or is constructed in soil with abrupt changes of soil properties.

The design should fully consider the seismic loads resulting from the deformation of the surrounding soil, from the inertia force of tanks and contained materials, and from the seismic earth pressure in the ultimate state for out-of plane stress of under-ground walls.

8.2.3   Soil properties for the seismic design model should include the effect of soil strain level during earthquakes.

8.2.4   Buoyancy should be taken into account if there is the possibility of surrounding soil liquefaction.

Commentary:

1. *Seismic performance of under-ground tanks depend upon seismic stability and the response of surrounding soil. Examples from recent earthquakes show that the following conditions contributed significantly to the resulting damage of under-ground tanks:*

    - under-ground structures built in soft ground,
    - under-ground structures built in ground with abrupt changes in profile or materials,
    - connecting section with different type of structures or incidental equipment.

    Sinking, lifting, inclination and translation of under-ground structures may take place during earthquakes in soft ground because of significant soil deformation or liquefaction. It is therefore recommended that under-ground tanks should be constructed in stable ground.

    Soft ground, or inclined ground which is subject to sliding and slope failure should be avoided, as should ground with abrupt changes in contours or materials, or at connecting sections with different structures where significant deformation and stress can be expected. However, when construction on unstable ground is unavoidable, it is preferable that a comprehensive geological survey is performed, and soil improvement, piled foundations, or other measures are adopted for better seismic safety, (refer to the "Recommendation for the design of building foundations" - Architectural Institute of Japan).

2. *Under-ground seismic intensity and soil displacement for the response displacement method may be calculated using the guidelines and formulae contained in Chapter 3.6.2. Similarly, seismic earth pressures may be calculated using the guidance and formulae given in Chapter 3.8.2.*

    As under-ground tanks are bounded by soil, their seismic behaviour will depend mainly on the displacement and deformation of the surrounding soil.   Whilst the dynamic characteristics of the structures themselves have less influence on their seismic response than above-ground tanks, the properties of the stored materials and their inertia force need to be taken into account.

    The response displacement method, seismic intensity method and dynamic analysis are the recommended evaluation methods and as such are explained in the following paragraphs. In these methods, both the surrounding soil and the structure are analysed and their displacement, deformation, and inertia forces are taken into account simultaneously.

It must be noted that utility tunnels, under-ground pipes and linear sealed tunnels etc., or horizontally long structures are excluded in this chapter. However, such kind of structures, when associated with under-ground storage tanks, should be examined for deformation in horizontal section, and reference should be made to the relevant standards and recommendations.

Figure 8.2.1 below is a flow chart for the three methods,

- *the response displacement method uses soil springs for the ground model where ground displacement, circumferential shear force, and inertia force are taken into consideration,*
- *the seismic intensity method, which normally uses a two dimensional FEM model for the ground and gives the static under-ground seismic intensity,*
- *and the dynamic analysis which also uses an FEM model for the ground and gives the dynamic load (earthquake motion).*

Response Displacement Method	Seismic Intensity Method	Dynamic Analysis

Modeling of Tank and Contents Modeling of Soil (Ground Spring)	Modeling of Tank and Contents Modeling of Soil (FEM and so on)	Modeling of Tank and Contents Modeling of Soil (FEM and so on)
Ground Deformation / Surround Shear Force / Inertia Force	Ground Intensity	Input Seismic Wave
Calculation of Seismic Stress	Calculation of Seismic Stress	Calculation of Seismic Stress

Fig. 8.2.1 Method flow chart for seismic analysis methods

The following paragraphs give a conceptual outline of the three evaluation methods.

a) Response displacement

Figure 8.2.2 shows a model for applying the response displacement method to an under-ground tank where the predominant consideration is the shear deformation in the cross section of the structure due to shear wave seismic motion of the ground.

The first step involves the calculation of the shear deformation for the free field using equation (3.16) or the1-D wave propagation theory. The second step involves calculating the relative displacement of the free field to the tank bottom level soil and through to the top of the tank level soil.

The relative displacement of the free field is applied to the soil springs around the tank structure as shown in Fig. 8.2.2.

Circumferential shear forces are applied to the outside under-ground walls, and inertia forces for under-ground seismic intensity, (refer to Chapter 3.6.2.2), are applied to the tank structure and stored material.

Refer also to Chapters 4, 5, and 7 for details of the inertia force of stored materials.

The response displacement method has a clear logical basis. The soil springs should preferably be calculated using FEM model of the ground, but may also be calculated using simpler methods. Appendix B shows dependence of the stress on soil springs, soil deformation, circumferential shear force and inertia force.
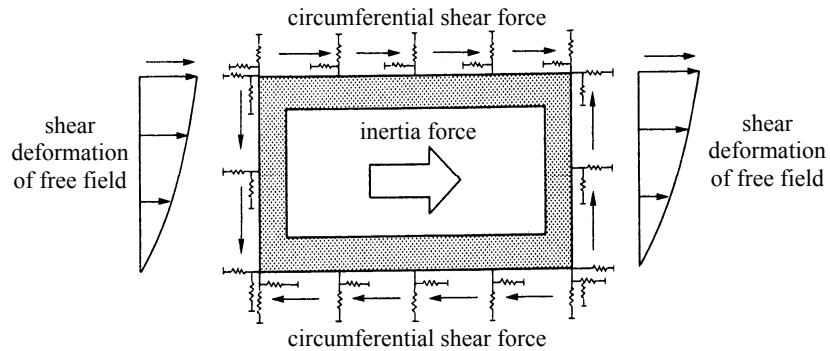
Fig. 8.2.2 Structural model and forces for the response displacement method

b) Dynamic analysis

Dynamic analysis gives the most reliable result because both the under-ground tank and the surrounding soil are analysed using an FEM model and the earthquake motion is given as a dynamic load. However, it is important that the modeling region, boundary conditions, and the input earthquake motions should carefully be chosen to ensure that the most reliable results are obtained. (Refer to Appendix B.)

c) Seismic intensity method

The seismic intensity method is similar to the dynamic analysis in that the under-ground tank and the surrounding soil are analysed using an FEM model, but the seismic intensity is given as static load. Because the method involves a static analysis, the modeling region and the boundary conditions may be different from the dynamic analysis. (Refer to Appendix B.)

Evidence taken from seismic damage shows that the most critical parts for under-ground structures are where there are abrupt changes in the soil conditions, structural properties, or sections connecting different types of structures. In such cases it is preferable that a detailed analysis, such as a dynamic analysis, is performed to ensure seismic safety.

3. *In general, the seismic response of the ground is non-linear. Therefore, the soil strain level should be taken into consideration together with the appropriate equivalent soil stiffness when the soil spring constants are evaluated. The equivalent soil stiffness may be calculated using the 1-D wave propagation theory with the equivalent linear method etc. (Refer to Appendix B). Some references give a simple estimation of the modification factor for grounds with a shear wave velocity of less than 300m/sec. But as an excessive reduction of soil stiffness reduces the safety margin, a careful estimation of the stiffness reduction is essential.*

4. *Because the unit weight of the surrounding soil is greater than that of under-ground tanks or other under-ground structures, they may be subject to lifting when liquefaction of the surrounding soil occurs. This was evident during the Niigata earthquake in 1964, and the Nihon-Kai-Chubu earthquake in 1983, when underpasses, under-ground oil tanks, water tanks and manholes to under-ground piping were damaged when they were pushed towards*

the surface due to the liquefaction of the surrounding soil. Therefore, due consideration should be given to this phenomenon when there is a possibility of liquefaction. It must be noted however, that stored materials should not be taken into consideration when evaluating these conditions. Figure 8.2.3 below shows the forces acting on under-ground tanks during liquefaction.
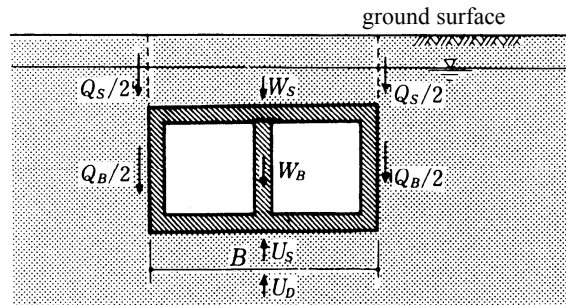
Figure 8.2.3   Forces acting on under-ground tanks during liquefaction.

In the event that liquefaction is possible, Q_S and Q_B are neglected. The forces shown are for unit thickness of the under-ground tank.

The safety factor F_S for lifting due to liquefaction is calculated using equation (8.2.1) below.

(8.2.1) $$F_S = \frac{W_S + W_B + Q_S + Q_B}{U_S + U_D}$$

where:

W_S *weight of the overburden (water included) (N/m)*

W_B *weight of the under-ground tank (stored material and levelling concrete included) (N/m)*

Q_S *shear strength of the overburden (N/m)*

Q_B *frictional strength of the side walls and soil(N/m)*

U_S *buoyancy on tank bottom caused by hydrostatic pressure (N/m)*

U_D *buoyancy caused by excess pore water pressure (N/m)*

8.3   Checking of Seismic Capacity

Stresses in the structure are compared with the design limits. However, sufficient ductility is necessary in the structure because the surrounding soil acts to deform all the members.

Commentary:

1. *Working stresses in under-ground tanks are calculated assuming the most severe combination of seismic loads, the dead load, stored material properties, static earth pressure, hydrostatic pressure, etc., these are then compared with allowable stresses. Stresses that fall within the elastic range of the materials are recommended. The surrounding soil acts to deform the structural members and therefore no reduction of seismic loads due to any plastic deformation of the structure can be expected. It is therefore recommended that seismic designs should have enough ductility to withstand all the stresses indicated above, and should take into account the lessons learned from the seismic damage caused to under-ground structures with insufficient ductility.*

APPENDIX A
DESIGN AND CALCULATION EXAMPLES

APPENDIX A1   STEEL WATER TOWER TANKS

A1.1   Description of water tower tank

A1.1.1   Outline

The structural outline and design conditions are shown in Table A1.1.

Table A1.1   Design Conditions

Description	Usage Structural type Shape	Tower for water supply Steel plate tower Vessel – Cylindrical shell Tower – Cylindrical column
Outline of structure	Height Vessel diameter Diameter of tower	GL + 35.35m 6.8m 1.6~3.4m
Outline of vessel	H.W.L L.W.L Water capacity Total volume	GL + 34.35m GL + 32.0m 80m^3 93.4m^3
Design Conditions	Standards and codes	a. Building Standard Law b. Design Recommendation for Storage Tanks and Their Supports (AIJ) c. Design Standard for Steel Structures (AIJ) d. Standard for Structural Calculation of RC Structures (AIJ) e. Japanese Industrial Standards (JIS)
		Steel – JIS G 3136 SN400B Concrete – Fc = 21N/mm^2 Reinforced bars – SD295
	Allowable stress	Refer to b. and c.

A1.2   Calculation of Tube Tower

A1.2.1   Assumed section of tube tower

The natural period of the tower is calculated with the thickness without reducing the 1 mm of corrosion allowance. The outline of the water tower tanks is shown in Figure A1.1.
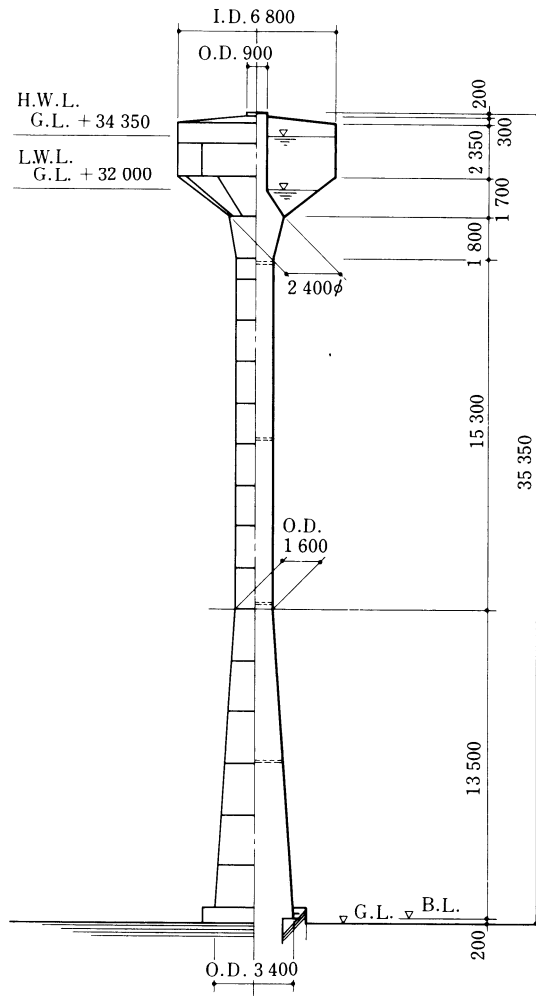
Fig. A1.1   Outline of Water Tower Tank

A1.2.2   Assumed loads

  (1) Vertical Load

The total vertical load upon its base plate: mass

Water   915.32k N (93,400 kg)

Vessel   107.80 kN (11,000 kg)

Pipe (1.47kN/m)   47.04 kN (4,800 kg)

Deck (26.46kN for each)   105.84 kN (10,800 kg)

Tube weight   107.80 kN (11,000 kg)

                        1,283.80 kN (131,000 kg)

The sectional dimensions and modeling of the tower are shown in Table A1.2 and Figrure A1.2, respectively.

Table A1.2   Sections of Tower

	Level B. L + (m)	h_n (cm)	OD (cm)	t (cm)
	30.6		240	
		180		0.9
	28.8		160	
		90		0.9
	27.9		160	
		360		1.2
	24.3		160	
		360		1.4
	20.7		160	
		360		1.4
	17.1		160	
		360		1.6
	13.5		160	
		450		1.6
	9.0		220	
		450		1.4
	4.5		280	
		450		1.4
	0		340	

Fig.A1.2   Modeling of Tower

A1.2.3   Stress Calculation

(1)   Modified Seismic Coefficient Method

The flexibility matrix and the mass matrix are obtained from the following equation:

Flexibility matrix,

$$[F] = \begin{bmatrix} 0.0343 & 0.1228 \\ 0.1228 & 1.0903 \end{bmatrix}$$

Mass matrix,

$$[M] = \begin{bmatrix} m_1 & 0 \\ 0 & m_2 \end{bmatrix}$$

$$\therefore T_1 = 1.572 \, \text{s}$$

$$T_2 = 0.106 \, \text{s}$$

$$B = 1.0, Z_s = 1.0, I = 1.0, D_s = 0.5, T_g = 0.96,$$

$$T_1 > T_g$$

From (3.2)

$$\therefore C = Z_s \cdot I \cdot D_s \cdot \frac{T_g}{T_1} = 0.305 > 0.3 Z_s I$$

$$W = W_1 + W_2 = 683.52 \, \text{kN}$$

$$Q_d = C \cdot W = 208.47 \, \text{kN}$$

$$Q_{ei} = Q_{di} / B$$

From (3.4)

$$f_{di} = Q_d \frac{\sum_{m=i}^{n} W_m \cdot h_m}{\sum_{m=1}^{n} W_m \cdot h_m}$$
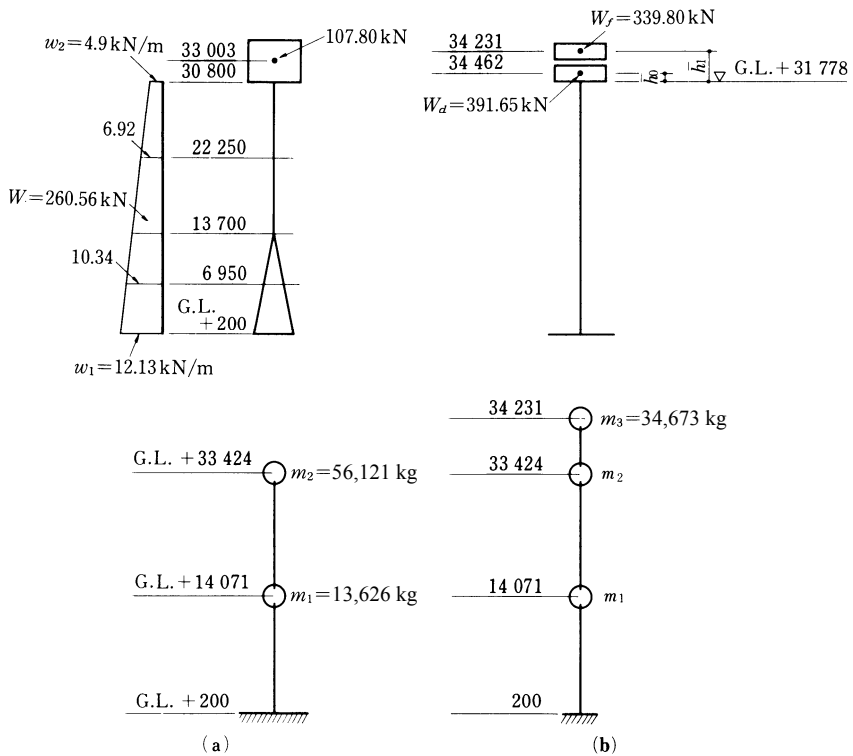
Fig.A1.3   Lumped Mass Model

Table.A1.3 Q_{ei} Obtained by Calculations

i	W_i (kN)	ΣW_i (kN)	h_i B. L.+ (m)	$\sum\limits_{m=i}^{n} W_m \cdot h_m$	$\dfrac{\sum\limits_{m=i}^{n} W_m \cdot h_m}{\sum\limits_{m=1}^{n} W_m \cdot h_m}$	$\dfrac{Q_d}{B}$	Q_{ei} (kN)	M_{ei} (kN·m)
2	549.99	549.99	33.224	18 272.9	0.908		189.14	3 650.5
1	133.53	683.52	13.871	20 125.1	1.0	208.47	208.47	6 552.3

(2) Modal Analysis

The flexibility matrix and the mass matrix are obtained from the model shown in Fig. A1.3(b) as follows:

$$[F] = \begin{bmatrix} 0.0343 & 0.1228 & 0.1265 \\ 0.1228 & 1.0903 & 1.1415 \\ 0.1265 & 1.1415 & 7.2404 \end{bmatrix}$$

$\delta'_{33} = 1/K_2$ is added to δ_{33} from stiffness coefficient, where K_2 is the spring constant for the convective mass.

$$[M] = \begin{bmatrix} m_1 & 0 & 0 \\ 0 & m_2 & 0 \\ 0 & 0 & m_3 \end{bmatrix}$$

$Q_{d1} = 157.09$ kN $< 0.3Z_sIW = 205.02$ kN

Stresses in modal analysis are obtained by multiplying with $\dfrac{0.3Z_sIW}{Q_{d1}}$ as follows:

$$Q_{ei} = \frac{Q_{di}}{B} \cdot \frac{0.3Z_sIW}{Q_{d1}}$$

Table.A1.4 Natural Periods, u, β and C

j (th)	i	T_j (s)	u_{ij}	β_j	S_{aj}	C_j
1	3	3.259	1.0	1.248	288.7	0.147
	2		0.196			
	1		0.0218			
2	3	1.402	1.0	−0.248	671.0	0.342
	2		−3.147			
	1		−0.358			
3	3	0.106	1.0	0.00015	980	0.500
	2		−162.54			
	1		5 895.3			

$Z_s = 1.0$, $I = 1.0$, $D_s = 0.5$, $T_o = 0.96$ s

Table.A1.5 Q_{ei} Obtained by calculation

mass	W_i (kN)	$\beta_1 \cdot u_{i1}$	$C_1 \sum\limits_{m=i}^{3} W_m \cdot \beta_1 \cdot u_{i1}$	$\beta_2 \cdot u_{i2}$	$C_2 \sum\limits_{m=i}^{3} W_m \cdot \beta_2 \cdot u_{i2}$	$\beta_3 \cdot u_{i3}$	$C_3 \sum\limits_{m=i}^{3} W_m \cdot \beta_3 \cdot u_{i3}$	Q_{di} (kN)
3	339.80	1.249	62.39	−0.249	−28.93	0.00015	0.03	68.80
2	549.99	0.246	82.27	0.778	117.40	−0.0246	−6.73	143.57
1	133.53	0.130	84.83	0.0894	121.48	0.884	52.28	157.09

Table.A1.6 Calculation of Q_{ei} and M_{ei}

i	h_i B. L. + (m)	Q_{ei} (kN)	M_{ei} (kN·m)
3	34.031	89.77	72.423
2	33.224	187.38	3 698.52
1	13.871	205.02	6 542.48
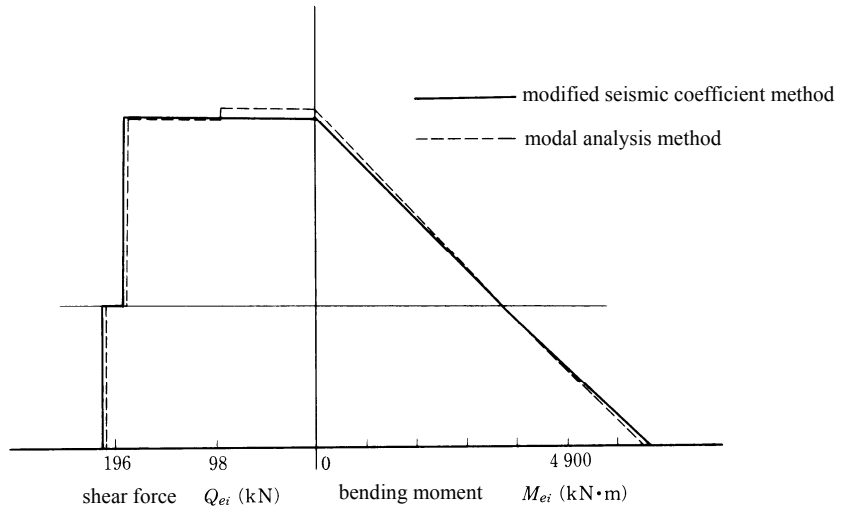
Fig.A1.4 Comparision of Stresses obtained using the Modified Seismic Coefficient Method and the Modal Analysis

A1.3   Water Pressure Imposed on the Tank

Impulsive mass (water),

$$Q = (Q_{e2} - Q_{e1})\frac{W_d}{56.21} = 69.39 \text{ kN} = \iint \overline{P} \cdot R d\varphi \cdot dy$$

Convective mass (water),

$$Q' = 89.77 \text{ kN} = \iint \overline{P} R d\varphi \cdot dy$$

Height of wave due to sloshing; from (7.9),

$$\eta_s = \frac{0.802 \cdot Z_s \cdot I \cdot S_{v1}}{B} \sqrt{\frac{D}{g} \tanh\left(\frac{3.682h}{D}\right)} = 1.104 \text{ m}$$

$$S_{v1} = 2.11 \times \frac{1}{1.2} = 1.758 \text{ m/s}$$
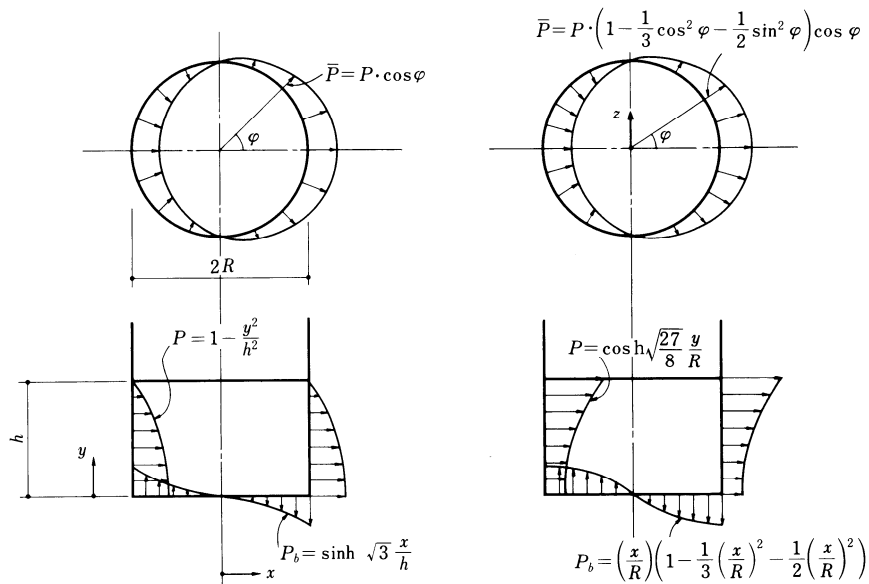
Fig.A1.5   Water Pressure due to Sloshing

A1.4   Wind Loads

(1) Wind loads

Wind loads are obtained from chapter 6 "Wind Loads" of Recommendations for Loads on Buildings (2004), AIJ.

a) Design wind speed

Basic wind speed $U_0 = 36 \text{ (m/s)}$

Height Coefficient

$$E_H = E_r \cdot E_g = 1.205 \times 1.0 = 1.205$$

From exposure II,

$$Z_b = 5 \text{ m}, \quad Z_G = 350 \text{ m}, \quad \alpha = 0.15$$

$$E_r = 1.7 \times \left(\frac{35.35}{350} \right)^{0.15} = 1.205$$

Return period conversion coefficient

$$k_{rw} = 0.63(\lambda_u - 1)I_{nr} - 2.9\lambda_u + 3.9 = 0.952$$

Return period $r = 50$ years, $\lambda_u = U_{500}/U_0 = 1.111$

Design wind speed at standard height

$$U_H = U_0 \cdot k_D \cdot E_H \cdot k_{rw} = 36 \times 1.00 \times 1.205 \times 0.952 = 41.29 \text{ (m/s)}$$

b) Design velocity pressure

$$q_H = \frac{1}{2} \times \rho \times U_H^2 = \frac{1}{2} \times 1.22 \times 41.29^2 = 1,040 \text{ (N/m}^2)$$

Air Density $\rho = 1.22$ (kg/m^3)

c) Pressure coefficient

From $H/D = 35.35/4.6 = 7.68$

$Z \leqq 5$m,

$$C_D = 1.2 \times k_1 \cdot k_2 \cdot k_Z = 1.2 \times 0.6 \times \left(\frac{H}{D} \right)^{0.14} \times 0.75 \times \left(\frac{Z_b}{H} \right)^{2\alpha}$$

$$= 1.2 \times 0.6 \times 7.7^{0.14} \times 0.75 \left(\frac{5.0}{35.35} \right)^{2 \times 0.15} = 0.400$$

28.28m > Z > 5m,

$$C_D = 1.2 \times k_1 \cdot k_2 \cdot k_Z = 1.2 \times 0.6 \times 7.7^{0.14} \times 0.75 \times \left(\frac{Z}{35.35} \right)^{0.3} = 0.247 \times Z^{0.3}$$

$Z \geqq 28.28$m,

$$C_D = 1.2 \times k_1 \cdot k_2 \cdot k_Z = 1.2 \times 0.6 \times 7.7^{0.14} \times 0.75 \times 0.8^{0.3} = 0.672$$

d) Gust effect factor

exponent for mode shape β	2.500
total building mass M	104420kg
generalized building mass M_D	84644kg
λ	0.633
mode correction factor ϕ_D	0.174
turbulence scale at reference height L_H	108.6m
turbulence intensity at reference height Ir_H	0.158

topography factor for the standard deviation

of fluctuating wind speed E_I 1.000

topography factor for turbulence intensity E_{gI} 1.000

$I_H = Ir_H \cdot E_{gI}$ 0.158

gust effect factor

natural frequency for the first mode in

along-wind direction f_D 0.713Hz

damping ratio for the first mode in

along-wind direction ζ_D 0.010

C_g 0.457

k 0.070

C'_g 0.127

R 0.386

F 0.075

S_D 0.404

F_D 0.033

R_D 2.593

v_D 0.606

g_D 3.604

gust effect factor G_D 2.044

e)   Wind load

$$W_D = q_H \cdot C_D \cdot G_D \cdot A$$

$Z \leqq 5\text{m}$

$$W_D = 1{,}040 \times 0.400 \times 2.044 \times A = 850 \times A$$

$28.28\text{m} > Z > 5\text{m}$

$$W_D = 1{,}040 \times 0.247 \times Z^{0.3} \times 2.044 \times A = 0.525 \times Z^{0.3} \times A$$

$Z \geqq 28.28\text{m}$

$$W_D = 1{,}040 \times 0.672 \times 2.044 \times A = 1{,}429 \times A$$

(2)   Wind load for vortex oscillation

a)   Calculation model

In this example, the calculation model is assumed to have the shape shown in Fig. A1.6, and the water content is assumed to be empty.

Natural period T_1,

From $[F] = \begin{bmatrix} 0.0343 & 0.1111 \\ 0.1111 & 0.7952 \end{bmatrix}$

$T_1 = 0.726$ s

$[M] = \begin{bmatrix} m_1 & 0 \\ 0 & m'_2 \end{bmatrix}$
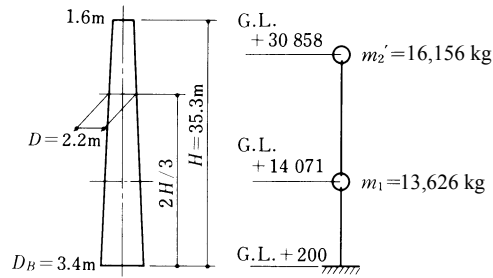
Fig.A1.6　Calculation Model

Table.A1.7　Sectional Forces by Wind Load in the Along Direction

Level GL + (m)	$q_H \cdot C_D \cdot G_D$ (kN/m²)	A_w (m²)	Q_n (kN)	h_n (m)	M (kN·m)
33.003	1.429	23.12	33.04		0 —
				2.203	
30.8	1.429	1.98	35.87		72.79 —
				1.8	
29.0	1.429	2.34	39.21		137.35 —
				0.9	
28.1	1.428	3.6	44.35		172.64 —
				3.6	
24.5	1.371	5.76	52.25		332.30 —
				3.6	
20.9	1.307	5.76	59.78		520.40 —
				3.6	
17.3	1.235	5.76	66.89		735.61 —
				3.6	
13.7	1.151	6.82	74.74		976.41 —
				4.5	
9.2	1.022	9.9	84.86		1312.74 —
				4.5	
4.7	0.850	12.6	95.57		1694.61 —
				4.5	
0.2	0.850	7.31	101.78		2124.68 —

b)　Calculation of wind load for vortex oscillation

The possibility of vortex oscillation is checked　according to Chapter 6 "Wind Load" of the "Recommendations for Loads on Buildings (2004)", AIJ as follows.

$$W_r = 0.8 \cdot \rho U_r^2 C_r \frac{Z}{H} A$$

in which,

$$U_r = 5 \cdot f_L \cdot D_m = 5 \times 1.38 \times 2.2 = 15.18 \, (\text{m/s}) : \text{resonance wind speed}$$

where,

$f_L = 1.38$: natural frequency of water tower tank (Hz)

$\rho = 1.22 \, (\text{kg/m}^3)$: air density

$H = 35.3 \, (\text{m})$: tower height

$D_m = 2.20 \, (\text{m})$: diameter at the level 2/3 H

$C_r = 4.03$: pressure coefficient in resonance

$$\left. \begin{array}{l} U_r \cdot D_m = 15.18 \times 2.2 = 33.4 > 6.0 \\ \rho_s \sqrt{\zeta_L} = 142 \times \sqrt{0.02} = 20.1 > 5.0 \end{array} \right\} \quad \text{then,} \quad C_r = \frac{0.57}{\sqrt{\zeta_L}} = 4.03$$

$\zeta_L = 0.02$: damping ratio of water tower tank

$$\rho_s = \frac{M}{H \cdot D_m \cdot D_B} = \frac{37,600}{35.3 \times 2.2 \times 3.4} = 142 \, (\text{kg/m}^3)$$

$M = 37,600 \, (\text{kg})$

Then,

$$W_r = 0.8 \rho U_r^2 C_r \frac{Z}{H} A = 0.8 \times 1.22 \times 15.18^2 \times 4.03 \times \frac{Z}{35.3} \times A = 25.7 \times Z \times A \, (\text{N})$$

The cross section of the tower should be designed with the composite force of obtained from the wind load itself and the wind load for vortex oscillation

Table.A1.8 Forces Caused by Wind Load Vortex Oscillation

Level GL+ (m)	$0.8\rho U_r^2 \frac{C_r}{H}$ (kN/m²)	A_w (m²)	W_r (kN)	Q_h (kN)	h_h (m)	M (kN·m)	Section forces in wind along direction		Composite forces	
							Q'_n (kN)	M'_n (kN·m)	Q (kN)	M (kN·m)
33.003	0.0257	23.12	19.61	19.61		0	33.04	0	39.41	0
					2.203					
30.8	0.0257	1.98	1.57	21.18		43.20	35.87	72.79	41.66	84.64
					1.80					
29.0	0.0257	2.34	1.74	22.92		81.32	39.21	137.35	45.42	159.62
					0.90					
28.1	0.0257	2.60	1.88	24.80		101.95	44.35	172.64	50.81	200.50
					3.60					
24.5	0.0257	5.76	3.63	28.43		191.23	52.25	332.30	59.48	383.40
					3.60					
20.9	0.0257	5.76	3.09	31.52		293.58	59.78	520.40	67.58	597.50
					3.60					
17.3	0.0257	5.76	2.56	34.08		407.05	66.89	735.61	75.07	840.72
					3.60					
13.7	0.0257	6.82	2.40	36.48		529.74	74.74	976.41	83.17	1110.86
					4.50					
9.2	0.0257	9.90	2.34	38.82		693.90	84.86	1312.74	93.32	1484.85
					4.50					
4.7	0.0257	12.60	1.52	40.34		868.59	95.57	1694.61	103.73	1904.25
					4.50					
0.2	0.0257	7.31	0.04	40.38		1050.12	101.78	2124.68	109.50	2370.02

Table.A1.9 Forces List

Joint No.	Axial force N (kN)		Seismic (modified seismic coefficient)		Seismic (modal analysis)		Wind in along dir.		Wind for vortex oscillation	
	Full	Empty	Q (kN)	M (kN·m)	Q (kN)	M (kN·m)	Q (kN)	M (kN·m)	Q (kN)	M (kN·m)
10	1 023.12	107.80	189.14	491.96	187.38	558.60	35.87	72.79	21.18	43.20
9	1 031.94	116.62	189.14	832.02	187.38	896.70	39.21	137.35	22.92	81.32
8	1 036.84	121.52	189.14	1 002.54	187.38	1 065.26	44.35	172.64	24.80	101.95
7	1 058.40	143.08	189.14	1 683.64	187.38	1 739.50	52.25	332.30	28.43	191.23
6	1 082.90	167.58	189.14	2 364.74	187.38	2 413.74	59.78	520.40	31.52	293.58
5	1 110.34	195.02	189.14	3 044.86	187.38	3 088.96	66.89	735.61	34.08	407.05
4	1 141.70	226.38	208.74	3 731.84	205.02	3 768.10	74.74	976.41	36.48	529.74
3	1 183.84	268.52	208.74	4 671.66	205.02	4 691.26	84.86	1312.74	38.82	693.90
2	1 231.86	316.54	208.74	5 610.50	205.02	5 613.44	95.57	1694.61	40.34	868.59
1	1 283.80	368.48	208.74	6 552.28	205.02	6 542.48	101.78	2124.68	40.38	1050.12

Table.A1.10　Section Properties and Allowable Stresses

Joint No.	OD (cm)	t (cm)	A (cm²)	Z (cm²)	Long term $_c\bar{f}_{cr}$ (kN/cm²)	Long term $_b\bar{f}_{cr}$ (kN/cm²)	Long term $_s\bar{f}_{cr}$ (kN/cm²)	Seismic $_c\bar{f}_{cr}$ (kN/cm²)	Seismic $_b\bar{f}_{cr}$ (kN/cm²)	Seismic $_s\bar{f}_{cr}$ (kN/cm²)
10	239.8	0.8	600.7	35 771	12.417	13.201	3.205	20.247	21.041	7.703
9	159.8	0.8	399.6	15 805	14.053	14.504	5.449	21.883	22.344	9.967
8	159.8	0.8	399.6	15 805	14.053	14.504	5.449	21.883	22.344	9.967
7	159.8	1.1	548.4	21 610	14.955	15.210	6.733	22.785	23.050	11.201
6	159.8	1.3	647.3	25 443	14.955	15.504	7.183	23.138	23.344	11.701
5	159.8	1.3	647.3	25 443	14.955	15.504	7.183	23.138	23.344	11.701
4	159.8	1.5	746.0	29 247	15.582	15.680	7.556	23.412	23.520	12.064
3	219.8	1.3	892.4	48 459	14.563	14.906	6.145	22.383	22.746	10.652
2	279.8	1.3	1 137.4	78 826	13.798	14.298	5.106	21.629	22.138	9.614
1	339.8	1.3	1 382.5	116 545	13.044	13.720	4.057	20.874	21.540	8.565

Table.A1.11　Design of Section

(1) Full water tank (modified seismic coefficient method)

Joint No.	N (kN)	M (kN·m)	Q (kN)	σ_t	$\dfrac{\sigma_c}{_c\bar{f}_{cr}}$ ①	σ_b	$\dfrac{\sigma_2}{_b\bar{f}_{cr}}$ ②	①+②	τ	$\dfrac{\tau_s}{_c\bar{f}_{cr}}$
10	1 023.12	491.96	189.14	1.705	0.084	1.372	0.065	0.149	0.627	0.082
9	1 031.94	832.02	189.14	2.587	0.118	5.263	0.236	0.354	0.951	0.095
8	1 036.84	1 002.54	189.14	2.597	0.119	6.341	0.284	0.402	0.951	0.095
7	1 058.40	1 683.64	189.14	1.931	0.085	7.791	0.338	0.423	0.686	0.062
6	1 082.90	2 364.74	189.14	1.676	0.072	9.290	0.398	0.470	0.588	0.050
5	1 110.34	3 044.86	189.14	1.715	0.074	11.966	0.513	0.587	0.588	0.050
4	1 141.70	3 731.84	208.74	1.529	0.065	12.760	0.543	0.608	0.559	0.046
3	1 183.84	4 671.66	208.74	1.323	0.059	9.643	0.424	0.483	0.470	0.044
2	1 231.86	5 610.50	208.74	1.088	0.050	7.115	0.322	0.372	0.363	0.038
1	1 283.80	6 552.28	208.74	0.931	0.044	5.625	0.261	0.305	0.304	0.035

(2) Full water tank (modal analysis)

Joint No.	N (kN)	M (kN·m)	Q (kN)	σ_c	$\dfrac{\sigma_c}{_c\bar{f}_{cr}}$ ①	σ_b	$\dfrac{\sigma_b}{_b\bar{f}_{cr}}$ ②	①+②	τ	$\dfrac{\tau_s}{_c\bar{f}_{cr}}$
10	1 023.12	558.60	187.38	1.705	0.084	1.558	0.074	0.158	0.627	0.080
9	1 031.94	896.70	187.38	2.587	0.118	5.674	0.254	0.372	0.941	0.094
8	1 036.84	1 065.26	187.38	2.597	0.119	6.742	0.302	0.420	0.941	0.094
7	1 058.40	1 739.50	187.38	1.931	0.085	8.046	0.349	0.434	0.686	0.062
6	1 082.90	2 413.74	187.38	1.676	0.072	9.486	0.406	0.479	0.588	0.050
5	1 110.34	3 088.96	187.38	1.715	0.074	12.142	0.520	0.594	0.588	0.050
4	1 141.70	3 768.10	205.02	1.529	0.065	12.887	0.548	0.613	0.549	0.046
3	1 183.84	4 691.26	205.02	1.323	0.059	9.682	0.426	0.485	0.451	0.044
2	1 231.86	5 613.44	205.02	1.088	0.050	7.125	0.322	0.372	0.382	0.036
1	1 283.80	6 542.48	205.02	0.931	0.045	5.615	0.261	0.305	0.294	0.034

(3) Wind with full water tank (in along direction)

Joint No.	N (kN)	M (kN·m)	Q (kN)	σ_c	$\dfrac{\sigma_c}{1.5_c\bar{f}_{cr}}$ ①	σ_b	$\dfrac{\sigma_b}{1.5_b\bar{f}_{cr}}$ ②	①+②	τ	$\dfrac{\tau}{1.5_s\bar{f}_{cr}}$
10	1 023.12	72.79	35.87	1.705	0.092	0.203	0.010	0.102	0.119	0.025
9	1 031.94	137.35	39.21	2.587	0.123	0.869	0.040	0.163	0.196	0.024
8	1 036.84	172.64	44.35	2.597	0.123	1.092	0.050	0.173	0.222	0.027
7	1 058.40	332.30	52.25	1.931	0.086	1.538	0.067	0.153	0.191	0.019
6	1 082.90	520.40	59.78	1.676	0.073	2.045	0.088	0.161	0.185	0.017
5	1 110.34	735.61	66.89	1.715	0.075	2.891	0.124	0.199	0.207	0.019
4	1 141.70	976.41	74.74	1.529	0.065	3.338	0.142	0.207	0.200	0.018
3	1 183.84	1312.74	84.86	1.323	0.061	2.709	0.121	0.182	0.190	0.021
2	1 231.86	1694.61	95.57	1.088	0.053	2.150	0.100	0.153	0.168	0.022
1	1 283.80	2124.68	101.78	0.931	0.048	1.823	0.089	0.137	0.147	0.024

(4) Wind with empty water tank (for vortex osc.)

Joint No.	N (kN)	M (kN·m)	Q (kN)	σ_c	$\dfrac{\sigma_c}{1.5_c\bar{f}_{cr}}$ ①	σ_b	$\dfrac{\sigma_b}{1.5_b\bar{f}_{cr}}$ ②	1.5 (①+②)	τ	$\dfrac{\tau}{1.5_s\bar{f}_{cr}}$ ③	1.5 ③
10	107.80	84.64	41.66	0.176	0.009	0.237	0.012	0.032	0.139	0.029	0.043
9	116.62	159.62	45.42	0.294	0.014	1.010	0.046	0.090	0.227	0.028	0.042
8	121.52	200.50	50.81	0.304	0.014	1.269	0.058	0.108	0.254	0.031	0.047
7	143.08	383.40	59.48	0.265	0.012	1.774	0.078	0.135	0.217	0.021	0.032
6	167.58	597.50	67.58	0.255	0.011	2.348	0.101	0.168	0.209	0.019	0.029
5	195.02	840.72	75.07	0.304	0.013	3.304	0.142	0.233	0.232	0.022	0.032
4	226.38	1110.86	83.17	0.304	0.013	3.798	0.161	0.261	0.223	0.020	0.030
3	268.52	1484.85	93.32	0.304	0.014	3.064	0.137	0.227	0.209	0.023	0.034
2	316.54	1904.25	103.73	0.274	0.013	2.416	0.113	0.189	0.182	0.024	0.036
1	368.48	2370.02	109.50	0.265	0.014	2.034	0.099	0.170	0.158	0.026	0.039

1.5(①+②) < 1.0   OK

1.5③   < 1.0   OK

APPENDIX   A 2

DESIGN EXAMPLE
STEEL SILO

The equations referred in this chapter correspond to those given in chapters 3 and 5 of the main body of this Recommendation.

A2.1   Specifications

Table A2.1   Specifications

Application	Silo for storing grain
Type	Welded steel silo
Configuration	A single free-standing, cylindrical shape
Height	34,500 mm
Diameter	8,600 mm
Angle of hopper : α	45°
Thicknesses of wall, skirt and hopper	$t_1 = 6 \sim 15.2$ mm, $t_2 = 6 \sim 8$mm
Stored product	Grain
Storage weight	1176×10^4N
Density — For long-term design	7.35×10^{-6}N/mm^3
Density — For seismic design	80% of the above
Angle of repose:	30°
Internal friction angle:	25°
Friction coefficient of tank wall:	0.3
Impact pressure coefficient:	1.5
Dynamic pressure coefficient: — Wall	1.92
Dynamic pressure coefficient: — Hopper	2.30(top), 1.0(bottom)
Safety factor of friction force:	1.5
Design codes	- Design Recommendation for Storage Tanks and Their Supports, AIJ - Design Standard for Steel Structures - Japanese Industrial Standards
Material	SS400(JIS G 3101)
Allowable stress	F=235N/mm^2
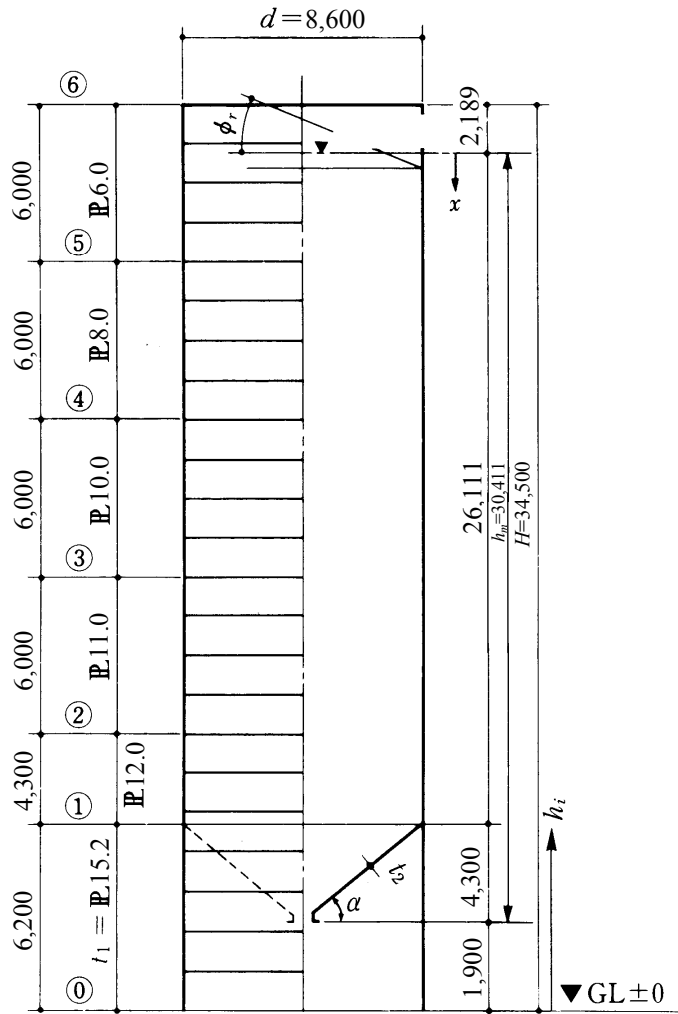
Fig. A2.1 Specifications of Calculated Silo (Unit:mm)

A2.2   Stress Calculation

(1)   Pressures and Forces Caused by the Stored Material
   a) Internal pressure in silo and axial force on tank wall:

Vertical pressure: P_v

From (5.1), $P_v = \dfrac{\gamma \cdot r_w}{\mu_f \cdot K_s} \cdot \left(1 - e^{-\mu_f \cdot K_s \cdot x / r_w}\right)$

where:

bulk density of the stored material, γ,   = 7.35×10^{-6} (N/mm³)
internal friction angle of the stored material, φ_i,   =   25 (°)
radius of water pressure, r_w, [as determined from (5.3)]   =   2,150 (mm)

From (5.3), r_w = A/l_c = $d/4$ = 8,600/4 = 2,150mm

depth from the free surface of the stored material, x, (mm)
friction coefficient of the tank wall, μ_f,= 0.3

From (5.2), $K_s = \dfrac{1 - \sin\varphi_i}{1 + \sin\varphi_i} = \dfrac{1 - \sin 25°}{1 + \sin 25°} = 0.40$

∴ $P_v = 0.13169\left(1 - e^{-0.000558x}\right)$

∴ $dP_v = C_i \cdot P_v = 1.5 \cdot P_v$

where:

dP_v = design vertical pressure per unit area
C_i = impact pressure factor when filling the silo with grain = 1.5

Fig.A2.2   Minimum Value of C_d and C'_d

Horizontal pressure: P_h (N/mm²)

From (5.4), $P_h = K_s \cdot P_v = 0.40 \cdot P_v$

$$\therefore \qquad dP_h = C_d \cdot P_h = 1.92 \cdot P_h$$

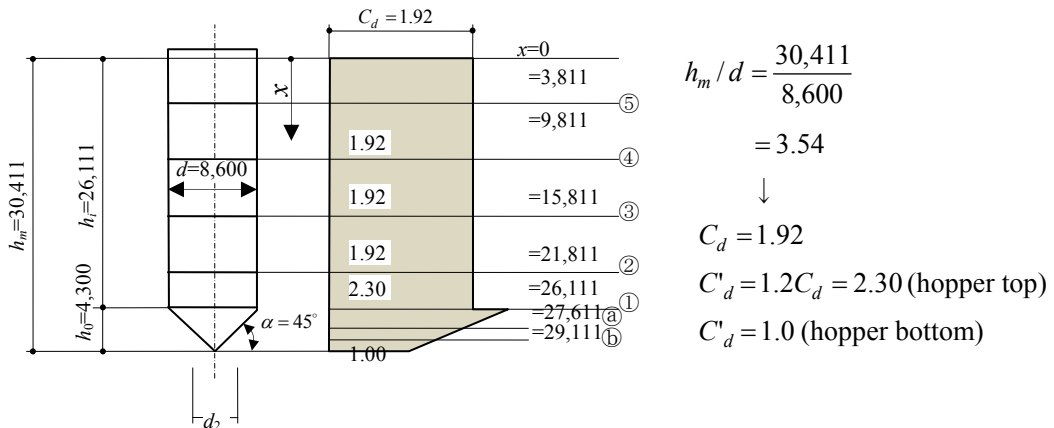for hopper $\qquad C'_d = 1.2 \times C_d = 2.30 \text{ (top)}$

$$C'_d = 1.00 \text{ (bottom)}$$

where:
dP_h design horizontal pressure per unit area on the tank wall (N/mm^2)
C_d, C'_d dynamic pressure coefficient when discharging grain from the silo $1.00 \sim$
      2.3 (defined by Fig. A2.2)

Friction force per unit area on the tank wall: P_f (N/mm^2)

From (5.5), $\qquad P_f = \mu_f \cdot P_h = 0.3 \cdot P_h$

b)   Normal pressure on hopper wall: P_a (N/mm^2)

From (5.6), $\qquad P_a = P_h \cdot sin^2\, \alpha + P_\upsilon \cdot cos^2\, \alpha$

where:
α incline of the hopper wall to the horizontal plane 45 (°)

$$\therefore \qquad\qquad P_a = 0.7 P_\upsilon$$

From (5.9),
$$dP_a = C'_d \cdot P_a = 1.61 P_\upsilon \sim 0.7 P_\upsilon (\because C'_d = 2.30 \sim 1.00)$$
$$dP_a = C_i \cdot P_a = 1.05 \cdot P_\upsilon \left(\because C_i = 1.5 \right)$$

where:
dP_a design vertical pressure per unit area on the hopper wall (N/mm^2)

Table A2.2(a)   Internal Pressure in Silo and Axial Force on Tank Wall

Calculation Point	Depth	Vertical Pressure (N/mm^2)		Horizontal Pressure (N/mm^2)			Axial Force on Tank Wall (N/mm)	
	x (mm)	P_υ	dP_υ	P_h	C_d	dP_h	Long Term dN_m	During Earthquakes dN_m
⑤	3,811	0.025	0.038	0.010	1.92	0.020	9.1	6.1
④	9,811	0.055	0.083	0.022	1.92	0.043	54.1	36.1
③	15,811	0.077	0.115	0.031	1.92	0.060	127.2	84.8
②	21,811	0.092	0.138	0.037	1.92	0.072	220.2	146.8
①	26,111	0.100	0.150	0.041	1.92	0.078	295.8	197.2

(b)   Internal Pressure and Axial Force in Hopper

Calculation Point	Depth	Pressure			Pressure Factor		Design Pressure	
	x (mm)	P_υ (N/mm²)	P_h (N/mm²)	P_a (N/mm²)	C_i (−)	C'_d (−)	dP_a (N/mm)	dP_υ (N/mm)
top	26,111	0.100	0.041	0.071	1.50	2.30	0.163	0.150
middle	27,544	0.102	0.041	0.072	1.50	1.87	0.135	0.153
bottom	28,977	0.105	0.042	0.074	1.50	1.44	0.111	0.158

c)   Design generator force acting on cross section of tank wall caused by wall friction force: dN_m (N/mm)

Long-term design generator force per unit length of the circumference of the tank wall, dN_m (N/mm).
Safety factor of the friction force between the tank wall and the granular material (long term), C_f, = 1.5 or 1.0. Then, from equation (5.11),

$$dN_m = (\gamma \cdot \chi - P_\upsilon) \cdot r_w \cdot C_f = (7.35 \times 10^{-6} \chi - P_\upsilon) \cdot 2150 \cdot (1.5)$$

Design generator force per unit length of the circumference of the tank wall during earthquakes, dN_m' (N/mm)

$$dN_m' = (\gamma \cdot \chi - P_\upsilon) \cdot r_w = (7.35 \times 10^{-6} \chi - P_\upsilon) \cdot 2150$$

(2) Calculation of Design Axial Force and Weight

a) Design axial force = (empty-weight) + (axial force of stored material caused by wall friction force)

Table A2.3   Design Axial Force

Calculation Point	Empty-weight (N/mm)		Axial Force of Stored Material Caused by Wall Friction Force: dN_m (N/mm)		Design Axial Force dN_m (N/mm)	
	Empty-weight	Cumulated Weight	Long Term	During Earthquakes	Long Term	During Earthquakes
⑥	12.7	12.7	-	-	12.7	12.7
⑤	3.2	15.9	9.1	6.1	25.0	22.0
④	4.2	20.1	54.1	36.1	74.2	56.2
③	4.9	25.0	127.2	84.8	152.2	109.8
②	4.5	29.5	220.2	146.8	249.7	176.3
①	9.2	38.7	295.8	197.2	334.5	235.9
⓪	1.5	40.2	-	-	475.5	388.4

b) Calculation of Weight

Table A2.4   Basic Design Weight and Weight for Calculating Seismic Force

Calculation Point	Empty-weight (kN)	Weight of Stored Material (kN)		Basic Design Weight W (kN)		Weight for Calculating Seismic Force W_t (kN)	
		$\gamma = 0.735 \times 10^{-2}$	$\gamma = 0.735 \times 10^{-2} \times 0.8$	Section	Cumulation	Section	Cumulation
⑥	344.0	346.2	277.0	690.2	690.2	621.0	621.0
⑤	87.4	2,561.8	2,049.4	2,649.2	3,339.4	2,136.8	2,757.8
④	112.4	2,561.8	2,049.4	2,674.2	6,013.6	2,161.8	4,919.6
③	131.1	2,561.8	2,049.4	2,692.9	8,706.5	2,180.5	7,100.1
②	122.4	2,198.9	1,759.1	2,321.3	11,027.8	1,881.5	8,981.6
①	290.9	1,529.9	1,223.9	1,820.8	12,848.6	1,514.8	10,496.4

(See Fig. A2.5)

(3) Evaluation of Wall Stress in Circumferential Direction

a) Fumigation Pressure with Long Term Design Pressure

$$\sigma_\theta = \frac{(dP_h + P_i) \cdot d}{2 \cdot t_i} \leqq f_t$$

where :

σ_θ : silo wall tensile stress in circumferential Direction (N/mm^2)

dP_h : horizontal pressure on tank wall (N/mm^2)

P_i : pressure other than dP_h (e. g., fumigation pressure) =500(mmAq)

$$=0.0049(N/mm^2)$$

t_i : thickness of tank wall (mm)

f_t : allowable tensile stress = 157 (N/mm^2)

Table A2.5　Evaluation of Wall Stress in Circumferential Direction
(fumigation pressure considered)

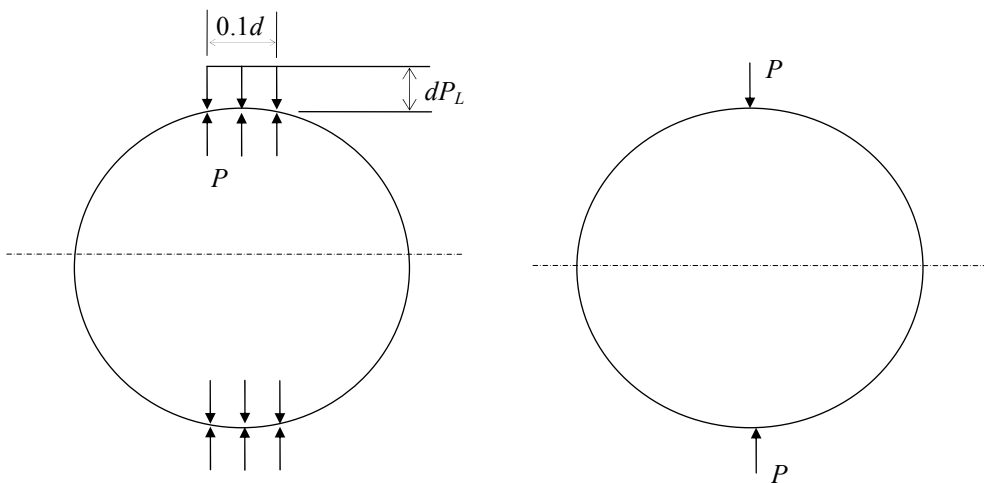| Calculation Point	t_i (mm)	d (mm)	dP_h (N/mm^2)	P_i (N/mm^2)	σ_θ (N/mm^2)	f_t (N/mm^2)	$\dfrac{\sigma_\theta}{f_t}$	Test Result
6	6.0	8,600	0.020	0.0049	17.8	157	0.11	$\leqq 1.0$
5	8.0	8,600	0.043	0.0049	25.7	157	0.16	$\leqq 1.0$
4	10.0	8,600	0.060	0.0049	27.9	157	0.18	$\leqq 1.0$
3	11.0	8,600	0.072	0.0049	30.1	157	0.19	$\leqq 1.0$
2	12.0	8,600	0.078	0.0049	29.7	157	0.19	$\leqq 1.0$
1	15.2	8,600	0.000	0.0000	0.0	157	0.00	$\leqq 1.0$

b) Local Pressure with dP_h

Fig. A2.3　Local Pressure

$$\sigma_t + \sigma_b \leqq f_t$$

$$\sigma_t = \frac{dP_h \cdot d}{2 \cdot t_i}$$

$$\sigma_b = \frac{M_b}{Z}$$

$$M_0 = 0.318 \cdot P \cdot (d/2) \quad (\text{N} \cdot \text{mm/mm})$$

$$M_b = k \cdot M_0 \quad (\text{N} \cdot \text{mm/mm})$$

$$k = 0.1 + 0.05 \cdot (h_m/d - 2), \text{ however, if } h_m/d < 2, \quad k = 0.1 \quad (-)$$

$$\quad = 0.177$$

$$P = 0.1 \cdot d \cdot dP_L \quad (\text{N/mm})$$

$$dP_L = C_L \cdot C_d \cdot P_h \quad (\text{N/mm}^2)$$

$$C_L = 0.15 + 0.5 \cdot (e/d) \quad (-) \quad \text{See Fig. A2.4}$$
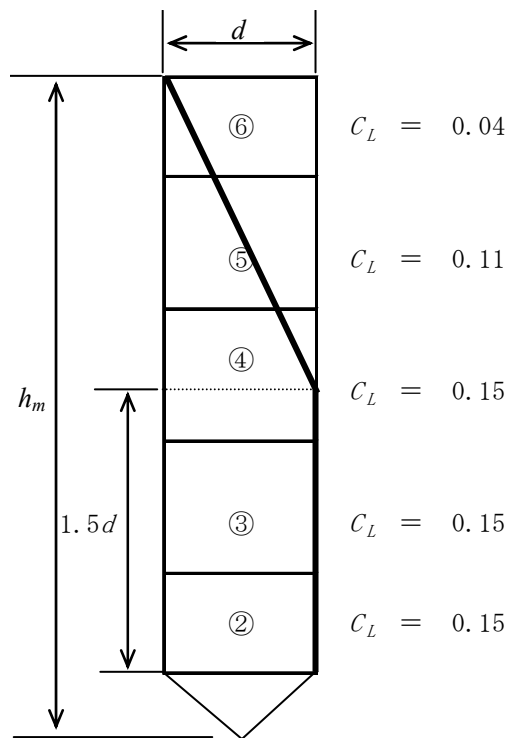

Fig. A2.4 C_L Value

where :

σ_t : tensile stress (N/mm^2)

σ_b : bending stress by the local pressure (N/mm^2)

M_b : design bending moment by the local pressure (N·mm/mm)

M_0 : maximum bending moment for ring model (N·mm/mm)

k : local stress coefficient (−)

h_m : effective height of material = 30,411 (mm)

P : local load (N/mm)

dP_L : design local horizontal pressure per unit area (N/mm^2)

$dP_L = C_L \cdot C_d \cdot P_h$ (N/mm^2)

C_L : ratio of the local pressure to the design horizontal pressure ($-$)

e : eccentricity = 0 (mm)

Table A2.6   Evaluation of Wall Stress in Circumferential Direction
(local pressure considered)

Calculation Point	t_i (mm)	d (mm)	dP_h (N/mm^2)	σ_t (N/mm^2)	f_t (N/mm^2)
6	6.0	8,600	0.020	14.3	157
5	8.0	8,600	0.043	23.1	157
4	10.0	8,600	0.060	25.8	157
3	11.0	8,600	0.072	28.1	157
2	12.0	8,600	0.078	28.0	157
1	15.2	8,600	0.0	0.0	157

Table A2.7-1   Evaluation of Wall Stress in Circumferential Direction
(local pressure considered)

Calculation Point	t_i (mm)	d (mm)	dP_h (N/mm^2)	C_L	dP_L (N/mm^2)	P (kN/m)
6	6.0	8,600	0.020	0.04	0.0008	0.69
5	8.0	8,600	0.043	0.11	0.0047	4.04
4	10.0	8,600	0.060	0.15	0.0090	7.74
3	11.0	8,600	0.072	0.15	0.0108	9.29
2	12.0	8,600	0.078	0.15	0.0117	10.06
1	15.2	8,600	0.0			

Table A2.7-2   Evaluation of Wall Stress in Circumferential Direction
(local pressure considered)

Calculation Point	M_b (kNm/m)	Z (mm^3/m)	σ_b (N/mm^2)	σ_t (N/mm^2)	$\dfrac{\sigma_t + \sigma_b}{f_t}$	Test Result
6	0.17	6,000.0	28.3	14.3	0.27	$\leqq 1.0$
5	0.98	10,666.7	91.9	23.1	0.73	$\leqq 1.0$
4	1.87	16,666.7	112.2	25.8	0.88	$\leqq 1.0$
3	2.25	20,166.7	111.6	28.1	0.89	$\leqq 1.0$
2	2.43	24,000.0	101.3	28.0	0.83	$\leqq 1.0$
1	0.0	38,506.7	0.0	0.0	0.00	$\leqq 1.0$

(4)   Calculation of Stress during Earthquakes

a)   Modified Sesmic Intensity Method

・Design shear force at the silo base: Q_d(N)

$$Q_d = C \cdot W_t$$

$$C = Z_s \cdot I \cdot D_s \cdot \frac{S_{a1}}{g}$$

where $C \geqq 0.3 \cdot Z_s \cdot I$

Symbols C :   design yield shear force coefficient at the silo base

W_t :   design weight imposed on the silo base = $10{,}496.4 \times 10^3$ (N)

Z_s :   seismic zone factor = 1.0 (Kanto area)

I :   importance factor = 0.8

D_s :   = $D_\eta D_h$ = $(0.5\sim0.7) \cdot 1.0 = 0.5\sim0.7$

D_η :   a constant determined by the plastic deformation of the silo = $0.5\sim0.7$
        (steel structure)

D_h :   a constant determined by the damping capacity of the silo = 1.0 (area of
        silo basement $S < 2{,}000$ m^2)

S_{a1} :   acceleration response spectrum of the first natural period = 9.80 (m/s^2)
        g = 9.80 (m/ s^2)

$C = 1.0 \cdot 0.8 \cdot (0.5\sim0.7) \cdot 9.80/9.80 = (0.4\sim0.56) > 0.3 \cdot Z_s \cdot I = 0.3 \cdot 1.0 \cdot 0.8 = 0.24$

$Q_d = (0.4\sim0.56) \cdot 10496.4 \times 10^3 = (4198.56\sim5877.98) \times 10^3$ (N)

・ Design yield shear force at each part of the structure: Q_{di} (N)

$$Q_{di} = Q_d \cdot \frac{\displaystyle\sum_{m=i}^{n} W_m \cdot h_m}{\displaystyle\sum_{m=1}^{n} W_m \cdot h_m}$$

Symbols Q_{di} : design horizontal yield shear force at the i-th mass when the structure is assumed to be a vibration system with n masses (N)

W_i : weight of the i-th mass (N)

h_i : height of the i-th mass from the ground (m)
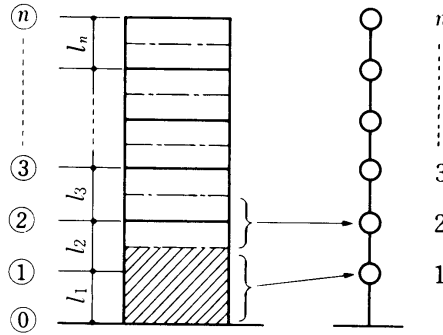
n : total number of masses

Fig. A2.5

・ Design shear force: Q_{ei} (N)

$$Q_{ei}=Q_{di} / B$$

Symbol B : ratio of the horizontal load-carrying capacity of the structure to the allowable strength during earthquakes 1.0

Table A2.8 was the calculated results of Q_{ei}.

Table A2.8 Design Shear Force/Bending Moment during Earthquakes Calculated by Modified Seismic Intensity Method

Calculation Point	Height from the Ground h (m)	Mass Point Number i	Section Length h_s (m)	Height of the i-th Point h_i (m)	Weight of the i-th Point W_i (kN)	$W = \sum W_i$ (kN)	$W_i \times h_i$ (kN-m)	$\sum W_i \times h_i$ (kN-m)	$\dfrac{\sum_{m=i}^{n} W_m \cdot h_m}{\sum_{m=1}^{n} W_m \cdot h_m}$ $(-)$	Q_d (kN)	Q_{di} (kN)	Q_{ei} (kN)	P_i (kN)	M_e $\times 10^5$ (N·m)
⑥	34.50	6		34.50	621.0	621.0	21,424.5	21,424.5	0.11		461.8		-	
⑤	28.50	5	6.00	28.50	2,136.8	2,757.8	60,898.8	82,323.3	0.42		1,763.4	461.8	461.8	27.7
④	22.50	4	6.00	22.50	2,161.8	4,919.6	48,640.5	130,963.8	0.67		2,813.1	1,763.4	1,301.6	133.5
③	16.50	3	6.00	16.50	2,180.5	7,100.1	35,978.3	166,942.1	0.85		3,568.8	2,813.1	1,049.7	302.3
②	10.50	2	6.00	10.50	1,881.5	8,981.6	19,755.8	186,697.9	0.95		3,988.7	3,568.8	755.7	516.4
①	6.20	1	4.30	6.20	1,514.8	10,496.4	9,391.8	196,089.7	1.00	4,198.6	4,198.6	3,988.7	419.9	687.9
⓪	0.00		6.20									4,198.6	209.9	948.3

* The axial compressive stress ratio for equations (3.7.12) and (3.7.13) is $\sigma_c / {}_c f_{cr}$ < 0.2, which gives 0.5 to D_s.

Therefore, Q_d = 4,198.6 x 10^3 (N) is used.

・ Bending Moment: M_{ei} (N・m)

When we use the model shown in Fig. A 2.5 the bending moment can be calculated as follows:
The seismic force P_i acting on each part of the structure (each mass point) is calculated from
the following equation using the design seismic-story shear force Q_{ei} described above:

$$P_i = Q_{ei} - Q_{e,i-1} \ (i = 1 \sim n)$$

The moment of each story(calculation point) can be calculated as follows:

$$M_{e,i-1} = \sum_{m=i}^{n} (P_m \cdot H_m) \ (i = 1 \sim n)$$

where the subscripts m of P, H and i of Q_{ei}, M_{ei} mean the mass and the calculation point,
respectively. H_m shows the height from the calculation point to each mass.

    b)   Modal Analysis

・ Design yield shear force at each part of the structure: Q_{di} (N)

$$Q_{di} = \sqrt{ \sum_{j=1}^{k} \left(C_j \cdot \sum_{m=i}^{n} W_m \cdot \beta_j \cdot u_{mj} \right)^2 }$$

$$C_j = Z_s \cdot I \cdot D_s \cdot S_{aj} / g$$

where $\quad Q_{di} \geqq 0.3 \cdot Z_s \cdot I \cdot W$

Symbols β_j :   participation factor of the j-th natural vibration

$$\beta_j = \frac{\sum\limits_{i=1}^{n} W_i \cdot u_{ij}}{\sum\limits_{i=1}^{n} W_i \cdot u_{ij}^2}$$

Symbols u_{ij} :   the j-th eigenfunction of the i-th mass

                     k :   maximum number of vibration mode having a significant effect on
                               the seismic response = 3

                     j :   order of natural frequency

                     C_j :   design yield shear force coefficient for the j-th natural mode

                     S_{aj} :   design acceleration response spectrum for the j-th natural period
                               defined in 3.6.1.6. (m/s^2)

                     Z_s :   seismic zone factor = 1.0 (Kanto area)

                     I :   essential facility factor = 0.8

             $D_s = D_\eta \cdot D_h$

Symbols D_η :   a constant determined by the ductility of the structure = $0.5 \sim 0.7$
                               (steel structure)

D_h : a constant determined by the damping of the structure = 1.0 (area of silo foundation $S < 2,000$ m^2)

$\therefore$ $D_s=(0.5\sim0.7)\cdot1.0=0.5\sim0.7$

$T_{j(max)}=0.559<T_G=1.28$s

Symbols T_j : the j-th natural period (s)

T_G : critical period determined by the ground class (s)

$S_{aj}=9.80$ m/s^2

$$C_j = Z_s \cdot I \cdot D_s \cdot \frac{S_{aj}}{g} = 1.0 \cdot 0.8 \cdot (0.5\sim0.7) \cdot \frac{9.80}{9.80} = (0.4\sim0.56) > 0.3 \cdot 1.0 \cdot 0.8 = 0.24$$

・ Design shear force: Q_{ei} (N)

$Q_{ei}=Q_{di}/B$

・ Bending Moment: M_{ei} (N・m)

$P_i=Q_{ei}-Q_{e,i-1}$ ($i=1\sim$n)

$$M_{e,i-1} = \sum_{m=i}^{n} (P_m \cdot H_m) \ (i=1\sim n)$$

Table A2.9　Natural Period, Mode, and Participation Factor

j	i	W_i (kN)	C_j	T_j	β_j	u_{mj}	$\beta_j \cdot u_{mj}$	$C_j \cdot W_i \cdot \beta_j \cdot u_{mj}$ (kN)	Q_{ij} (kN)	$(Q_{ij})^2$ (10^9N^2)
1	6	621.0	0.40	0.511	1.606	1.0000	1.6060	398.93	398.93	159.1
	5	2,136.8				0.7776	1.2488	1,067.37	1,466.30	2,150.0
	4	2,161.8				0.5473	0.8790	760.09	2,226.39	4,956.8
	3	2,180.5				0.3335	0.5356	467.15	2,693.54	7,255.2
	2	1,881.5				0.1564	0.2512	189.05	2,882.59	8,309.3
	1	1,514.8				0.0651	0.1046	63.38	2,945.97	8,678.7
2	6	621.0	0.40	0.125	0.894	-1.0000	-0.8940	-222.07	-222.07	49.3
	5	2,136.8				-0.3007	-0.2688	-229.75	-451.82	204.1
	4	2,161.8				0.3694	0.3302	285.53	-166.29	27.7
	3	2,180.5				0.6711	0.6000	532.32	357.03	127.5
	2	1,881.5				0.5588	0.4996	376.00	733.03	537.3
	1	1,514.8				0.3171	0.2835	171.78	904.81	818.7
3	6	621.0	0.40	0.064	0.464	1.0000	0.4640	115.26	115.26	13.3
	5	2,136.8				-0.1279	-0.0593	-50.68	64.58	4.2
	4	2,161.8				-0.5866	-0.2722	-235.38	-170.80	29.2
	3	2,180.5				0.0670	0.0311	27.13	-143.67	20.6
	2	1,881.5				0.6349	0.2946	221.72	78.05	6.1
	1	1,514.8				0.5039	0.2338	141.66	219.71	48.3

* The axial compressive stress ratio for equations (3.7.12) and (3.7.13) is $\sigma_c/_cf_{cr}< 0.2$, which gives $D_s= 0.5$ and $C_j = 0.4$.

Table A2.10　Design Shear Force/Bending Moment during Earthquakes Calculated by Modal Analysis

	h_i (m)	i	Q_{di} (kN)	B	Q_{ei} (kN)	P_i (kN)	h_s (m)	M_{ei} $\times 10^5 (\text{N} \cdot \text{m})$
⑥	34.5	6	470.9					
⑤	28.5	5	1,535.7		470.9	470.9	6.00	28.3
④	22.5	4	2,239.1		1,535.7	1,064.8	6.00	120.4
③	16.5	3	2,720.9	1.0	2,239.1	703.4	6.00	254.7
②	10.5	2	2,975.3		2,720.9	481.8	6.00	418.0
①	6.2	1	3,089.6		2,975.3	254.4	4.30	545.9
⓪	0.00	0			3,089.6	114.3	6.20	737.5

(5)　Calculation of Stress under Wind Pressure

The construction site is assumed to be Tsurumi Port in the City of Yokohama. Considering the ground surface conditions of the surrounding area (inland port where mid-rise buildings lie scattered), the roughness of the ground surface is estimated to be class II.

For load calculation, we calculate the horizontal load for the structural frame. The design return period (r) is assumed to be 50 years.

i)　Calculation of Design Wind Velocity　U_H

・　Basic wind velocity　U_0 = 38 m/s (Tsurumi Port, Yokohama City)

・　Vertical distribution coefficient of wind velocity　$E = E_r \cdot E_g$

　Z_b = 5 m, Z_G= 350 m, α= 0.15 (because the roughness of the ground surface is classII)

　$E_r = 1.7(Z/Z_G)^{\alpha} = 1.7 \times (34.5/350)^{0.15} = 1.20$

　E_g = 1.0 (topography factor)

∴　　　E = 1.20 x 1.0 = 1.20

・　Return period conversion factor of the wind velocity　k_{rw}

　$k_{rw} = 0.63(\lambda_U - 1)\ln r - 2.9\lambda_U + 3.9$

　$\lambda_U = \dfrac{U_{500}}{U_0}$

U_{500} : 500 - year - recurrence 10 - minute mean wind speed at 10m above ground over a flat and open terrain = 44 (m/s)

∴ $k_{rw} = 0.93$

Therefore, design wind velocity U_H and design velocity pressure q_H are

$$U_H = U_0 K_D E_H k_{rw}$$
$$= 42.4 \text{ (m/s)}$$
$$q_H = 0.5\rho U_H^2$$
$$= 1,096.6 \text{ (N/m}^2)$$

Wind force coefficient for circular-planned structures C_D

$$C_D = 1.2 k_1 k_2 k_Z$$

k_1 : factor for aspect ratio

$$\frac{H}{D} = 4.01$$

∴ $k_1 = 0.73$

k_2 : factor for surface roughness = 0.75

k_Z : factor for vertical profile

$$k_Z = (Z_b / H)^{2\alpha} \quad Z \leqq Z_b$$
$$= (Z / H)^{2\alpha} \quad Z_b < Z \leqq 0.8H$$
$$= 0.8^{2\alpha} \quad 0.8H \leqq Z$$

Table A2.11   Calculation of Wind Force Coefficient

Calculation Point	Height from the Ground (m)	k_1 (—)	k_2 (—)	k_Z (—)	Wind Force Coefficient C_D (—)
6	34.5			1.00	0.66
5	28.5			0.94	0.62
4	22.5	0.73	0.75	0.88	0.58
3	16.5			0.80	0.53
2	10.5			0.70	0.46
1	6.2			0.60	0.39

Gust Effect Factor G_D

$$G_D = 1 + g_D \frac{C'_g}{C_g} \sqrt{1 + \phi^2{}_D R_D}$$

$$g_D = \sqrt{2 \ln(600\nu_D) + 1.2}$$

$$C_g = \frac{1}{3 + 3\alpha} + \frac{1}{6} = 0.457$$

$$C'_g = 2I_H \frac{0.49 - 0.14\alpha}{\left\{1 + \frac{0.63(BH/L_H)^{0.56}}{(H/B)}\right\}}$$

$$k = \begin{cases} 0.07 & H/B \geqq 1 \\ 0.15 & H/B < 1 \end{cases}$$

$$\phi_D = 1.1 - 0.1\beta$$

β : exponent for mode = 1

$\therefore \quad \phi_D = 1.0$

$$\nu_D = f_D \sqrt{\frac{R_D}{1 + R_D}}$$

$$R_D = \frac{\pi F_D}{4\zeta_D}$$

$$F_D = \frac{I_H^2 F S_D (0.57 - 0.35\alpha + 2R\sqrt{0.053 + 0.042\alpha}}{C'^2_g}$$

$$R = \frac{1}{1 + 20\dfrac{f_D B}{U_H}}$$

$$F = \frac{\dfrac{4 f_D L_H}{U_H}}{\left\{1 + 71\left[\dfrac{f_D L_H}{U_H}\right]^2\right\}^{5/6}}$$

$$S_D = \frac{0.9}{\left\{1 + 6\left[\dfrac{f_D H}{U_H}\right]^2\right\}^{0.5}\left[1 + 3\dfrac{f_D B}{U_H}\right]}$$

ϕ_D : mode correction factor ($-$)

f_D : natural frequency for the first mode in along-wind direction = 1.1 (Hz)

ζ_D : damping ratio for the first mode in along wind direction = 0.01 ($-$)

H : reference height = 34.5 (m)

B : width of building = 8.60 (m)

U_H : design wind speed = 38.0 (m/s)

I_H : turbulence intensity at reference height ($-$)

L_H : turbulence scale at reference height ($-$)

α : exponent of power law in wind speed profile = 0.15 ($-$)

$$\therefore S_D = \frac{0.9}{\left\{1+6\left[\frac{1.1\times 34.5}{38}\right]^2\right\}^{0.5}\left[1+3\times\frac{1.1\times 8.6}{38}\right]} = 0.195$$

$$\therefore L_H = 100\times\left[\frac{H}{30}\right] = 115.0(-)$$

$$\therefore F = \frac{\dfrac{4\times 1.1\times 115.0}{38.0}}{\left\{1+71\left[\frac{1.1\times 115.0}{38.0}\right]^2\right\}^{5/6}} = 0.051$$

$$\therefore R = \frac{1}{1+20\dfrac{1.1\times 8.6}{38.0}} = 0.167$$

$$F_D = \frac{I_H^2 F S_D\left(0.57-0.35\alpha + 2R\sqrt{0.053+0.042\alpha}\right)}{C_g'^2}$$

$$I_H = I_{rz}E_{g1}$$

I_{rz} : turbulence intensity at height H on the flat terrain categories

E_{gI} : topography factor

$$I_{rz}\begin{cases} 0.1\left(\dfrac{H}{Z_G}\right)^{-\alpha-0.05} & Z_b < H \leqq Z_G \\ 0.1\left(\dfrac{Z_b}{Z_G}\right)^{-\alpha-0.05} & H \leqq Z_b \end{cases}$$

$$\therefore I_{rz} = 0.159$$

$$E_{gI} = \frac{E_I}{E_g}$$

E_I : topography factor for the standard deviation of fluctuating wind speed = 1

E_g : topography factor for mean wind speed = 1

$$\therefore E_{gI} = 1$$

$$\therefore I_H = 0.159$$

$$C_g' = 2I_H\frac{0.49-0.14\alpha}{\left\{1+\dfrac{0.63(BH/L_H)^{0.56}}{(H/B)^k}\right\}} = 0.0756$$

$$\therefore F_D = \frac{I_H^2 F S_D\left(0.57-0.35\alpha + 2R\sqrt{0.053+0.042\alpha}\right)}{C_g'^2} = 0.026$$

$$\therefore R_D = \frac{\pi F_D}{4\zeta_D} = 2.082$$

$$\therefore v_D = f_D \sqrt{\frac{R_D}{1 + R_D}} = 0.903$$

$$g_D = \sqrt{2\ln(600 v_D) + 1.2} = 3.71$$

Therefore, gust effect factor G_D is defined as follows.

$$G_D = 1 + g_D \frac{C'_g}{C_g} \sqrt{1 + \phi^2{}_D R_D} = 2.08$$

Along-wind Load W_D

Table A2.12　Calculation of Along-wind Load W_D

Calculation Point	Height from the Ground Surface (m)	Design Velocity Pressure q_H (N/m²)	Wind Force Coefficient C_D (－)	Gust Effect Factor G_D (－)	Projected Area A (m²)	Along-Wind Load W_D (kN)	Wind Shear-Force Q (kN)
6	34.5		0.66		51.67	56.84	56.84
5	28.5		0.62		51.70	53.43	110.27
4	22.5	1,096.6	0.58	1.52	51.72	50.00	160.27
3	16.5		0.53		51.73	45.70	205.97
2	10.5		0.46		37.08	28.43	234.40
1	6.2		0.39		53.51	34.78	269.18

Table A2.13　Calculation of Overturning Moment $(M_w)_i$

Calculation Point	Height from the Ground Surface h_i (m)	Section Length h_r (m)	Projected Area A_w (m²)	Along-Wind Load W_D (kN)	Moment $(M_w)_i$ (kN·m)
⑥	34.5				
⑤	28.5	6.0	51.67	56.84	170.50
④	22.5	6.0	51.70	53.43	671.90
③	16.5	6.0	51.72	50.00	1,483.50
②	10.5	6.0	51.73	45.70	2,582.20
①	6.2	4.3	37.08	28.43	3,529.00
⓪	0.0	6.2	53.51	34.78	5,090.10

A2.3 Evaluation

A2.3.1 Evaluation of cylindrical buckling is made by the following equations:

From (3.21)

$$\frac{\sigma_c}{{}_c f_{cr}} + \frac{\sigma_b}{{}_b f_{cr}} \leq 1$$

and

(3.22)

$$\frac{\tau}{{}_s f_{cr}} \leq 1$$

Notations :

σ_c	average compressive stress	=	W / A (N/mm^2)
σ_b	compressive bending stress	=	M / Z (N/ mm^2)
τ	shear stress	=	$2 Q / A$ (N/ mm^2)
W	compressive force (N)		
M	bending moment (N·mm)		
Q	shear force (N)		
A	cross section (mm^2)		
Z	section modulus (mm^3)		
${}_c f_{cr}$	allowable compressive stress (N/mm^2)		
${}_b f_{cr}$	allowable bending stress (N/mm^2)		
${}_s f_{cr}$	allowable shear stress (N/mm^2)		

where:

r	=	$d/2$ = 4,300 (mm)	
t	=	6.0 ~ 15.2 (mm)	
v	=	0.3	
E	=	2,058 x 10^2 (N/mm^2)	SS 400
F	=	2.35 x 10^2 (N/mm^2)	
r/t	=	282.9 ~ 716.7	

$$\sigma_h = \frac{P_h \cdot d}{2 \cdot t} = 4,300 \cdot \frac{P_h}{t} \quad \text{(N/mm}^2\text{)}$$

For the calculation of the shear stress the following values are used:

$l/r = 1.0$

$\sigma_h = 0$

A2.3.1.1 The allowable long-term stress is given by the following equations:

(1) Allowable compressive stress, ${}_c f_{cr}$ (N/mm^2)

- In the case of $0 \leq \dfrac{\sigma_h}{F} \leq 0.3 \rightarrow 0 \leq \sigma_h \leq 70.5$

From (3.23), $\quad {}_c f_{cr} = \overline{{}_c f_{cr}} + \dfrac{0.7 \cdot f_{cr0} - \overline{{}_c f_{cr}}}{0.3} \cdot \left(\dfrac{\sigma_h}{F} \right)$

- In the case of $\quad \dfrac{\sigma_h}{F} > 0.3 \rightarrow \sigma_h > 70.5$

   From (3.24), $\quad {}_cf_{cr} = f_{cr0}\cdot\left(1-\dfrac{\sigma_h}{F}\right)$

   where,
   average tensile hoop stress caused by the internal pressure, σ_h, (N/mm^2)
   standard compressive buckling stress, f_{cro}, (N/mm^2)

   ${}_cf_{cr}$ is equal to $\overline{{}_cf_{cr}}$ (N/mm^2), when no internal pressure exists

- In the case of $\quad \dfrac{r}{t} \le 0.069\cdot\left(\dfrac{E}{F}\right) \rightarrow \dfrac{r}{t} \le 60.43$

   From (3.25), $\quad f_{cr0} = \dfrac{F}{1.5} = 1.567\times10^2$

- In the case of $\quad 0.069\cdot\left(\dfrac{E}{F}\right) \le \dfrac{r}{t} \le 0.807\cdot\left(\dfrac{E}{F}\right) \rightarrow 60.43 \le \dfrac{r}{t} \le 706.7$

   From (3.26),

   $$f_{cr0} = 0.267\cdot F + 0.4\cdot F\cdot\left\{\dfrac{0.807 - \left(\dfrac{r}{t}\right)\cdot\left(\dfrac{F}{E}\right)}{0.738}\right\} = 1.655\times10^2 - 0.145\left(\dfrac{r}{t}\right)$$

- In the case of $\quad 0.807\cdot\left(\dfrac{E}{F}\right) \le \dfrac{r}{t} \rightarrow 706.7 \le \dfrac{r}{t}$

   From (3.27), $\quad f_{cr0} = \dfrac{0.8\cdot E}{2.25\sqrt{3\cdot\left(1-v^2\right)}}\bigg/\left(\dfrac{r}{t}\right) = 4.429\times10^4\bigg/\left(\dfrac{r}{t}\right)$

- In the case of $\quad \dfrac{r}{t} \le 0.377\cdot\left(\dfrac{E}{F}\right)^{0.72} \rightarrow \dfrac{r}{t} \le 49.53$

   From (3.29), $\quad \overline{{}_cf_{cr}} = \dfrac{F}{1.5} = 1.567\times10^2$

- In the case of $\quad 0.377\cdot\left(\dfrac{E}{F}\right)^{0.72} \le \dfrac{r}{t} \le 2.567\cdot\left(\dfrac{E}{F}\right)^{0.72} \rightarrow 49.53 \le \dfrac{r}{t} \le 337.3$

   From (3.30), $\quad \overline{{}_cf_{cr}} = 0.267\cdot F + 0.4\cdot F\cdot\left\{\dfrac{2.567 - \left(\dfrac{r}{t}\right)\cdot\left(\dfrac{F}{E}\right)^{0.72}}{2.190}\right\}$

   $$= 1.729\times10^2 - 0.326\left(r/t\right)$$

- In the case of $\quad 2.567 \cdot \left(\dfrac{E}{F}\right)^{0.72} \le \dfrac{r}{t} \rightarrow 337.3 \le \dfrac{r}{t}$

From (3.31),

$$\overline{_c f_{cr}} = \dfrac{0.6 \cdot E}{2.25} \cdot \left[1 - 0.901 \cdot \left\{1 - \exp\left(-\dfrac{1}{16} \cdot \sqrt{\dfrac{r}{t}}\right)\right\}\right] \Bigg/ \left(\dfrac{r}{t}\right)$$

$$= 5.488 \times 10^4 \left[1 - 0.901 \cdot \left\{1 - \exp\left(-\dfrac{1}{16} \cdot \sqrt{\dfrac{r}{t}}\right)\right\}\right] \Bigg/ \left(\dfrac{r}{t}\right)$$

(2) Allowable bending stress, $_b f_{cr}$, (N/mm^2)

- In the case of $\quad 0 \le \dfrac{\sigma_h}{F} \le 0.3 \rightarrow 0 \le \sigma_h \le 0.705 \times 10^2$

From (3.33), $\quad _b f_{cr} = \overline{_b f_{cr}} + \dfrac{0.7 \cdot f_{cr0} - \overline{_b f_{cr}}}{0.3} \cdot \left(\dfrac{\sigma_h}{F}\right)$

- In the case of $\quad \dfrac{\sigma_h}{F} > 0.3 \rightarrow 0.705 \times 10^2 < \sigma_h$

From (3.34), $\quad _b f_{cr} = f_{cr0} \cdot \left(1 - \dfrac{\sigma_h}{F}\right)$

$\overline{_b f_{cr}} \quad$ is equal to $\quad _b f_{cr} \quad$ when no internal pressure exists (N/mm^2)

$\overline{_b f_{cr}}$ is given by the following equations:

- In the case of $\quad \dfrac{r}{t} \le 0.274 \cdot \left(\dfrac{E}{F}\right)^{0.78} \rightarrow \dfrac{r}{t} \le 54.05$

From (3.35), $\qquad \overline{_b f_{cr}} = \dfrac{F}{1.5} = 1.567 \times 10^2$

- In the case of $\quad 0.274 \cdot \left(\dfrac{E}{F}\right)^{0.78} \le \dfrac{r}{t} \le 2.106 \cdot \left(\dfrac{E}{F}\right)^{0.78} \rightarrow 54.05 \le \dfrac{r}{t} \le 415.4$

From (3.36), $\quad \overline{_b f_{cr}} = 0.267 \cdot F + 0.4 \cdot F \cdot \left\{\dfrac{2.106 - \left(\dfrac{r}{t}\right)\left(\dfrac{F}{E}\right)^{0.78}}{1.832}\right\}$

$$= 1.708 \times 10^2 - 0.260\left(\dfrac{r}{t}\right)$$

e) In the case of $2.106 \cdot \left(\dfrac{E}{F}\right)^{0.78} \le \dfrac{r}{t} \to 415.4 \le \dfrac{r}{t}$

From (3.37),
$$\overline{{}_b f_{cr}} = \frac{0.6 \cdot E}{2.25} \cdot \left[1 - 0.731 \cdot \left\{1 - exp\left(-\frac{1}{16} \cdot \sqrt{\frac{r}{t}}\right)\right\}\right] \bigg/ \left(\frac{r}{t}\right)$$

$$= 5.488 \times 10^4 \cdot \left[1 - 0.731 \cdot \left\{1 - exp\left(-\frac{1}{16} \cdot \sqrt{\frac{r}{t}}\right)\right\}\right] \bigg/ \left(\frac{r}{t}\right)$$

(3) Allowable shear stress, ${}_s f_{cr}$, (N/mm²)

From (3.39),
$$\quad {}_s f_{cr} = \overline{{}_s f_{cr}} + \frac{\dfrac{F}{1.5\sqrt{3}} - \overline{{}_s f_{cr}}}{0.3} \cdot \left(\frac{\sigma_h}{F}\right)$$

$$= \overline{{}_s f_{cr}} \quad (\because \sigma_h = 0)$$

$\overline{{}_s f_{cr}}$ is given by the following equations:

- In the case of $\dfrac{r}{t} \le \dfrac{0.204 \cdot \left(\dfrac{E}{F}\right)^{0.81}}{\left(\dfrac{l}{r}\right)^{0.4}} \to \dfrac{r}{t} \le 49.31$

From (3.41),
$$\overline{{}_s f_{cr}} = \frac{F}{1.5 \cdot \sqrt{3}} = 0.905 \cdot 10^2$$

- In the case of $\dfrac{0.204 \cdot \left(\dfrac{E}{F}\right)^{0.81}}{\left(\dfrac{l}{r}\right)^{0.4}} \le \dfrac{r}{t} \le \dfrac{1.446 \cdot \left(\dfrac{E}{F}\right)^{0.81}}{\left(\dfrac{l}{r}\right)^{0.4}} \to 49.31 \le \dfrac{r}{t} \le 349.54$

From (3.42),
$$\overline{{}_s f_{cr}} = \frac{0.267 \cdot F}{\sqrt{3}} + \frac{0.4 \cdot F}{\sqrt{3}} \cdot \left\{\frac{1.446 - \left(\dfrac{r}{t}\right) \cdot \left(\dfrac{l}{r}\right)^{0.4} \cdot \left(\dfrac{F}{E}\right)^{0.81}}{1.242}\right\}$$

$$= 0.994 \times 10^2 - 0.182\left(\frac{r}{t}\right)$$

- In the case of
$$\frac{1.446 \cdot \left(\frac{E}{F}\right)^{0.81}}{\left(\frac{l}{r}\right)^{0.4}} \le \frac{r}{t} \to 349.54 \le \frac{r}{t}$$

From (3.43),
$$\overline{_s f_{cr}} = \frac{4.83 \cdot E \cdot 0.8}{2.25 \cdot \left(\frac{l}{r} \cdot \sqrt{\frac{r}{t}}\right)^2} \cdot \sqrt{1 + 0.0239 \cdot \left(\frac{l}{r} \cdot \sqrt{\frac{r}{t}}\right)^3} \Big/ \left(\frac{r}{t}\right)$$

$$= 3.534 \times 10^5 \cdot \sqrt{1 + 0.0239 \cdot \left(\frac{r}{t}\right)^{3/2}} \Big/ \left(\frac{r}{t}\right)^2$$

where: l is the section length of the buckling (mm).

A2.3.1.2   The values of allowable short-term stresses in normal times are assumed to be 1.5 times those of allowable long-term stresses.

A2.3.1.3   Allowable stress during earthquakes is given by the following equations:

(1) Allowable compressive stress, $_c f_{cr}$, (N/mm^2)

$$0 \le \frac{\sigma_h}{F} \le 0.3 \to 0 \le \sigma_h < 0.705 \times 10^2$$

From (3.45),
$$_c f_{cr} = \overline{_c f_{cr}} + \frac{0.7 \cdot f_{crs} - \overline{_c f_{cr}}}{0.3}\left(\frac{\sigma_h}{F}\right)$$

$$\frac{\sigma_h}{F} > 0.3 \to 0.705 \times 10^2 < \sigma_h$$

From (3.46),
$$_c f_{cr} = f_{crs} \cdot \left(1 - \frac{\sigma_h}{F}\right)$$

Symbols: $\overline{_c f_{cr}}$: $_c f_{cr}$ when no internal pressure exists (N/mm^2)

f_{crs} :   basic compressive buckling stress under earthquakes (N/mm^2)

・ In the case of $\frac{r}{t} \le 0.069 \cdot \left(\frac{E}{F}\right) \to \frac{r}{t} \le 60.43$

From (3.47), $f_{crs} = F = 2.35 \times 10^2$

・ In the case of $0.069 \cdot \left(\frac{E}{F}\right) \le \frac{r}{t} \le 0.807 \cdot \left(\frac{E}{F}\right) \to 60.43 \le \frac{r}{t} \le 706.7$

From (3.48),

$$f_{crs} = 0.6 \cdot F + 0.4 \cdot F \cdot \left\{ \frac{0.807 - \left(\frac{r}{t}\right) \cdot \left(\frac{F}{E}\right)}{0.738} \right\} = 2.438 \times 10^2 - 0.145 \left(\frac{r}{t}\right)$$

- In the case of $0.807 \cdot \left(\frac{E}{F}\right) \leq \frac{r}{t} \rightarrow 706.7 \leq \frac{r}{t}$

From (3.49), $\quad f_{crs} = \dfrac{0.8 \cdot E}{\sqrt{3 \cdot (1 - v^2)}} \Big/ \left(\dfrac{r}{t}\right) = 9.965 / \left(\dfrac{r}{t}\right)$

$\overline{_c f_{cr}}$ is given by the following equations:

- In the case of $\dfrac{r}{t} \leq 0.377 \cdot \left(\dfrac{E}{F}\right)^{0.72} \rightarrow \dfrac{r}{t} \leq 49.53$

From (3.50), $\quad \overline{_c f_{cr}} = F = 2.35 \times 10^2$

- In the case of $0377 \cdot \left(\dfrac{E}{F}\right)^{0.72} \leq \dfrac{r}{t} \leq 2.567 \cdot \left(\dfrac{E}{F}\right)^{0.72} \rightarrow 49.53 \leq \dfrac{r}{t} \leq 337.2$

From (3.51), $\quad \overline{_c f_{cr}} = 0.6 \cdot F + 0.4 \cdot F \cdot \left\{ \dfrac{2.567 - \left(\dfrac{r}{t}\right) \cdot \left(\dfrac{F}{E}\right)^{0.72}}{2.190} \right\}$

$$= 2.511 \times 10^2 - 0.327 \left(\frac{r}{t}\right)$$

- In the case of $2.567 \cdot \left(\dfrac{E}{F}\right)^{0.72} \leq \dfrac{r}{t} \rightarrow 337.2 \leq \dfrac{r}{t}$

From (3.52), $\overline{_c f_{cr}} = 0.6 \cdot E \cdot \left[1 - 0.901 \cdot \left\{ 1 - exp\left(-\frac{1}{16} \cdot \sqrt{\frac{r}{t}} \right) \right\} \right] \Big/ \left(\frac{r}{t}\right)$

$$= 1.235 \times 10^5 \cdot \left[1 - 0.901 \cdot \left\{ 1 - exp\left(-\frac{1}{16} \cdot \sqrt{\frac{r}{t}} \right) \right\} \right] \Big/ \left(\frac{r}{t}\right)$$

(2) Allowable bending stress, $_b f_{cr}$, (N/mm^2)

$$0 \leq \frac{\sigma_h}{F} \leq 0.3 \rightarrow 0 \leq \sigma_h \leq 0.705 \times 10^2$$

From (3.53), $\quad _b f_{cr} = \overline{_b f_{cr}} + \dfrac{0.7 \cdot f_{crs} - \overline{_b f_{cr}}}{0.3} \left(\dfrac{\sigma_h}{F}\right)$

- In the case of $\dfrac{\sigma_h}{F} > 0.3 \rightarrow 0.705 \times 10^2 < \sigma_h$

  From (3.54), $\quad _b f_{cr} = f_{crs} \cdot \left(1 - \dfrac{\sigma_h}{F}\right)$

  Symbols: $\qquad \overline{_b f_{cr}}$: $_b f_{cr}$ when no internal pressure exists (N/mm²)

- In the case of $\quad \dfrac{r}{t} \leq 0.274 \cdot \left(\dfrac{E}{F}\right)^{0.78} \rightarrow \dfrac{r}{t} \leq 54.05$

  From (3.55), $\quad \overline{_b f_{cr}} = F = 2.35 \times 10^2$

- In the case of $\quad 0.274 \cdot \left(\dfrac{E}{F}\right)^{0.78} \leq \dfrac{r}{t} \leq 2.106 \cdot \left(\dfrac{E}{F}\right)^{0.78} \rightarrow 54.05 \leq \dfrac{r}{t} \leq 415.4$

  From (3.56), $\quad \overline{_b f_{cr}} = 0.6 \cdot F + 0.4 \cdot F \cdot \left\{ \dfrac{2.106 - \left(\dfrac{r}{t}\right)\left(\dfrac{F}{E}\right)^{0.78}}{1.832} \right\}$

  $$= 2.49 \times 10^2 - 0.260\left(\dfrac{r}{t}\right)$$

- In the case of $\quad 2.160 \cdot \left(\dfrac{E}{F}\right)^{0.78} \leq \dfrac{r}{t} \rightarrow 415.4 \leq \dfrac{r}{t}$

From (3.57), $\quad \overline{_b f_{cr}} = 0.6 \cdot E \cdot \left[1 - 0.731 \cdot \left\{1 - exp\left(-\dfrac{1}{16} \cdot \sqrt{\dfrac{r}{t}}\right)\right\}\right] \Big/ \left(\dfrac{r}{t}\right)$

$$= 1.235 \times 10^5 \cdot \left[1 - 0.731 \cdot \left\{1 - \exp\left(-\dfrac{1}{16} \cdot \sqrt{\dfrac{r}{t}}\right)\right\}\right] \Big/ \left(\dfrac{r}{t}\right)$$

(3)　Allowable shear stress, $_s f_{cr}$, (N/mm²)

$\qquad$ From (3.58), $\quad _s f_{cr} = \overline{_s f_{cr}} + \dfrac{\dfrac{F}{\sqrt{3}} - \overline{_s f_{cr}}}{0.3} \cdot \left(\dfrac{\sigma_h}{F}\right) = \overline{_s f_{cr}} \quad (\because \sigma_h = 0)$

- In the case of $\quad \dfrac{r}{t} \leq \dfrac{0.204 \cdot \left(\dfrac{E}{F}\right)^{0.81}}{\left(\dfrac{l}{r}\right)^{0.4}} \rightarrow \dfrac{r}{t} \leq 49.31$

From (3.60), $\quad \overline{{}_s f_{cr}} = \dfrac{F}{\sqrt{3}} = 1.357 \times 10^2$

▪ In the case of $\quad \dfrac{0.204 \cdot \left(\dfrac{E}{F}\right)^{0.81}}{\left(\dfrac{l}{r}\right)^{0.4}} \leq \dfrac{r}{t} \leq \dfrac{1.446 \cdot \left(\dfrac{E}{F}\right)^{0.81}}{\left(\dfrac{l}{r}\right)^{0.4}} \rightarrow 49.31 \leq \dfrac{r}{t} \leq 349.54$

From (3.61), $\quad \overline{{}_s f_{cr}} = \dfrac{0.6 \cdot F}{\sqrt{3}} + \dfrac{0.4 \cdot F}{\sqrt{3}} \cdot \left\{ \dfrac{1.446 - \left(\dfrac{r}{t}\right) \cdot \left(\dfrac{F}{E}\right)^{0.81} \cdot \left(\dfrac{l}{r}\right)^{0.4}}{1.242} \right\}$

$$= 1.446 \times 10^2 - 0.181 \left(\dfrac{r}{t}\right)$$

▪ In the case of $\quad \dfrac{1.446 \cdot \left(\dfrac{E}{F}\right)^{0.81}}{\left(\dfrac{l}{r}\right)^{0.4}} \leq \dfrac{r}{t} \rightarrow 349.54 \leq \dfrac{r}{t}$

From (3.62), $\quad \overline{{}_s f_{cr}} = \dfrac{0.8 \cdot 4.83 \cdot E}{\left(\dfrac{l}{r} \cdot \sqrt{\dfrac{r}{t}}\right)^2} \cdot \sqrt{1 + 0.0239 \cdot \left(\dfrac{l}{r} \cdot \sqrt{\dfrac{r}{t}}\right)^3} \Big/ \left(\dfrac{r}{t}\right)$

$$= 7.952 \times 10^5 \sqrt{1 + 0.0239 \cdot \left(\dfrac{r}{t}\right)^{3/2}} \Big/ \left(\dfrac{r}{t}\right)^2$$

A2.3.1.4   Evaluation Results

(1)   For Long-term Loading

Table A2.14

Calculation Point	t (mm)	r/t (—)	Allowable Stress				Working Stress			Test Results	
			σ_h (N/mm²)	$_cf_{cr}$ (N/mm²)	$_bf_{cr}$ (N/mm²)	$_sf_{cr}$ (N/mm²)	σ_c (N/mm²)	σ_b (N/mm²)	τ (N/mm²)	$\sigma_c/_cf_{cr}+\sigma_b/_bf_{cr}$ $\leqq 1$	$\tau/_sf_{cr}$ $\leqq 1$
⑤	6.0	716.7	7.3	22.9	32.4	14.8	4.16	0.0	0.0	0.18+0.0=0.18 <1	0<1
④	8.0	537.5	12.1	36.8	47.8	21.2	9.27	0.0	0.0	0.25+0.0=0.25 <1	0<1
③	10.0	430.0	13.4	49.5	62.2	28.0	15.20	0.0	0.0	0.31+0.0=0.31 <1	0<1
②	11.0	390.9	14.6	56.0	70.6	31.5	22.67	0.0	0.0	0.40+0.0=0.40 <1	0<1
①	12.0	358.3	14.6	62.0	78.0	35.2	27.83	0.0	0.0	0.45+0.0=0.45 <1	0<1
⓪	15.2	282.9	0.0	80.6	97.3	48.3	31.23	0.0	0.0	0.39+0.0=0.39 <1	0<1

(2)   For Seismic Loading (Modified Seismic Coefficient Method)

Table A2.15

Calculation Point	t (mm)	r/t (—)	Allowable Stress				Working Stress			Test Results	
			σ_h (N/mm²)	$_cf_{cr}$ (N/mm²)	$_bf_{cr}$ (N/mm²)	$_sf_{cr}$ (N/mm²)	σ_c (N/mm²)	σ_b (N/mm²)	τ (N/mm²)	$\sigma_c/_cf_{cr}+\sigma_b/_bf_{cr}$ $\leqq 1$	$\tau/_sf_{cr}$ $\leqq 1$
⑤	6.0	716.7	7.3	51.5	72.9	33.2	3.66	7.94	5.7	0.07+0.11= 0.18<1	0.17<1
④	8.0	537.5	12.1	79.0	103.8	47.6	7.02	28.70	16.3	0.09+0.28= 0.37<1	0.34<1
③	10.0	430.0	13.4	104.6	133.3	63.0	10.97	51.98	20.8	0.10+0.39= 0.49<1	0.33<1
②	11.0	390.9	14.6	117.6	144.1	71.0	16.01	80.71	24.0	0.14+0.56= 0.70<1	0.34<1
①	12.0	358.3	14.6	130.4	151.6	79.2	19.63	98.55	24.6	0.15+0.65= 0.80<1	0.31<1
⓪	15.2	282.9	0.0	158.9	175.7	93.6	25.51	107.21	20.4	0.16+0.61= 0.77<1	0.22<1

(3)   For Seismic Loading (Modal Analysis)

Table A2.16

Calculation Point	t (mm)	r/t (—)	Allowable Stress				Working Stress			Test Results	
			σ_h (N/mm^2)	$_cf_{cr}$ (N/mm^2)	$_bf_{cr}$ (N/mm^2)	$_sf_{cr}$ (N/mm^2)	σ_c (N/mm^2)	σ_b (N/mm^2)	τ (N/mm^2)	$\sigma_c/_cf_{cr}+\sigma_b/_bf_{cr}$ $\leqq 1$	$\tau/_sf_{cr}$ $\leqq 1$
⑤	6.0	716.7	7.3	51.5	72.9	33.2	3.66	8.11	5.8	0.07+0.11= 0.18<1	0.17<1
④	8.0	537.5	12.1	79.0	103.8	47.6	7.02	25.88	14.2	0.09+0.25= 0.34<1	0.30<1
③	10.0	430.0	13.4	104.6	133.3	63.0	10.97	43.80	16.6	0.10+0.33= 0.43<1	0.26<1
②	11.0	390.9	14.6	117.6	144.1	71.0	16.01	65.33	18.3	0.14+0.45= 0.59<1	0.26<1
①	12.0	358.3	14.6	130.4	151.6	79.2	19.63	78.21	18.3	0.15+0.52= 0.67<1	0.23<1
⓪	15.2	282.9	0.0	158.9	175.7	93.6	25.51	83.38	15.0	0.16+0.47= 0.63<1	0.16<1

(4)   For Short-term Loading (under Wind Pressure)

Table A2.17

Calculation Point	t (mm)	r/t (—)	Allowable Stress				Working Stress			Test Results	
			σ_h (N/mm^2)	$_cf_{cr}$ (N/mm^2)	$_bf_{cr}$ (N/mm^2)	$_sf_{cr}$ (N/mm^2)	σ_c (N/mm^2)	σ_b (N/mm^2)	τ (N/mm^2)	$\sigma_c/_cf_{cr}+\sigma_b/_bf_{cr}$ $\leqq 1$	$\tau/_sf_{cr}$ $\leqq 1$
⑤	6.0	716.7	7.3	34.4	48.6	22.2	4.16	0.489	0.7	0.12+0.01= 0.13<1	0.03<1
④	8.0	537.5	12.1	55.2	71.7	31.8	9.27	1.445	1.0	0.17+0.02= 0.19<1	0.03<1
③	10.0	430.0	13.4	74.3	93.3	42.0	15.20	2.551	1.2	0.20+0.03= 0.23<1	0.03<1
②	11.0	390.9	14.6	84.0	105.9	47.3	22.67	4.036	1.4	0.27+0.04= 0.31<1	0.03<1
①	12.0	358.3	14.6	93.0	117.0	52.8	27.83	5.056	1.4	0.30+0.04= 0.34<1	0.03<1
⓪	15.2	282.9	0.0	120.9	146.0	72.5	31.23	5.755	1.3	0.26+0.04= 0.30<1	0.02<1

A2.3.2   Evaluation of Stresses in Hopper Wall

The axial stress σ_ϕ in the longitudinal direction and the circumferential tensile stress σ_θ in the hopper wall are evaluated by the following equations:

From (5.15),
$$\sigma_\phi = \frac{(W_h + W_s)}{l_c \cdot t_2 \cdot \sin\alpha} + \frac{dP_v \cdot d'}{4 \cdot t_2 \cdot \sin\alpha} \le f_t$$

From (5.16)
$$\sigma_\theta = \frac{dP_a \cdot d'}{2 \cdot t_2 \cdot \sin\alpha} \le f_t$$

Symbols:
W_h :   weight of stored material in the hopper (N)
W_s :   weight of the hopper beneath the section (N)
t_2 :   thickness of the hopper wall (mm)
l_c :   perimeter of the hopper wall (mm)
d' :   diameter of the hopper wall (mm)
dP_v :   design vertical pressure (N/mm^2)
α :   inclination of the hopper wall (°)
dP_a :   perpendicular design pressure of the hopper wall (N/mm^2)

Table A2.18   Stresses in Hopper Wall

t_2 (mm)	d' (mm)	W_h (kN)	W_s (kN)	l_c (m)	dP_v (N/mm^2)	$t_2 \sin\alpha$ (mm)	C_d' (—)	dP_a (N/mm^2)	f_t (N/mm^2)	σ_ϕ (N/mm^2)	σ_θ (N/mm^2)
8.0	8,600	612.00	50.60	27.02	0.150	5.657	2.30	0.163	157	61.3	123.9
6.0	5,733	181.50	16.90	18.01	0.153	4.243	1.87	0.135	157	54.3	91.2
6.0	2,867	22.60	4.20	9.01	0.158	4.243	1.44	0.111	157	27.4	37.5

APPENDIX A3

DESIGN EXAMPLE
SUPPORTING STRUCTURES FOR SPHERICAL TANKS
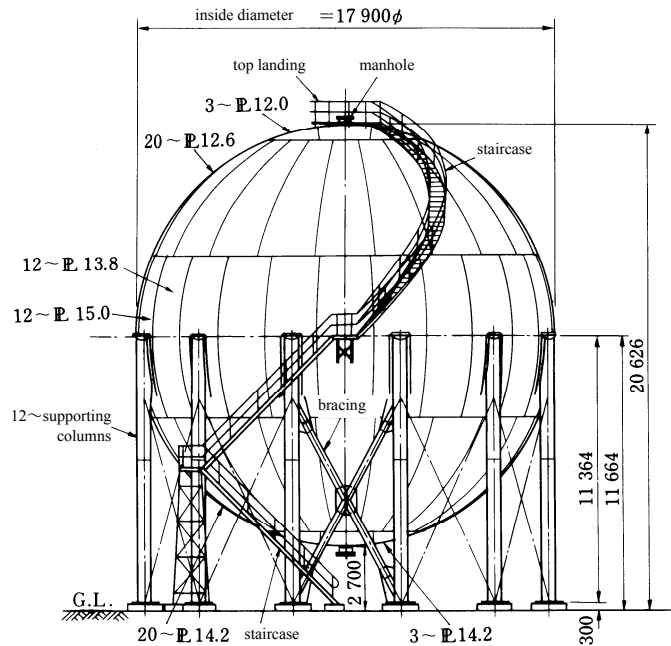
Fig.A3.1　General View of Spherical Tank

Specifications:

- Classification of ground: Type 3

- Importance factor, $I = 1.5$ (Classification of seismic design IV)

- Structural type:　pipe columns and pipe bracings

- Stored contents:　liquefied butane (specific gravity 0.587)

- Sphere:　　$D = 1\ 790$ cm, $t = 12.0{\sim}15.0$ mm, material SPV 490 ($F = 42.7$ kN/ cm^2)

- Columns:　$d_c = {}^\phi 609.6$, $t_c = 14$, $n = 12$, material SPV 490

- Bracings:　$d_b = {}^\phi 267.4$, $t_b = 7$, $L = 1\ 012$, material STK 400 ($F = 23.5$ kN/ cm^2)

- h_o　　$= 1\ 136.4$ cm

- h_1　$= 900$ cm

- l　　$= 463$ cm

- θ = 1.096 rad

The dead weight of the structure W_D and weight of the stored contents W_I are calculated as follows:

$W_D = 1\,980$ kN

$W_I = 15\,550$ kN

As $f(\xi)$ is obtained as 0.7 from Figure 6.1, the design weight imposed on the base of structure W is calculated at;

$W = W_D + f(\xi)\,W_I = 12\,865$ kN

Those basic values to assess the retaining strength and elastic modulus of the structure are obtained as follows:

$$l_r = \sqrt{\frac{Dd_c}{2}} = 233.5 \text{ cm}$$

$$h = h_0 - \frac{l_r}{2} = 1019.7 \text{cm}$$

$$h_2 = h - h_1 = 119.7 \text{ cm}$$

Axial force in the column: $\quad N = \frac{W_D + W_I}{n} = 1\,461$ kN

Sectional properties of the column:

$A_c = 262 \text{ cm}^2$

$Z_c = 3\,810 \text{ cm}^3$

$I_c = 1.160 \times 10^5 \text{ cm}^4$

$i_c = 21.1 \text{ cm}$

$\lambda_c = h / i_c = 48.3 < 60$

Sectional properties of the bracing:

$A_c = 57.3 \text{ cm}^2$

$i_b = 9.21 \text{ cm}$

Short-term allowable bending moment of the column:

$$M_y = FZ_c\left(1 - \frac{N}{FA_c}\right) = 42.7 \times 3\,810 \times \left(1 - \frac{1461}{42.7 \times 262}\right) = 1\,414 \text{ kN·m}$$

Short-term allowable shear force of the column:

$$Q_{ca} = \frac{F}{\sqrt{3}} \times \frac{A_c}{2} = 3\ 230 \text{ kN}$$

Short-term allowable compressive force of the bracing:

$$\lambda_b = (L/\ i_b) \times \frac{1}{2} = 54.9$$

$$1.5f_c = 19.7 \text{ kN/cm}^2, \quad \therefore \quad N_c = 1.5f_c A_b = 1\ 129 \text{ kN}$$

$$S_y = N_c \cos\theta = 516 \text{ kN}$$

Stresses in the column in *Figure 6.3.2* of the Commentary are calculated as follows:

From Eq. *(6.3.8)*,

$$M_{a1} = 198.9S$$

$$M_{b1} = -35.7S$$

$$R_a = (M_{a1} - M_{b1})/h_2 = 1.960S$$

From Eq. *(6.3.9)*,

$$M_{a2} = 31.4S$$

$$M_{b2} = 27.7S$$

$$R' = M_{a2}/h_2 = 0.031S$$

$$Q = R_a + R' = 1.99S$$

From Eq. *(6.3.12)* and *(6.3.13)*,

$$M_a = 230.3S$$

$$M_b = -8.0S$$

From Eq. *(6.3.7)*,

$$\delta = 0.00458S$$

The yield shear force Q_y in the plain where the maximum shear stress takes place is given as follows:

$$Q_y = 1.99S_y = 1,027 \text{ kN}$$

From Eq. *(6.3.1)*, the yield shear force F_y of the supporting structure is given as follows:

$$F_y = \frac{nQ_y}{2} = 6\,161\text{kN}$$

The yield deformation δ_y is given as follows:

$$\delta_y = 0.00458S = 2.363 \text{ cm}$$

The spring constant k is obtained from Eq. *(6.3.18)*.

$$k = \frac{F_y}{\delta_y} = 2\,607\text{kN/cm}$$

The natural period: $T = 2\pi\sqrt{\dfrac{W}{gk}} = 0.446\,\text{s}$

The yield shear force coefficient: $\alpha = \dfrac{F_y}{W} = 0.479$

The bending moment $_eM_a$ in *Figure 6.3.3* of the Commentary is calculated as per Eq. *(6.3.19)*:

$$_eM_a = M_a - \frac{l_rQ}{4} = 114.1S$$

$$\therefore \left(_eM_a\right)_y = 114.1S_y = 589 \text{ kN}\cdot\text{m}$$

From Eq. *(6.3.21)*,

$$\Delta M = M_y - (_eM_a)_y = 1414 - 589 = 825 \quad \text{kN}\cdot\text{m}$$

From Eq. *(6.3.22)*,

$$\Delta M_a = \Delta M \times \frac{h}{h - l_r/4} = 875 \quad \text{kN}\cdot\text{m}$$

From Eq. *(6.3.23), (6.3.24)*,

$$\eta = \frac{\Delta M_a h^2}{3EI}/\delta_y = 5.397$$

$$\therefore \quad a\eta = 0.75 \times 5.397 = 4.048 > 3.0 \ \rightarrow \ 3.0$$

From Eq. (6.3),

$$D_s = \frac{1}{\sqrt{1 + 4a\eta}} = 0.278$$

From Eq. (6.2),

$$C = Z_s \cdot I \cdot D_s \cdot \frac{S_{a1}}{g} = 1.0 \times 1.5 \times 0.278 \times 1.0 = 0.417$$

Evaluation of anti-seismic characteristics is made in accordance with Eq. (6.5).

$F_y = 6{,}161$ kN

$Q_d = CW = 0.417 \times 12{,}865 = 5{,}365$ kN

$F_y \geq Q_d$

APPENDIX A4

DESIGN EXAMPL
ABOVE-GROUND, VERTICAL, CYLINDRICAL STORAGE TANKS

A seismic capacity evaluation is conducted for a small tank which suffered elephant foot bulge type damage during the Hanshin-Awaji Great Earthquake in Japan. The evaluation is performed according to the flow scheme shown in *Fig. 7.3.1*.

A4.1   Tank size

Diameter of the cylindrical tank	D	=	13.54 m
Weight of the stored contents	W_l	=	1.905 x 10^4 kN
Depth of the stored liquid	H_l	=	13.5 m
Static pressure imposed on the bottom plate	p	=	0.0132 kN/cm^2
Slope angle of the conical roof			15° (estimated)
Wall thickness of the cylindrical tank			
- bottom course	t_0	=	8 mm
- one-third height above the bottom	$t_{1/3}$	=	6 mm
- thickness of the bottom annular plate	t	=	6 mm
Anchor			unanchored

A4.2   Design specification:

Yield point of bottom plate and wall plate	σ_y	=	23.5 kN/cm^2
Young's modulus of bottom plate and wall plate:	E	=	2.06 x 10^4 kN/cm^2
Poisson's ratio	v	=	0.3
Ratio of yield stress to ultimate tensile strength	Y_r		below 0.8 (estimated)
Seismic zone factor	Z_S	=	1.0
Importance factor	I	=	1.2
Damping ratio	h	=	0.1
			(for impulsive mass)
		=	0.001
			(for convective mass)
Critical period	T_G	=	0.96 sec.
- (determined by the ground classification)			

A4.3   Evaluation for the mass of impulsive pressure

Natural period T_f is obtained using Eq. *(7.2.20)*:

$$
\begin{aligned}
T_f &= \frac{2}{\lambda}\sqrt{\frac{W_l}{\pi g E t_{1/3}}} \\
&= \frac{2}{0.23}\sqrt{\frac{1.905 \times 10^4}{\pi \times 980 \times 2.06 \times 10^4 \times 0.6}} \\
&= 0.196 \, \text{sec}
\end{aligned}
$$

Weight percent of the effective mass of the tank contents is given by *Fig.7.2.1*.

$$f_f(D/H_l) = f_f(1.00) = 0.77$$

1) Evaluation for buckling

Substituting values into Eq. (7.6):

$$D_s = \frac{0.71}{1+3h+1.2\sqrt{h}} \cdot \frac{1}{0.5\sqrt{1+3\left(\dfrac{T_f}{T_e}\right)^2}}$$

$$= \frac{0.71}{1+3\times0.1+1.2\sqrt{0.1}} \cdot \frac{1}{0.5\sqrt{1+3\left(\dfrac{0.196}{0.397}\right)^2}}$$

$$= 0.423 \times 0.76 / 0.5$$

$$= 0.642$$

Design shear force of the impulsive mass vibration, Q_{dw}, is given by Eq. *(7.3.1)* as:

$$Q_{dw} = Z_s \cdot I \cdot D_s \cdot S_{a1} \cdot f_f \cdot W_l / g$$
$$= 1.0\times1.2\times0.642\times980\times0.77\times1.905\times10^4 / 980$$
$$= 1.130\times10^4\,\text{kN.}$$

Mean hoop tensile stress in the cylindrical wall, $_Q\sigma_{hd}$, is calculated by Eq. *(7.3.2)* as:

$$_Q\sigma_{hd} = \frac{Q_{dw}}{2.5H_l t_0} + \frac{W_l}{\pi r t_0}$$

$$= \frac{1.13\times10^4}{2.5\times1350\times0.8} + \frac{1.905\times10^4}{\pi\times677\times0.8}$$

$$= 4.185 + 11.20$$

$$= 15.38\,\text{kN/cm}^2$$

Allowable bending stress in the cylindrical wall, $_b f_{cr}$, and basic axial compressive buckling stress f_{crs} are calculated by Eqs. (3.54) and (3.28) as:

$$_b f_{cr} = f_{crs}(1-\sigma_{hd}/Q_y)$$
$$= 11.79(1-15.38/23.5)$$
$$= 4.072\,\text{kN/cm}^2$$

$$f_{crs} = \frac{0.8E}{\sqrt{3(1-v^2)}\left(\dfrac{r}{t_0}\right)}$$

$$= \frac{0.8\times2.06\times10^4}{\sqrt{3(1-0.09)}\times(677/0.8)}$$

$$= 11.79\,\text{kN/cm}^2$$

Yield shear force of the storage tank for buckling as shown in Eq. *(7.3.6)* is:

$$_eQ_y \quad = \quad \frac{\pi \cdot r^2 \cdot _bf_{cr} \cdot t_0}{0.44H_l}$$

$$= \quad \frac{\pi(677)^2 \times 4.072 \times 0.8}{0.44 \times 1350}$$

$$= \quad 7.896 \times 10^3 \text{ kN}$$

It can be concluded that the buckling strength is insufficient as $_eQ_y < Q_{dw}$.

2) Evaluation for bottom plate

The yielding force of the bottom plate q_y, the uplifting deformation for the yielding force δ_y, the spring constant of unit circumferential length for uplifting resistance k_1, the spring constant K_1 as the one degree of freedom system that represents the horizontal directional motion of tank and the natural period of the storage tank when only the bottom plate deforms, T_1, are calculated from Eqs. *(7.2.11)*, *(7.2.15)*, *(7.2.17)* and *(7.2.18)*, respectively, as:

$$q_y \quad = \quad \frac{2t\sqrt{1.5P\sigma_y}}{3}$$

$$= \quad \frac{2 \times 0.6 \times \sqrt{1.5 \times 0.0132 \times 23.5}}{3}$$

$$= \quad 0.273 \text{ kN/cm}$$

$$\delta_y \quad = \quad (3t\sigma_y^2)/(8Ep)$$

$$= \quad (3 \times 0.6 \times 23.5^2)/(8 \times 2.06 \times 10^4 \times 0.0132)$$

$$= \quad 0.457 \text{ cm}$$

$$k_1 \quad = \quad q_y/\sigma_y$$

$$= \quad 0.273/0.457$$

$$= \quad 0.597 \text{ kN}/\text{cm}^2$$

$$K_1 \quad = \quad 48.7r^3 k_1/H_l^2$$

$$= \quad 48.7 \times (677)^3 \times 0.597/1350^2$$

$$= \quad 4950 \text{ kN}/\text{cm}$$

$$T_1 \quad = \quad 2\pi\sqrt{\frac{f_fW_l}{gK_1}}$$

$$= \quad 2\pi\sqrt{\frac{0.77 \times 1.905 \times 10^4}{980 \times 4950}}$$

$$= \quad 0.345 \text{ sec}$$

The modified natural period of the storage tank considering deformation of both the wall plate and the bottom plate, T_e, the coefficient determined by the ductility of the bottom plate uplifting, D_η, and the structural characteristic coefficients, D_s are calculated from Eqs. *(7.2.19)*, *(7.2.24)* and *(7.3)*, respectively, as

$$T_e \quad = \quad \sqrt{T_f^2 + T_1^2}$$
$$= \quad \sqrt{0.196^2 + 0.345^2}$$
$$= \quad 0.397\,\text{sec}$$

$$D_\eta \quad = \quad \frac{1}{\sqrt{1 + 84(T_1/T_e)^2}}$$
$$= \quad \frac{1}{\sqrt{1 + 84(0.345/0.397)^2}}$$
$$= \quad 0.125$$

$$D_s \quad = \quad \frac{1.42}{1 + 3h + 1.2\sqrt{h}} \cdot D_\eta$$
$$= \quad 0.846 \times 0.125$$
$$= \quad 0.105$$

Design shear force of the impulsive mass vibration, Q_{dw}, and the design yield shear force of the storage tank, Q_y, are obtained from Eqs. *(7.3.1)* and *(7.3.5)* as:

$$Q_{dw} \quad = \quad Z_s \cdot I \cdot D_s \cdot S_{a1} \cdot f_f \cdot W_l / g$$
$$= \quad 1.0 \times 1.2 \times 0.105 \times 1.0 \times 0.77 \times 1.905 \times 10^4$$
$$= \quad 1848\ \text{kN}$$

$$Q_y \quad = \quad (2\pi\,r^2 q_y) / (0.44 H_l)$$
$$= \quad (2\pi \times (677)^2 \times 0.273) / (0.44 \times 1350)$$
$$= \quad 1324\ \text{kN}.$$

Therefore it can be concluded that the uplifting strength is insufficient because $_e Q_y < Q_{dw}$.

A4.4   Evaluation for the mass of convective pressure

As f_f is obtained from *Fig.7.2.1*, f_s, the natural period of sloshing response T_s, and acceleration response spectrum of the first natural period S_{a1} are calculated by Eqs.*(7.2.5)* and *(7.2.32)* as

$$f_s \quad = \quad 1 - f_f$$
$$= \quad 1 - 0.77$$

$$= \quad 0.23$$

$$T_s \quad = \quad \frac{2\pi\sqrt{D}}{\sqrt{3.682g\tanh(3.682H_l/D)}}$$

$$= \quad \frac{2\pi\sqrt{1354}}{\sqrt{3.682\times980\tanh(3.682\times1350/1354)}}$$

$$= \quad 3.85\,\text{sec}$$

$$IS_v \quad = \quad 2\cdot\frac{1.10}{1+3h+1.2\sqrt{h}}$$

$$= \quad 2.11\,\text{m/s}$$

$$\therefore IS_{a1} \quad = \quad IS_v\times\frac{2\pi}{T_s}$$

$$= \quad 3.45\,\text{m/s}^2$$

Design shear force of the convective mass vibration Q_{ds} is obtained from Eq. *(7.3.3)* as:

$$Q_{ds} \quad = \quad Z_s\cdot I\cdot S_{a1}\cdot f_s\cdot W_l/g$$

$$= \quad 1.0\times345\times0.23\times1.905\times10^4/980$$

$$= \quad 1542\text{ kN.}$$

The design yield shear force for buckling, $_sQ_y$ is obtained by Eq. *(7.3.4)* as

$$_sQ_y \quad = \quad 0.44\,_eQ_y$$

$$= \quad 0.44\times7.896\times10^3$$

$$= \quad 3474\text{ kN}$$

and the design yield shear force for uplifting, $_sQ_y$ is obtained from Eq. *(7.3.4)* as:

$$_sQ_y \quad = \quad 0.44Q_y$$

$$= \quad 0.44\times1324$$

$$= \quad 583\text{ kN.}$$

From these results, it can be concluded that buckling strength is sufficient as $_sQ_y > Q_{ds}$, and uplifting strength is insufficient because $_sQ_y < Q_{ds}$.

In conclusion, this tank has insufficient capacity for impulsive mass vibration concerning both buckling and uplifting strength, and for convective mass vibration concerning uplifting strength. This therefore, explains the actual seismic damage, namely buckling type damage, to the subject tank.

A4.5   Sloshing force acting on the fixed roof

When only the 1st mode is considered, sloshing height ζ_R is equal to η_s.
Therefore,

$$\zeta_R \quad = \quad 0.802 \cdot Z_s I \cdot S_{v1} \sqrt{\frac{D}{g} \tanh\left(\frac{3.682 H_i}{D}\right)}$$

$$= \quad 0.802 \cdot 1.0 \cdot 2.11 \cdot \sqrt{\frac{13.54}{9.8} \tanh\left(\frac{3.682 \cdot 13.5}{13.54}\right)}$$

$$= \quad 1.99 m$$

Since the roof angle $\varphi = 0.262$ rad., the impulsive pressure P_i is, from equation *(7.2.37)*,

$$P_i \quad = \quad \frac{\pi}{2} \rho \cot \varphi (\dot{\zeta}_r^A \cos \theta)^2 = \frac{\pi}{2} \cdot 10^3 \cdot \cot\left(\frac{15\pi}{180}\right) \cdot (1.99 \cdot 1.63)^2$$

$$= \quad 6.17 \times 10^4 \, \text{N/m}^2$$

The hydrodynamic pressure P_h at the connection of the roof and wall is, from equation *(7.2.38)*,

$$P_h \quad = \quad \rho g(\zeta_r - h_r)\cos\theta = 1000 \cdot 9.8 \cdot (1.99 - 0)$$

$$= \quad 1.95 \times 10^4 \, \text{N/m}^2$$

APPENDIX B

ASSESSMENT OF SEISMIC DESIGNS
FOR
UNDER-GROUND STORAGE TANKS

B.1 Introduction

This chapter addresses that the seismic design for under-ground tanks has been revised in the response displacement method. Some sample calculations are provided to evaluate the response displacement method comparing with other analytical methods.

B.2 Analytical Methods

The recommended analytical methods are; the response intensity method and dynamic analysis using an FEM model other than the response displacement method. The main change in the response displacement method from the 1990 version [B.1] is to consider an inertia force and surrounding shear forces in the new version. The five analytical methods shown in Figure B.1 are assessed in the following sections whereas Figure B.2 compares the new preferred analytical methods with the one in the previous (1990) version of the Design Recommendation.
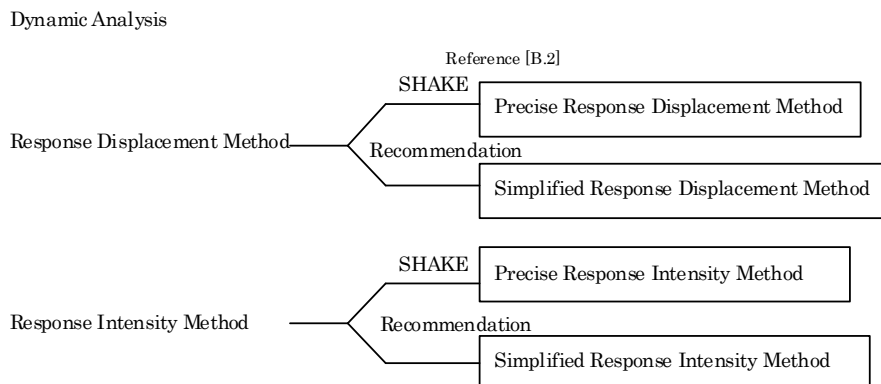
Figure B.1
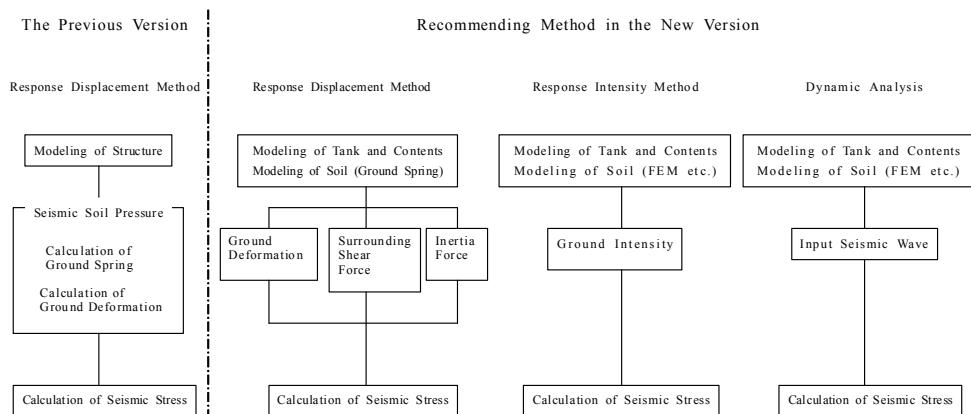
Figure B.2

Par.3.6.2.3 generally recommends the use of a reverse triangle distribution for calculating ground displacement by the simplified response displacement method. However, it recommends that a cosine-curve distribution is used where the bedrock is located at the base of the under-ground tank. This appendix reports the assessment result of the ground displacement with an assumption of a cosine-curve distribution used in the 1990 version of the Design Recommendation and compares to the one with an assumption of a reverse triangle distribution (see Figure B.2).

B.3   Assessment of Structure with Ground

Figure B.3 illustrates the model of an under-ground water tank with a flat slab structure, which is to be analysed. Table B.1 shows the physical properties of the ground which, for the purposes of this example, is assumed as sandy ground.
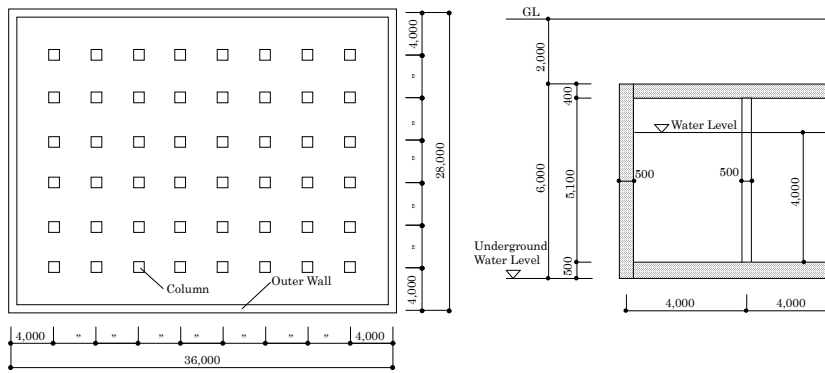
Figure B.3

Table B.1

Soil	Thickness (m)	N Value	Vs (m/s)	ρ (kN/m³)	G_0 (kN/m²)	ν	E_0 (kN/m²)	P (N/c m²)
Reclaimed Clay	2.0	5	100	15.68	15,680	0.33	42,140	0.98
Grain	3.0	10	170	16.66	49,000	0.33	127,400	3.92
Sand	3.0	15	200	16.66	67,620	0.33	176,400	6.86
Sand ∼ Gravel	12.0	30	250	16.66	107,800	0.49	323,400	11.76
Sand	20.0	50	300	18.62	166,600	0.49	499,800	20.58
	30.0	>50	400	18.62	303,800	0.49	901,600	35.28
Bed Rock		>50	500	18.62	470,400	0.49	−	−

Grand Water Level : GL−8m

Vs　　:　S-Wave Velocity = $80.6 N^{0.331}$
ρ　　:　Unit Volume Weight
G_0　　:　Shear Modulus of Elastic Ground
ν　　:　Poisson's Ratio
E_0　　:　Young's Modulus of Elastic Ground
P　　:　Restraint Pressure = $(1+2K_0)/3 \times \sigma_v$
K_0　　:　Static Soil Pressure Coefficient = 0.5
σ_v　　:　Imposed Load

B.4 Outline of Analytical Method

Figure B.4 shows a model of dynamic analysis and its assessment flow. The structure with the surrounding ground is modeled with a two dimensional FEM model on the assumption that an energy transmission boundary is provided at the side of the model, and there is a viscous boundary at the bottom of the model.   The frequency response analysis is adopted by use of the EL CENTRO seismic wave as an input, and the convergence stiffness is adopted as a stiffness of the ground as the result of SHAKE [B.2].

Figure B.5 illustrates the structure's model so that the outer wall in the model plane is modeled as plane elements, and the outer wall perpendicular to the plane, columns, bottom slab and top slab as beam elements.
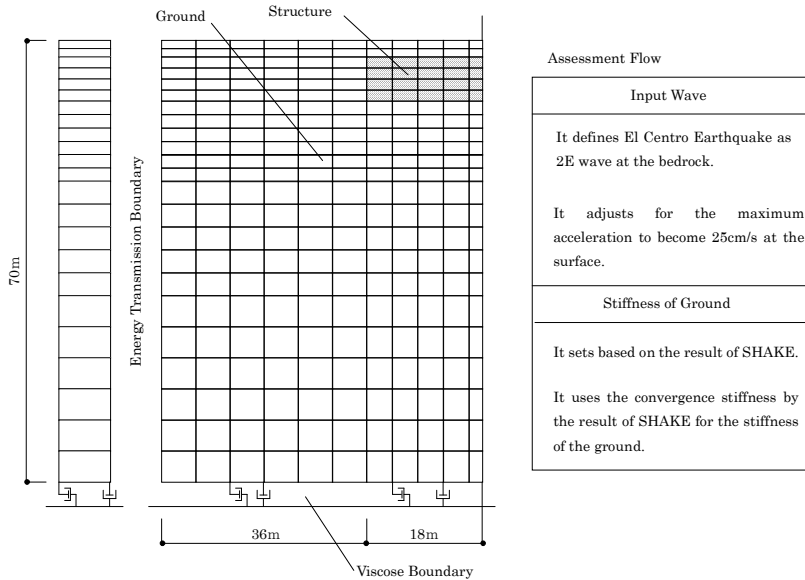
Figure B.4
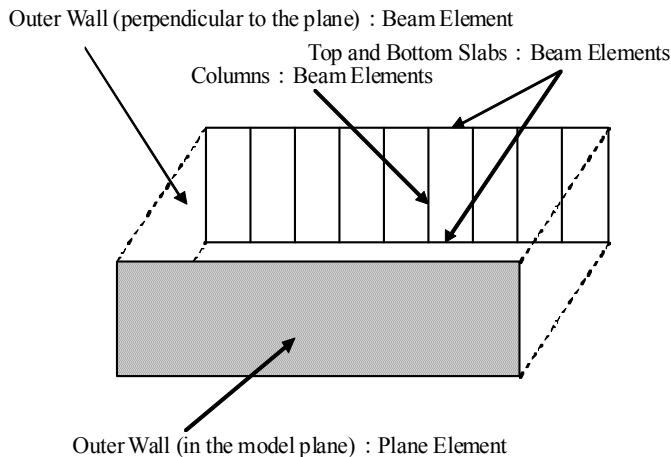
Figure B.5

Figure B.6 shows a design flow of the response intensity method and Figure B.7 shows its analytical model. The structure, together with the surrounding ground, is modeled with a two dimensional FEM model on the assumption that a ground seismic coefficient is provided in the ground, and there is a static inertia force in the structure. An assessment of the ground stiffness and the seismic ground coefficient, (the inertia force), is made by means of both the simplified calculation based on the 1990 version of the Design Recommendation and the precise calculation based on the result of SHAKE.

| Analysis Flow		Method	
		Simplified Calculation	Precise Calculation
Modeling of Structure — Modeling of Ground — Calculating Stiffness of Ground	Ground Stiffness	The initial stiffness is calculated considering the non-linear characteristics of soil. · to calculate the ground deformation in accordance with the previous recommendation. · to calculate the ground stiffness considering the degradation of rigidity due to the shear strain.	It is provided by the result of SHAKE. · The ground stiffeness is considered as the convergence stiffness based on the result of one-dimensional equivalent linear analysis.
Calculating Inertia Force — Horizontal Coefficient (Seismic Ground Coefficient) — Response Intensity Method	Seismic Ground Coefficient	The Design Recommendation calls for; $$K_{hs} = Z_S \cdot R_G \cdot K_0$$	It is provided by the result of SHAKE. · It is calculated from the maximum shear force of one-dimensional equivalent linear analysis. $$K_h = \frac{2(|\tau_{imax}| - |\tau_{i\text{-}1max}|)}{h_{i\text{-}1} \cdot \rho_{i\text{-}1} + h_i \cdot \rho_i}$$

Figure B.6
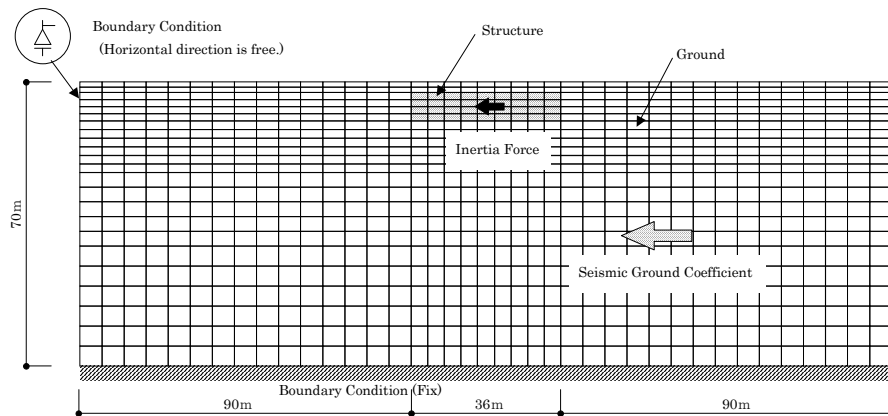
Figure B.7

Figure B.8 shows the design flow of the response displacement method, and Figure B.9 shows its analytical model. The structure, together with the surrounding ground, is modeled with a two dimensional FEM model on the assumption that the ground springs, (the axial and shear springs), are provided to the structure and the under-ground deformation, ground seismic coefficient (inertia force) and the boundary shear forces are provided statically. An assessment of the springs, seismic coefficient and shear forces is made by means of both the simplified calculation based on the Specifications for Highway Bridges [B.3], the 1990 version of the Design Recommendation, and the precise calculation based on the result of SHAKE (Refer to Figure B.10).

| Analysis Flow	Analytical Method		
		Simplified Calculation	Precise Calculation
	Ground Stiffness	Specifications for Highway Bridges Kv=12.8Kvo・Bv-3/4 Kh=12.8Kho・Bh-3/4 Kvo=Kho=1/30・α・Eo Eo=28N α=2.0	It is provided by the result of the Static FEM analysis. ・ The ground stiffness is considered as the convergence stiffness based on the result of one-dimensional equivalent linear analysis.
	Ground Deformation	The Design Recommendation calls for; $UH(Z) = \frac{2}{\pi^2} \cdot Sv \cdot Khb \cdot Ts \cdot \cos\left(\frac{\pi Z}{2H}\right)$	It is provided by the result of SHAKE. ・ Maximum ground deformation of one-dimensional equivalent linear analysis.
	Seismic Ground Coefficient	The Design Recommendation calls for; $K_{hs} = Z_S \cdot R_G \cdot K_\theta$,etc.	It is provided by the result of SHAKE. ・ It is calculated from the maximum shear force of one-dimensional equivalent linear analysis. $K_h = \frac{2(|\tau_{imax}| - |\tau_{i-1max}|)}{h_{i-1} \cdot \rho_{i-1} + h_i \cdot \rho_i}$
	Surround Shear Force	$\tau = G \times \gamma$ ・ It calculates the shear strain γ from the ground deformation in accordance with the Design Recommendation. ・ It calculates the ground stiffness G considering the degradation of the stiffness due to the shear strain.	It is provided by the result of SHAKE. ・ Maximum ground Shear Force of one-dimensional equivalent linear analysis.

Figure B.8
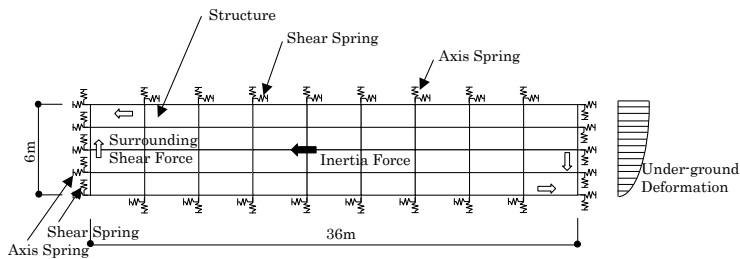
Figure B.9
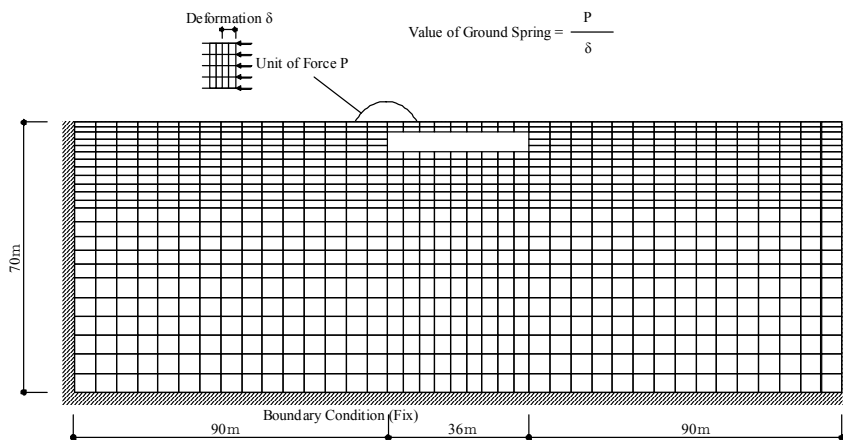
Figure B.10

B.5   One-dimensional Seismic Motion Analysis (SHAKE)

The outline of one dimensional seismic motion analysis is shown in Figure B.11. The stiffness and damping of the ground have strain dependent and restraint pressure dependent characteristics [B.4]. The non-linear characteristic shown in Figure B.12 is assumed as a sandy ground.

The EL CENTRO seismic wave is adopted as the design seismic wave as being the 2E wave at -70 m level from G.L. (Ground Level), and the maximum seismic velocity of approximately 25 cm/s at the ground surface.

Figure B.13 shows the result of SHAKE. The maximum seismic acceleration at the ground surface is approximately 220cm/s^2, the maximum relative displacement at the ground surface is approximately 2.6 cm to -70 m level from G.L., the maximum ground shear strain near the ground surface is approximately 4 - 6×10^{-4} and the ratio of the convergence stiffness to the initial stiffness (the degradation percentage of the ground stiffness) is 0.4 - 0.8.
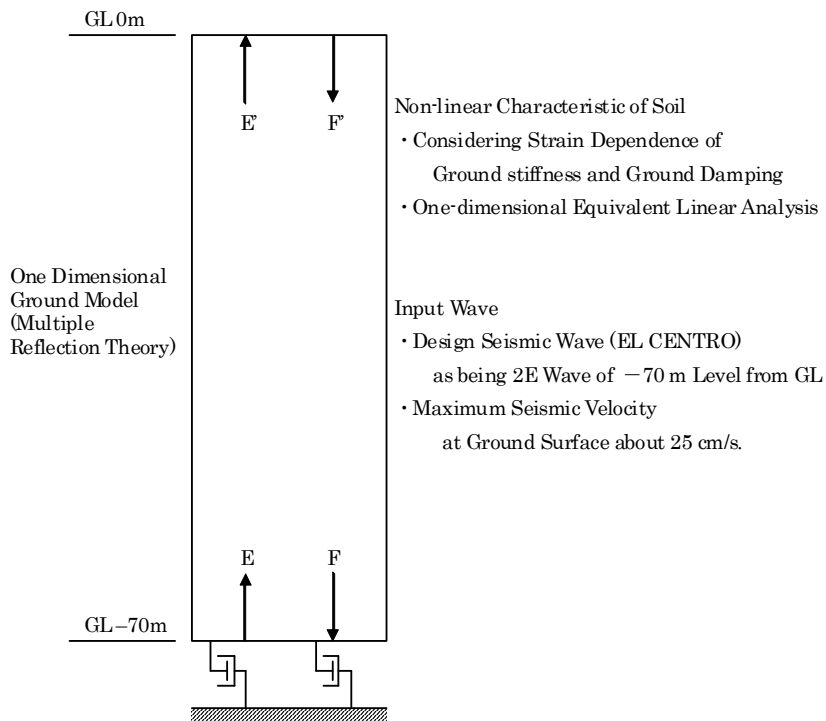
GL 0m

E'   F'

Non-linear Characteristic of Soil
・Considering Strain Dependence of
   Ground stiffness and Ground Damping
・One-dimensional Equivalent Linear Analysis

One Dimensional
Ground Model
(Multiple
Reflection Theory)

Input Wave
・Design Seismic Wave (EL CENTRO)
   as being 2E Wave of －70 m Level from GL
・Maximum Seismic Velocity
   at Ground Surface about 25 cm/s.
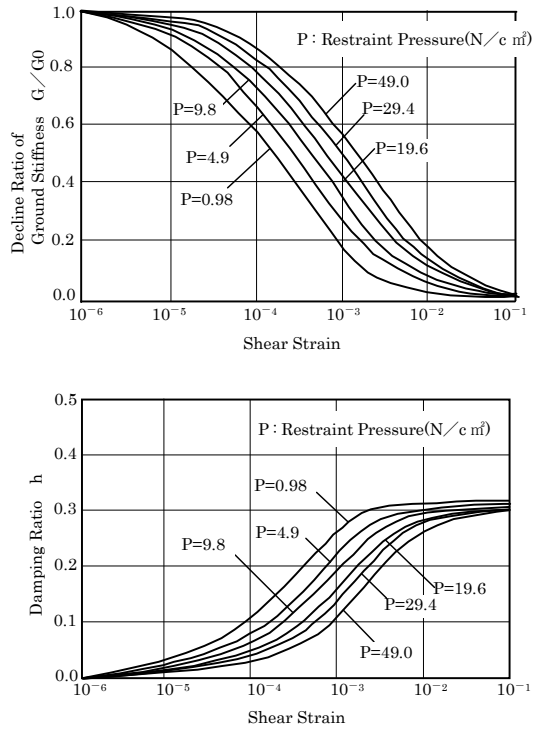
E   F

GL －70m
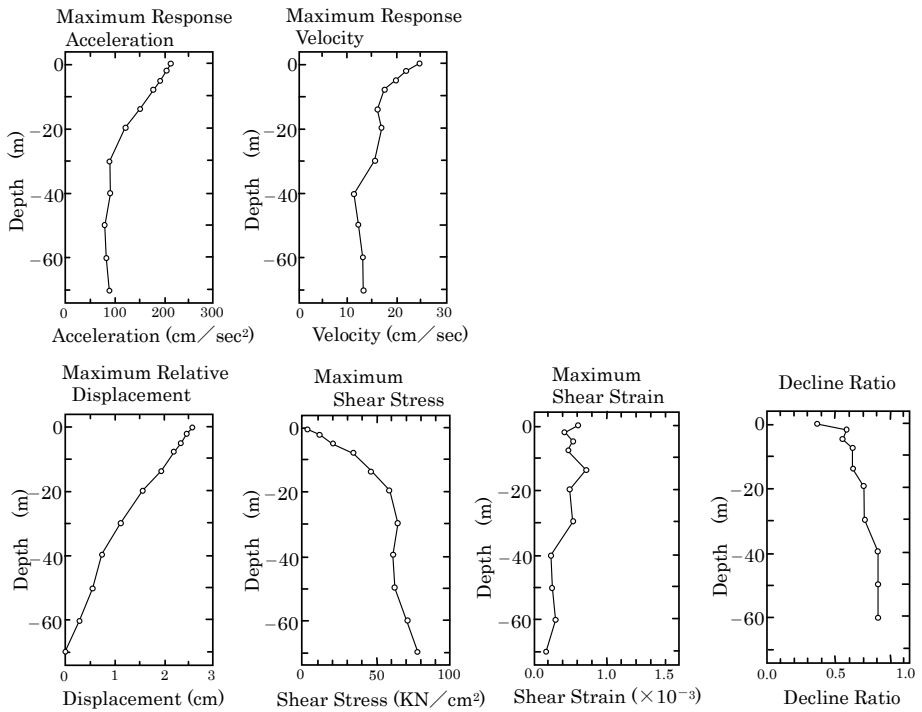
Figure B.11

Figure B.12

Figure B.13

B.6 Results of Analyses

1) Ground Stiffness and Seismic Ground Coefficient

Figure B.14 shows a comparison of the ground stiffness and seismic ground coefficient between the simplified calculation and the precise calculation. The seismic coefficient of the precise calculation was calculated by the maximum ground shear stress of SHAKE, and the ground stiffness was the convergence stiffness of SHAKE.

The seismic ground coefficient of the simplified calculation is based on the current version of the Design Recommendation whilst the ground stiffness was calculated by the ground deformation based on the 1990 version considering the strain dependent characteristic of the ground stiffness (the effective strain is 65 % of the maximum strain).
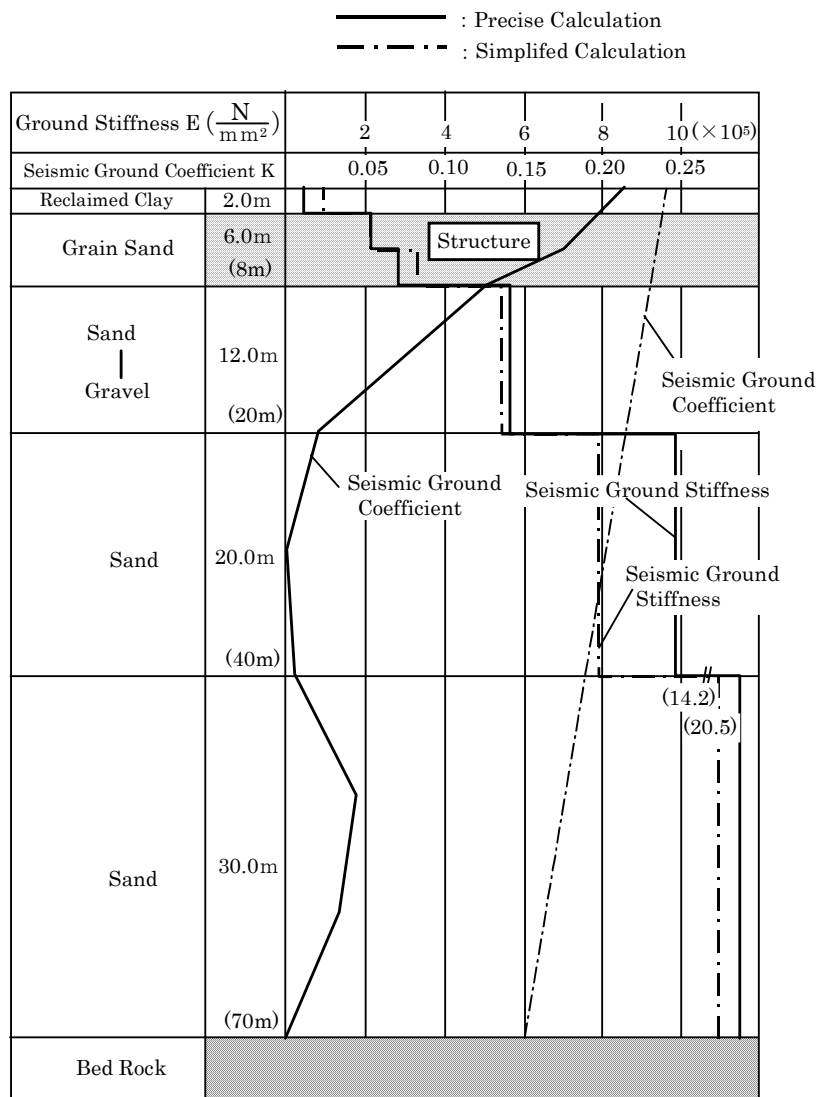

Figure B.14

2) Ground Displacement, Surrounding Shear Force, Ground Spring.

Figure B.15 shows a comparison of the ground displacement, the surrounding shear force and the ground springs (the axis springs) between the simplified calculation and the precise calculation.

As the ground displacement obtained from the simplified calculation based on the 1990 version is given in the cosine-curve distribution, the magnitude of the ground displacement is relatively big near the bedrock, but smaller near the structure at the ground surface layer, therefore the ground displacement obtained from the response displacement method and the surrounding shear force calculated by this ground displacement are small.

The ground springs calculated by the N values obtained from the simplified calculation following the Specifications for Highway Bridges are bigger than the ones calculated by the convergence stiffness of SHAKE obtained from the static FEM analysis.
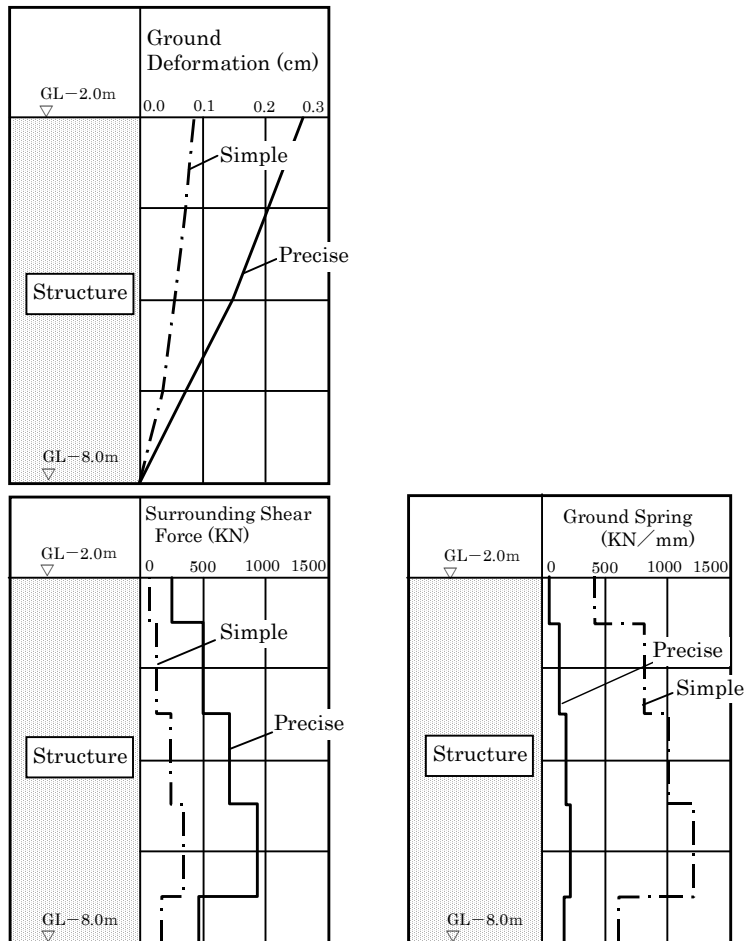
Figure B.15

3) Comparison of the Stresses Shared in the Supporting Structure

Figure B.16 shows a comparison of the stresses shared in the frame components (i.e. the outer wall perpendicular to the model plane, columns, bottom slab and top slab) and the wall component (i.e. the outer wall in the model plane) in the supporting structure for the various analyses. The figure shown at the bottom of each rectangular bar indicates the ratio for each analysis compared to 1.0 for the dynamic analysis.

It is noted that the stress shared in the frame is extremely small in that all analysis cases show values of only a few percent. The total stresses obtained from the response intensity method and the response displacement method (except for the simplified calculation of the latter), indicate a relatively larger value which is 1.1 - 1.4 times the total stress of the dynamic analysis.
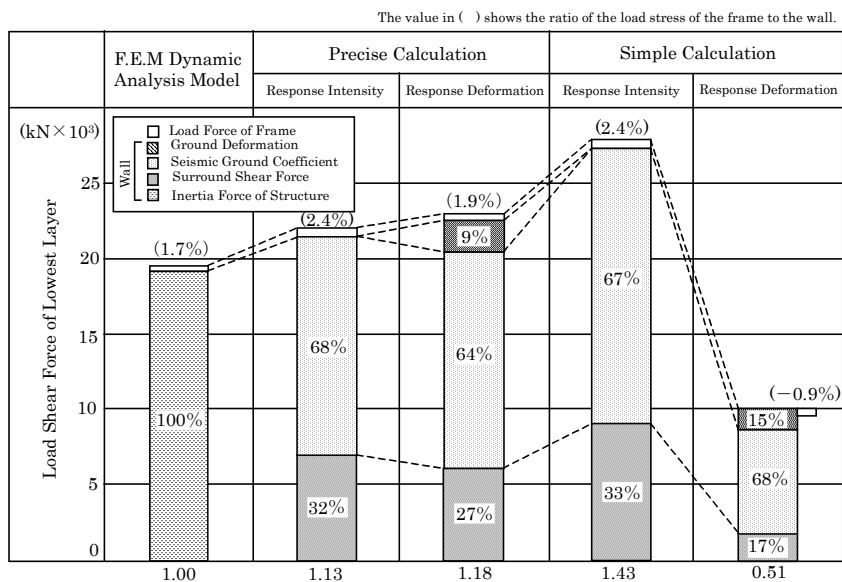

Figure B.16

4) Examination about the Simplified Calculation in the Response Displacement Method.

As the total stress obtained from the simplified calculation of the response displacement method is smaller compared to the other analysis result, an examination is carried out with three cases in Table B.2. CASE 1 is of an examination to see the effect of the ground spring, and CASE 2 and CASE 3 are examinations to see the effect of the ground displacement.

Figure B.17 shows the ground displacements and the surrounding shear forces of the simplified response displacement method, the precise response displacement method and the three cases. The analysis results of the sheared stresses at the lowest layer of the structure are shown in Figure B.18. Although the total stress for CASE 1 indicates approximately 1.4 times of the simplified calculation due to the different ground spring, it is still smaller than that of the dynamic analysis. The total stresses for CASE 2 and

CASE 3 indicate 1.0 - 1.4 times of the dynamic analysis due to the increased surrounding shear force.

Figure B.19 shows the analysis result in the case that a fall of the ground stiffness is not considered to calculate the surrounding shear force. All cases indicate the bigger total stress due to the increase of the surround shear force. It is noted that the total stresses for CASE 2 and CASE 3 indicate considerably larger when compared with the dynamic analysis.

From the above, and with the consideration that the selected structure is a proper example for the examination, the ground displacement of CASE2 (see Figure B.18) is recommended as for the simplified calculation of the response displacement method.

Table B.2

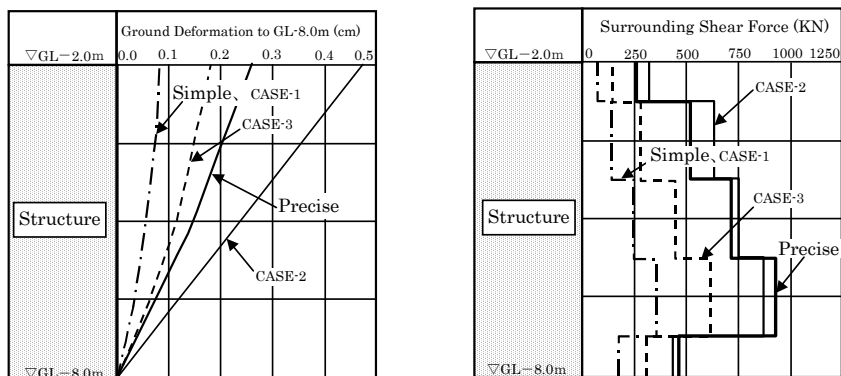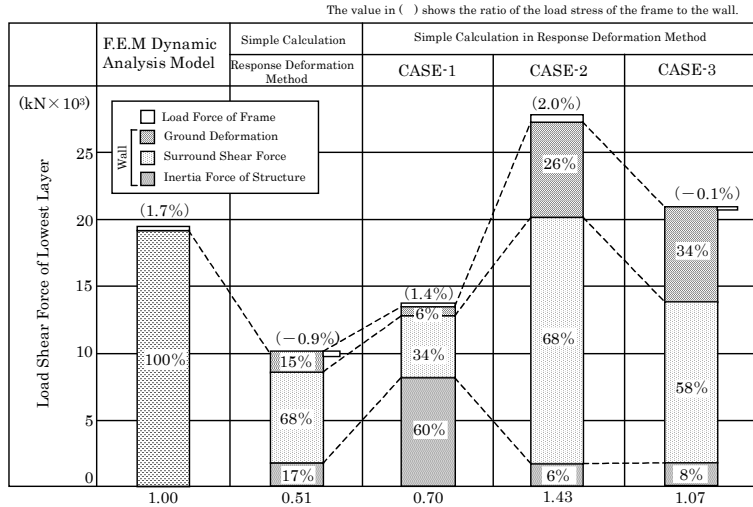| CASE－1	It uses the ground spring calculated by the precise analysis.
CASE－2	The ground deformation is an opposite triangle distribution setting the same deformation at the ground surface.
CASE－3	It changes the position of the bedrock into GL-40m from GL-70m.

Figure B.17

The value in ( ) shows the ratio of the load stress of the frame to the wall.

	F.E.M Dynamic Analysis Model	Simple Calculation	Simple Calculation in Response Deformation Method		
		Response Deformation Method	CASE-1	CASE-2	CASE-3

(kN×10³)

Load Shear Force of Lowest Layer

Wall
- ☐ Load Force of Frame
- ▨ Ground Deformation
- ▨ Surround Shear Force
- ▨ Inertia Force of Structure

(1.7%) 100%
(−0.9%) 15% 68% 17%
(1.4%) 6% 34% 60%
(2.0%) 26% 68% 6%
(−0.1%) 34% 58% 8%

1.00   0.51   0.70   1.43   1.07

Figure B.18

The value in ( ) shows the ratio of the load stress of the frame to the wall.

	F.E.M Dynamic Analysis Model	Simple Calculation	Simple Calculation in Response Deformation Method		
		Response Deformation Method	CASE-1	CASE-2	CASE-3

(kN×10³)

Load Shear Force of Lowest Layer

Wall
- ☐ Load Force of Frame
- ▨ Ground Deformation
- ▨ Surround Shear Force
- ▨ Inertia Force of Structure

(1.7%) 100%
(−0.7%) 11% 76% 13%
(1.2%) 5% 42% 53%
56180 (1.0%) 13% 84% 3%
(−0.1%) 24% 70% 6%

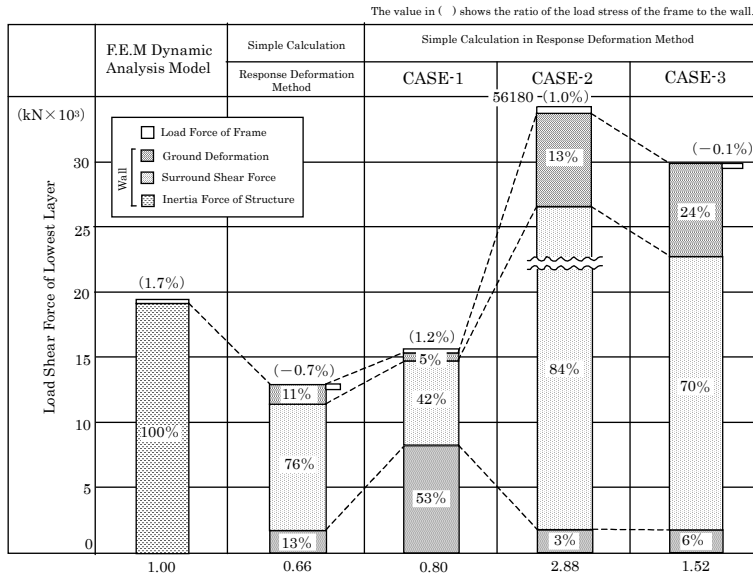1.00   0.66   0.80   2.88   1.52

Figure B.19

References
[B.1] The Architectural Institute of Japan: Design Recommendation for Storage Tanks and Their Supports, 1990
[B.2] Per B.Schnabel, John Lysmer and H.Bolton Seed : SHAKE-A Computer Program for Earthquake Response Analysis of Horizontally Layered Sites. EERC 72-12(University of California Berkeley), December.1972
[B.3] Japan Road Associations : Specifications for Highway Bridges Part Ⅴ Seismic Design. February.1990 and march. 2002
[B.4] Experimental Study on Dynamic Deformation Characteristics of Soils（Ⅱ） Toshio Iwasaki, Fumio Tatsuoka, Yoshikazu Takagi. Public Works Research Institute Report No.153 March.1980